International Journal of
Science, Engineering and Technology

Volume 4 Issue 1, January- February 2016

A Bi-Monthly Multi-Disciplinary Peer Reviewed/ Referred International Journal

ISSN (O) : 2348-4098 I ISSN (P) : 2395-4752

Published by: IJSET Journal Publication, E 310 A, Katariya Colony, Ram Nagar Ext., Sodala, Jaipur, Rajasthan, INDIA- 302019

Printed at: Madhu Offset, Barkat Nagar, Jaipur, Rajasthan, INDIA- 302015

Contents

Manuscript Title *Author*	Page No.
Performance analysis of Effect of Cyclic Prefix on Data Rates in Wi-MAX System with Variation in Signal to Noise Ratio and Coding Rates for Different Modulation Techniques: A Survey *Sachin Kumar Barmase, Kanak Kumar*	5
Nanoantenna – A Review on Present and Future Perspective *Sanjay Kumar, Sanju Tanwar, Sumit Kumar Sharma*	8
Optimization of Process Parameters in Extraction of Thyme Oil Using Response Surface Methodology (RSM) *Nadiya Rashid Malik, K. C. Yadav, Anurag Verma*	16
Robust Facial Landmark Detection Using a Mixture of Synthetic and Real Images with Dynamic Weighting: A Survey *Om Prakash Gupta, Kanak Kumar*	25
Comparative Study of Bio-Ethanol Production from Kokum and Butter Fruit Waste Samples by Employing Microbial Fermentation Technology *Thouseef Ahamad, M. Y., G. Panduranga Murthy*	28
Countering Smart Attack and Selective Capture in Wireless Sensor Networks Using Genetic Algorithm *M. Shamuganapriya, S. Divakar*	42
Study on 3D Visual Attention for Stereoscopic Image Quality and Compression Assessment *Vikas Kumar, Sanjay Sharma*	49
Significance of Various Fibres on Engineered Cementitious Concrete *Sathishkumar. P, Sampathkumar. P, Karthik. M, Vignesh. C*	52
Novel Technique for Video Segmentation and Image Matching *Shakuntala Satyawana, Surendra Kumar Agarwal*	59

A Review Paper on Image Segmentation and Object Recognition Procedures 67

Shakuntala Satyawana, Surendra Kumar Agarwal

Removal of Flouride from Industrial Waste Water Using Mosambi Peel as Biosorbent: Kinetics Studies 72

Deepankar Dev Pandey, Apoorva Tripathi, Tej Pratap Singh

Design and Fabrication of a Hybrid Solar & Micro Wind Power Generator 82

Vishnu Khetan, Hari Kumar Singh, Rohit Kumar

A Geographical Study of Food Security and Agriculture in India 92

Ashish Sharma

Synthesis and Characterization of Silver Nanoparticles using Delonix Elata Leaf Extract and Its Anti- Inflammatory Activity against Human Blood Cells 98

P. Anitha, P. Sakthivel

Development and Performance Evaluation of Forced Convection Batch Type Steam Blancher 99

Mohd Kaleem, Er. Kailash Chandra Yadav, Md Jafri Ahsan

Sachin Kumar Barmase et al. 2016, Volume 4 Issue 1
ISSN (Online): 2348-4098
ISSN (Print): 2395-4752

International Journal of Science, Engineering and Technology
An Open Access Journal

Performance analysis of Effect of Cyclic Prefix on Data Rates in Wi-MAX System with Variation in Signal to Noise Ratio and Coding Rates for Different Modulation Techniques: A survey

[1]Sachin Kumar Barmase, [2]Kanak Kumar

Abstract

Orthogonal frequency division Multiplexing (OFDM) has become the chosen modulation technique for wireless communications because it provides a high data rate wireless transmission. From the Process of this development, the mechanism of an OFDM system can be studied; and with a completed MATLAB program, the characteristics of an OFDM system can be explored. Implementation of the OFDM system entails several difficulties. One of the major drawbacks is the high peak-to-average power ratio (PAPR) which causes large number of sub-carriers, which make restrictions for practical applications. Results are verified using MATLAB software. The simulation is used to study the effect of the cyclic prefix on the bit error rate (BER) with different types of modulation techniques (BPSK, 4QAM, 16QAM, and 64QAM) based on the variation in signal to noise ratio (SNR).

Keywords- Orthogonal frequency division multiplexing (OFDM); SNR (Signal to Noise Ratio), BER (Bit Error Rate), MIMO (Multi-Input Multi-Output), Wi-Max, IFFT (Inverse Fast Fourier Transform), LTE

Introduction

Wi-Max is a wireless broadband technology based on IEEE 802.16 standard. Long Term Evolution (LTE) is standardized by the 3rd Generation Partnership Project (3GPP) as an evolution of the 3G systems to meet the requirements of increasing the data rates, high mobility and low latency over a bandwidth of up to 20 MH. In fourth generation (4G) communication systems to provide a comprehensive and secure IP solution where voice, data and multimedia can be offered to users at "anytime, anywhere" with higher data rates than previous generations . Multiple input multiple outputs (MIMO) and Orthogonal Frequency Division Multiplexing (OFDM) modulation have therefore been adopted due to their superior performance. These developing modulation used in LTE which promise to become the key for high-speed wireless communication technologies and combining them can provide wireless industry evolution from 3G to 4G systems. In OFDM systems which are use MIMO state that, the output is the superposition of multiple sub-carriers in this case, instantaneous power outputs increases and may demand higher powers than the mean power of the system since the phases of these carriers are the same. OFDM is a special form of spectrally efficient Multi-Carrier Modulation (MCM) technique, which involves densely spaced orthogonal sub-carriers and overlapping spectrums. Due to orthogonality nature of the sub-carriers, the use of band pass filters is not required in OFDM. Hence, the available bandwidth is used very efficiently without causing the Inter – Carrier Interference (ICI).

Our aim is to implement and find the effect the cyclic prefix (CP) on BER with different of modulation techniques based on the venation in gain vector, delay vector, SNR. This modulation technique gives a good performance of a Wi-MAX system.

Proposed Block Diagram for Transmitter & Receiver of Wi-Max System

[1]Corresponding Author's Email: barmasesachin@gmail.com

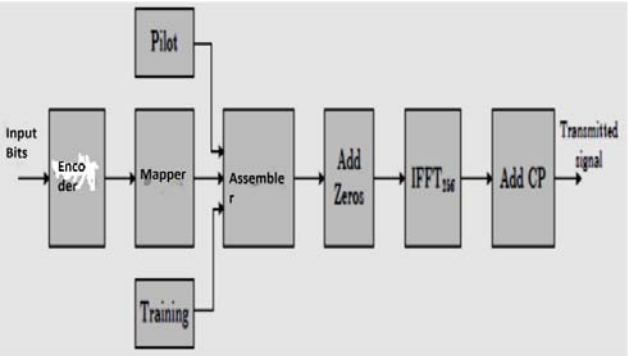

Figure 1: Transmitter of the Wi-MAX system

In the transmitter section, the digital data that is to be transmitted is first converted into several symbols of digital data of low bit rate using the serial to parallel converter. Each data stream is then converted into subcarrier amplitude and phase using a mapping technique and also according to the value of each symbol represented in digital form. The spectral representation of each data stream is then converted into time domain using the Inverse Fast Fourier Transform (IFFT).In this system, Physical layer uses Orthogonal Frequency Division multiplexing (OFDM) with 256 subcarriers. Each OFDM symbol is composed of 192 data subcarriers, 1 zero DC subcarrier, 8 pilot subcarriers, and 55 guard carriers. Therefore, a process of assembling the zero DC subcarrier, data, and pilots is needed to build the symbols. After wards zero padding is performed. Then, the signal is converted to the time domain by means of the inverse fast Fourier transform (IFFT) algorithm, and finally, a cyclic prefix (CP) is added.

Cyclic Prefix

A multipath channel can affect the subcarrier orthogonality of an OFDM system. Cyclic-Prefix is used to combat Inter Symbol Interference and Inter career Interference (ICI) introduced by the multipath channel. The length of the CP (Tg) must be longer than the maximum delay spread of the target multipath environment.

$$t_{max} < T_x < T_g \quad (1)$$

Where t_{max}= maximum multipath spread.

When above equation is satisfied, there is no ISI (Inter symbol Interference) and there is no ICI (Inter carrier Interference).

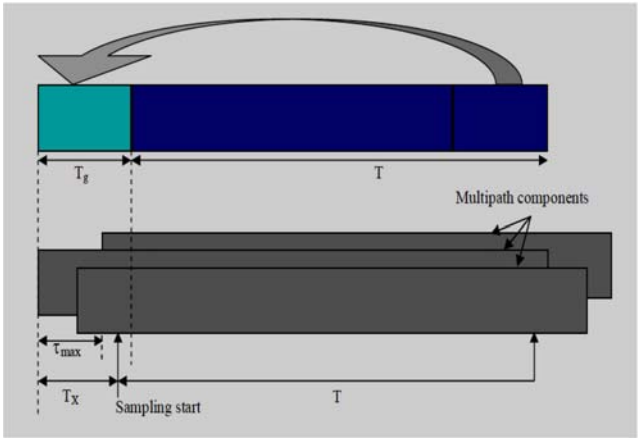

Figure 2: Cyclic Prefix in OFDM

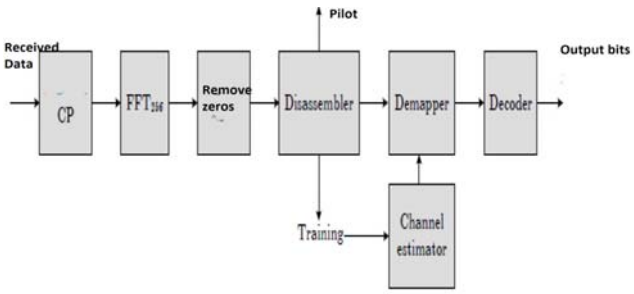

Figure 3: Receiver of the WI-MAX system

At the receiver end, the Cyclic-prefix (CP) is removed and the received signal is converted to the frequency domain using the Fast Fourier Transform (FFT). The receiver performs the reverse operation of the transmitter, mixing the RF signal to base band for processing, then using a Fast Fourier Transform (FFT) to analyze the signal in the frequency domain. The amplitude and phase of the sub carriers is then picked out and converted back to digital data.

Proposed Methodology

To judge the OFDM system performance, we have to do some performance analysis. There are a lot of criteria to analyze a systems performance. In mobile wireless system Bit Error Rate (BER), Signal to Noise Ratio (SNR), Peak to Average Signal Power Ratio (PAPR), channel coherence bandwidth, Quality of Service (QoS), transmission speed in bit per second (bps), delay profile etc are very common parameters to judge a system. It is always desirable to have a good wireless technique which has all the necessary qualities like lower BER, lower SNR, and higher Quality of Services values and so on. The main objective of this proposed research is to study and investigate the effect of several wireless channel impairment factors to the performance of OFDM

system and also to find out the best signal parameters to overcome the detrimental effects of the mobile wireless channel environment to the system. We may compare following modulation techniques such as: BPSK (Binary Phase Shift Keying), QPSK (Quadrature Phase Shift Keying), I6PSK, 32PSK and 64PSK are used in the OFDM transceiver to show the tradeoff between system capacity and system robustness. The OFDM system is simulated using MATLAB and all the simulation results are represented in term of Bit Error Rate (BER) versus Signal to Noise Ratio (SNR) in 2-D graph for four different channels.

Expected Outcomes

OFDM technology can be substituted by the sum of PSK/QAM modulators in quantity m, so that with the same error probability , what is acceptable for the voice communication, speed will be higher in m times or their possibility appears to optimize another parameters like power, antenna amplification and radiation pattern.

Conclusion and Future Work

For urban, rural, terrain and rician channels the BPSK and QPSK modulation techniques works well with small SNR value in the presence of any amount of clip compression in the channel. The higher the clip compression the higher the SNR value is required for 16 PSK or above PSK modulation techniques. Finally, the signal parameters must fulfill the condition of flat fading in a wireless environment to get a reasonable error free result.

References

[1] T. S. Rappaport, Wireless Communications Principles and Practice, 2nd ed., Upper Saddle River: Prentice Hall, 2002, pp. 2S- 40.

[2] P. Nicopolitidis, A. S.Pomportsis, G. I. Papadimitriou, and M. S. Obaidat, "Wireless Networks", John Wiley and Sons: New York, 2003, pp.190-192.

[3] Cho, Y. MIMO-OFDM Wireless communications with MATLAB / Y.Cho, J. Kim, W. Yang, Ch. Kang. – Singapore: John Wiley & Sons (Asia) Pte Ltd, 2010, c. 136.

[4] Patyukov, V. G., Errors estimation of the Doppler systems / V. G.Patyukov, E. V. Patyukov, □. N. Rychkov. – Journal of the radio engineering: electronic journal. 2014. URL:http://jre.cplire.ru/jre/may14/3/text.pdf

[5] J. Heiskala, and J. Terry, "OFDM Wireless LANs: A Theoretical and Practical Guide", Sams Publishing: USA, pp.SI -90, December 200l.

[6] Payaswini P, and Manjaiah D.H, "Analysis of effect of cyclic prefix on data rates in OFDM modulation techniques", International Journal of Adv. Computer and mathematical Sciences, Vol. 3, Issue 4, pp. 465-470, 20 12.

[7] Mohammad Azizul Hasan, Performance Evaluation of WiMAX/IEEE 802. 16 OFDM Physical Layers, June 2007

[8] IEEE 802.11, Part 11: Wireless LAN medium access control (MAC) and physical layer (PHY) specifications, IEEE 802.11 Std., Mar. 2012.

Author's details

[1]M.Tech. Scholar, Department of EC, MIT, Bhopal, India, Email: barmasesachin@gmail.com

[2]Assistant Professor, Department of EC, MIT Bhopal, India

Copy for Cite this Article- Sachin Kumar Barmase and Kanak Kumar, "Performance analysis of Effect of Cyclic Prefix on Data Rates in Wi-MAX System with Variation in Signal to Noise Ratio and Coding Rates for Different Modulation Techniques: A survey', *International Journal of Science, Engineering and Technology,* Volume 4 Issue 1: 2016, pp. 220- 222.

Sanjay Kumar et al. 2016, Volume 4 Issue 1
ISSN (Online): 2348-4098
ISSN (Print): 2395-4752

International Journal of Science, Engineering and Technology
An Open Access Journal

Nanoantenna – A Review on Present and Future Perspective

[1]Sanjay Kumar, [2]Sanju Tanwar, [3]Sumit Kumar Sharma

Abstract

The day-by-day increasing demand of energy for this world enforces to find alternative energy sources. At present lots of R&D is going on to improve photovoltaic devices so as to improve their efficiency but the limit is that they can extract energy only from visible region of the electromagnetic spectrum. Therefore, a new device called Nanoantenna has been designed that can convert thermal energy extracted from infrared region of the spectrum into electricity. In near future its contribution will be in various fields like space communication, broadband wireless links, wireless optical communication, mobile communication (5G), radar detection and higher order frequency applications. Nanoantenna can be fabricated by different techniques like electron beam lithography, focused ion beam and nanoimprinting lithography. In this paper we will discuss only about nanoimprinting lithography technique, because it is a cost effective and high throughput technique. The material selection for nanoantenna is also a big problem, so we will also discuss how to eliminate it.

Keywords: Nanoantenna, Photovoltaic devices, Infrared, Communication, Lithography, etc.

Introduction

A nanoantenna is a solar collection device based on rectifying antennas. Nanoantenna is a recent device, so it does not have an old history. It is worthy to mention that the idea of using antennas to collect solar energy was first proposed by Robert L. Bailey in 1972. In 1973, Robert Bailey, along with James C. Fletcher, received a patent for an electromagnetic wave converter. The patented device was similar to modern day nanoantenna devices. Alvin M. Marks received a patent in 1984 for a device explicitly stating the use of sub-micron antennas for the direct conversion of light into electricity.

The nanoantenna consists of three main parts: the ground plane, the optical resonance cavity and the antenna (See fig. 1). The antenna absorbs the electromagnetic wave, the ground plane acts to reflect the light back towards the antenna and the optical resonance cavity bends and concentrates the light back towards the antenna via the ground plane.

Figure 1: Nanoantenna Structure, (Copyright, IJRETR)

One of the main advantages of using nanoantennas is their high theoretical efficiency. For example, the theoretical efficiency of single junction solar cells is only 30%. In contrast, in the case of nanoantenna the theoretical efficiency found is nearly 85%. Another advantage of nanoantennas over semiconductor photovoltaic devices is that nanoantenna arrays can be designed to absorb any frequency of light. Nanoantennas can absorb energy from sunlight as well as the earth's heat emitted in the form of infrared radiations.

Theory of Operation

The theory behind nanoantennas is essentially the same for rectifying antennas. Incident light on the antenna causes electrons in the antenna to move back and forth at the same frequency as the incoming light. This is caused by the oscillating

[1]Corresponding Author's Email: sanjaysihag91@gmail.com

electric field of the incoming electromagnetic wave. The movement of electrons is an alternating current in the antenna circuit. To convert this into DC power, the AC current must be rectified, which is typically done with some kind of diode. The resulting DC current can then be used to power an external load.

Fabrication of Nanoantenna

The fabrication of nanoantenna has been done using several techniques like Electron Beam Lithography (EBL), Focused Ion Beam lithography (FIB) and Nanoimprinting Lithography (NIL). Electron beam lithography and Focused ion beam lithography are costly, time consuming and low throughput fabrication techniques. So, another fabrication technique, nanoimprinting lithography has been used later on to fabricate nanoantenna. It is low cost, less time consuming and high throughput technique. As opposed to serial beam-based lithographies, where photons, electrons or ions are used to define nanopatterns, the NIL process uses a hard mold that contains all the surface topographic features to be transferred onto the sample and is pressed under controlled temperature and pressure into a thin polymer film, thus creating a thickness contrast. Resolutions on the order of 10 nm have been demonstrated more than a decade ago [1]. A promising variation of this technique is UV-NIL, where a transparent mold, such as glass or quartz, is pressed at room temperature into a liquid precursor which is then cured by UV radiation. In order to reduce the cost of mold fabrication and to achieve patterning over larger areas at lower pressures, soft nano-imprinting techniques, based on polymeric flexible stamps replicated from a single master mold, have also been developed [1]. In future, NIL might become the ideal technique for low-cost, highly reproducible realization of antenna arrays covering large areas, e.g. for the realization of bio-optical sensors on substrates or on fiber facets. (See fig. 2)

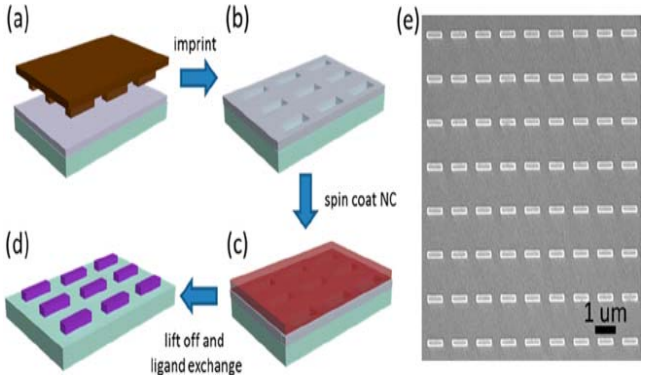

Figure 2: Nanoantenna fabrication by (a) thermal nanoimprint lithography to (b) transfer the master pattern into the resist, followed by (c) spin- coating of colloidal Au NCs and (d) ligand exchange and resist lift- off. (e) SEM image of a representative NC-based nanoantenna array fabricated by the nanoimprinting method [1], (Copyright, ResearchGate)

Material Issue

The material selection in nanoantenna fabrication is a difficult problem, because currently we used gold (Au) and silver (Ag) which have skin effect at higher frequency. It affects the efficiency of nanoantenna. At frequencies above infrared, almost in all the metals, current is being carried near the surface of the wire which reduces the effective cross sectional area of the wire leading to an increase in resistance. This effect is known as the skin effect. To eliminate this problem we switch the materials like graphene and carbon nanotube, because they do not show skin effect at higher frequency. Here we discuss the nanoantenna based on CNT and graphene in detail.

Carbon Nanotube Antennas

CNTs facilitate an extreme miniaturization due to slow wave propagation effects. CNTs exhibit exceptional electron transport properties, yielding ballistic carrier transport at room temperature with a mean free path of around 0.7 mm and a carrier mobility of 10,000 cm^2/Vs. Due to the slow-wave propagation of electromagnetic waves in CNT structures, the wavelength of electromagnetic waves propagating in CNT structures is considerably smaller than the free-space wavelength [2,3,4]. This effect occurs due to quantum transport effects in the CNT yielding a quantum capacitance and a kinetic inductance in addition to the geometric capacitance and inductance. CNTs exhibit a very high inductance per unit length due to the high kinetic energy of the electrons. The high inductance results in an electromagnetic slow-wave propagation along a CNT transmission line configuration with a phase velocity in the order of $c_0/100$ to $c_0/50$, where c_0 is the speed of light in free space [3,4]. CNT based nanoantennas are much shorter than the operating wavelength can be brought into resonance and potentially be used as radiation elements. A CNT nanoantenna is usually an extremely short antenna, considerably shorter than the free-space wavelength. The appearance of slow waves makes CNT antennas interesting for

wireless communication between circuits at the micro and nanoscale.

Copper and carbon dipole nanoantennas are investigated using modified Hallén and Pockling ton integral equations, which incorporate the CNT surface conductance. It was found that CNT dipoles start to go into resonance at much lower frequencies than initially assumed. This can be explained from the fact that electromagnetic waves are propagating along CNTs, forming surface plasmons, which have are induced propagation velocity and thus have shorter wavelengths. So, CNT dipoles with several micrometer sin length starts to resonate in the low terahertz region, where the wavelengths are 50–100 times larger compared to the length of the CNT dipole [5, 6].

Linear nanoscale dipole antennas either made of metal such as gold or silver or CNTs have been investigated. Due to the extremely high aspect ratio (length/cross sectional area), both metal nanowires as well as CNTs have AC resistances per unit length in the order of several kilo-ohm per micrometer. This high resistance causes high conduction losses and thus seriously decreases the efficiency and the achievable gain of nanoantennas. The efficiency of a CNT dipole antenna is estimated to being the range of –60 to –90 dB, which results from the high conductance losses. The situation in the case of metal nanoantennas is similar. Although low power levels are sufficient in modern communication links, the inherent loss introduced by metallic or CNT nanoantennas limits their applicability considerably. One approach to bypass the resistance problem could be the usage of arrays of nanoantennas or a bundle of parallel nanowires. In this case, the resistance can be decreased to an acceptable value; however, the slow wave effect is lost, as discussed in. Therefore, by an appropriate choice of geometry and the number of nanowires, the properties of nanoantenna structures have to be optimized.

Graphene Antennas

A promising alternative to CNT antennas could be planar structures such as two-dimensional (2-D) graphene layers. Graphene is a 2-D material consisting of a monoatomic layer of carbon atoms arranged in a honey-comb structure (See fig. 3). It exhibits an excellent crystal quality and unique electronic properties [2, 6]. Morozov et.al .have shown that electron-phonon scattering in graphene is so weak that room temperature electron mobility as high as 200,000 cm^2/Vs can be expected if extrinsic disorder is eliminated. Like CNTs, graphene also exhibits excellent conductivity and slow wave properties. The achievable slow-wave effect in plasmon modes is in the order of c_0/100. At terahertz frequencies, a population inversion in the graphene layer can be realized by optical pumping or forward bias, which yields an amplification of the surface plasmon. Graphene allows the realization of planar structures and active circuits.

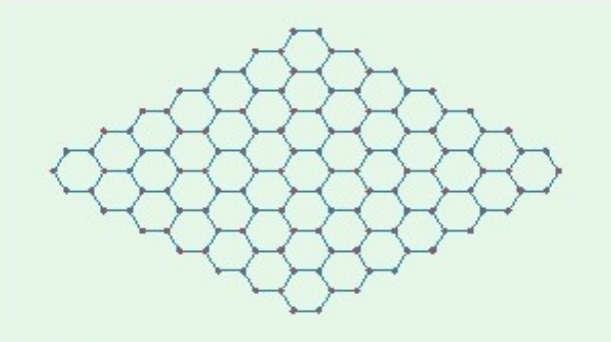

Figure 3: Structure of a graphene layer [6], (Copyright, IEEE Magazine)

Figure 4 shows patch antennas based on CNTs and graphene nanoribbons (GNRs). Theoretical investigations have shown that antennas with sizes in the order of several hundred nanometers are suitable to radiate electromagnetic waves in the terahertz band, that is, 0.1–1 THz. Graphene has also been used as substrate for metallic antennas. In metallic dipole antennas and arrays of dipole antennas have been patterned on a graphene layer. The antennas have been operated at 120 GHz using the high-resistivity and low-resistivity state of the graphene, the antenna radiation patterns could be controlled [6, 7].

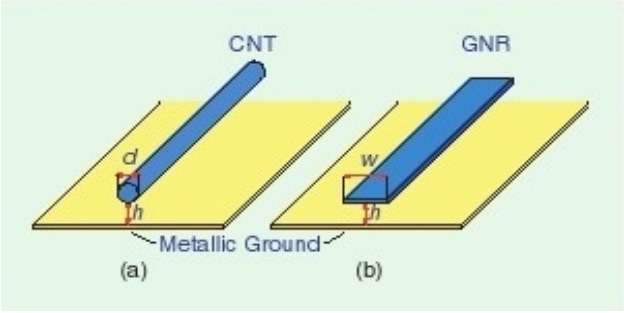

Figure 4: Nanopatch antenna based on (a) carbon nanotube and (b) graphene nanoribbon (GNR), [6], (Copyright, IEEE Magazine).

Nanoantenna Applications

Nanoantenna plays an important role in many fields like, space communication, optical wireless communication, mobile communication, object detection in radar technology, broadband wireless links, nanoantenna for terahertz detection, wireless data transfer at very high speed, and nanophotonic applications. These all applications will be possible in near future. Here we are discussing some of the applications based on nanoantenna in detail.

Optical Wireless Link

Owing to their capacity to control the direction and angular distribution of optical radiation over a broad spectral range, nanoantennas are promising components for optical communication in nanocircuits. Here we are discussing about the wireless optical power transfer between plasmonic nanoantennas in the far-field and changeable signal routing to different nanoscopic receivers via beam steering [8, 10]. The radiation pattern of single optical nanoantennas using a photoluminescence techniqueallows mapping of the unperturbed intensity distribution around plasmonic structures. The distance dependence of the power transmission between transmitter and receiver by deterministically positioning nanoscopic fluorescent receivers around the transmitting nanoantenna. By adjusting the wave front of the optical field incident on the transmitter directional control of the transmitted radiation over a broad range of 29° can be achieved. This enables wireless power transfer from one transmitter to different receivers [9, 11]. One of the envisioned applications of plasmonics is optical on chip circuitry with nanoscale footprints to combine photonics with integrated electronics for high speed computing and high bandwidth communication.

Wireless power transfer

Figure 5(a) depicts the concept of optical power transfer via free space between transmitting antenna T and receiving antenna R. The lower panel of Fig. 5a compares the power transmission as a function of distance d of such a nanoantenna link to a plasmonic waveguide. Here we consider an absorption constant $\alpha = (2\ \mu m)^{-1}$ for lithographically fabricated waveguides with a width of 100 nm at the near infrared wavelength λ=785 nm [12, 13]. There is a tradeoff between field confinement and propagation length, for example, for a cylindrical plasmonic waveguide, a decrease in the wire width leads to higher field confinement but results in a strong increase of the losses. In contrast, for the antenna link, absorption losses occur only at the antennas and are thus much lower than for a waveguide. The antenna link performs even better when plasmonics antennas with high directivity D are used as transmitters and receivers as shown by the red curve in Fig. 5(a). In the RF domain, antenna arrays achieve extremely high directivities because of constructive interference of the radiation of the individual antennas [14, 16]. They furthermore enable tunable redirection, that is, steerability of the transmitted radiation by phasing the individual antennas (see Fig. 5b). These properties make antenna arrays irreplaceable in steerable far distant communication where direct connections are no option. Bringing this concept to the optical frequency domain by employing optical nanoantenna arrays, opens up a new perspective of realizing low loss changeable optical interconnects where direct waveguide connections are not suited [15, 17].

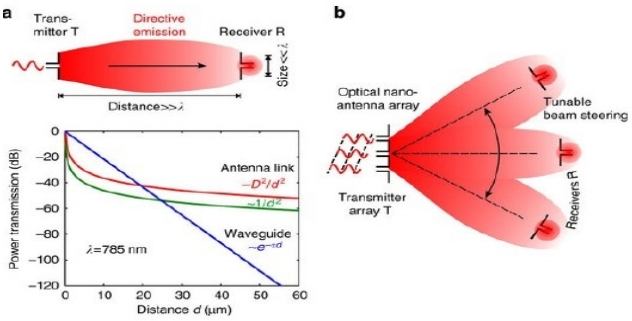

Figure 5: Optical nanoantennas enhance transmission and reception of electromagnetic waves via impedance matching and high directivity, allowing efficient power transfer between source and receiver [17], (Copyright, Nature publication Group).

Nanoantenna for Terahertz Detection

Infrared detectors are important devices in e.g., security and medical fields. Antenna-coupled metal–oxide–metal diodes (ACMOMDs) are a promising candidate for infrared (IR) detectors due to their small size, CMOS compatibility, and ability to offer full functionality without cooling or applied bias. The concept of ACMOMD was first introduced in the 1970s. The device consists of two main components: the dipole antenna for receiving electromagnetic waves in a certain wavelength range and a metal–oxide–metal (MOM) diode that serves as the rectifying device [18, 21, 22]. Tunneling diodes are

promising candidates for the rectification of terahertz signals because of the femtosecond tunneling times of an electron through a thin barrier in a MOM diode. All of the ACMOMDs, fabricated through either the evaporation technique or the two step EBL technique that pass the dc test of showing nonzero curvature coefficient are subjected to IR characterization for full detector functionality. A linearly polarized continuous wave (CW) CO_2 laser has been used as the IR source. The shape of the IR beam has been characterized through the knife-edge experiment and the $1/e^2$ beam width was found to be 4 mm [19, 21]. The laser beam passes through a polarizer, mechanical chopper, and a half-wave plate before it hits the device-under-test, the ACMOMDs. The half-wave plate is used to rotate the polarization of the IR laser without changing the orientation of devices or the laser.

According to classical antenna theory, if the polarization of the IR laser is rotated with respect to the orientation of the ACMOMD, the IR response of the ACMOMD should show a cosine-squared behavior, i.e., if δ_{IR} is the angle between the orientation of the ACMOMD and the electric field vector, the IR response should follow $\cos(\delta_{IR})^2$ type variation. The IR response of ACMOMDs consists of polarization-dependent response that is varying cosine squared, as discussed, and the polarization-independent response, which is believed to be of thermal origin [23. 25]. In a co-polarized condition, the electric field is fully aligned with the ACMOMD, and in a cross-polarized condition, the electric field vector is perpendicular to the ACMOMD orientation. The ratio of the corresponding IR responses of the co-polarized and cross-polarized conditions gives the polarization ratio of an ACMOMD. A typical IR response of an ACMOMD is shown in Fig. 6 [26].

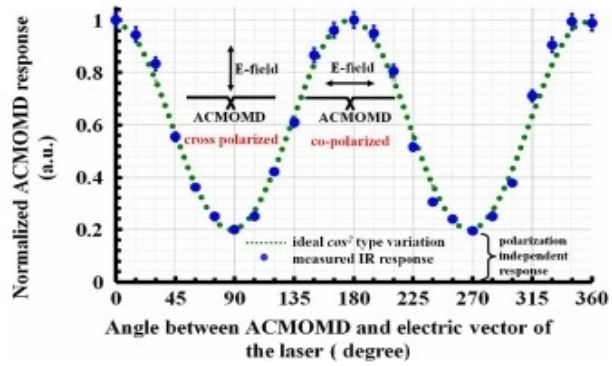

Figure 6: IR response of ACMOMDs [26], (Copyright, IEEE)

It consists of a polarization-dependent part, which varies as $\cos^2$ and a polarization-independent response, which is believed to be of thermal origin. The device shows a polarization ratio of 5. It is seen that the polarization-dependent signal is cosine squared varying with a dc off-set provided by the polarization-independent signal [28]. Presence of a polarization dependent component in the IR response of the ACMOMDs shows that ACMOMDs behave as classical antennas and their radiation characteristics and other antenna parameter are governed by classical antenna theory.

Nanoantenna for Nanophotonic Application

Antennas play an important role traditionally for many microwave applications [30]. However, recently developments of antennas in the near-infrared and optical regions are showing great promises with better manipulation, emission control and radiation of light waves into free space. In recent years, nano scale optical antennas are proposed for several applications in near-infrared, far-infrared and visible range. For example, nano-antennas have been considered as efficient and promising element in scattering, sensing, photo-detection, heat-transfer, inter and/or intra chip optical communications, energy harvesting etc. Moreover, optical nano-antenna can play a vital role in reducing power consumption and allow higher speed for on chip optical interconnects [31, 32, 33]. As a result, it is now considered of as a prominent alternative to optical waveguide based interconnects for on-chip wireless communication that meets high spectral efficiency.

To design a novel broadband optical nano-antenna including a transmission-line (which will be directly connected to waveguide), the fore mentioned hybrid plasmonic structure is considered here. The nano-antenna can be fabricated using standard CMOS processing techniques which can be incorporated with the electronic circuit of an optical communication device. The perspective view of our designed optical nanoantenna is shown in Fig. 7(a). Fig. 7(b) shows the top view of our proposed nano-antenna. Visually this antenna is almost similar to the 'Vivaldi Antenna' often used in radio frequency range. To cover all optical communication windows, we fix our target frequency range of operation as 150THz-390THz (λ_c = 2000nm-769.2nm) with the center frequency at f_c = 270THz (λ_c = 1111.1nm). We set our antenna's overall length, $L = L_P + L_T$ = 250nm + 300nm = 550nm; which is almost equal to half

center wavelength, $\lambda_c/2$ = 1111.1nm/2 = 555.55nm [34, 35]. The width is set to W_P = 500nm. Each tapered-slot is designed as quarter-portion of a circle considering each lower-side corner of the nano-antenna as center and L_P = 250nm is estimated as the radius of each circle. The width of transmission-line, W_T remains same as the width of the hybrid plasmonic waveguide described above ($W_T = W_{co}$ = 100nm). The overall dimension of the Si slab and its underneath SiO_2 insulator substrate is1100nm * 850nm [37, 38, 39].

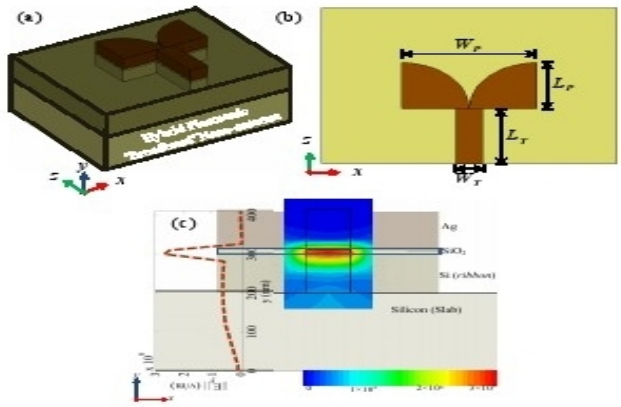

Figure 7: Schematic of the proposed hybrid plasmonic nano-antenna where a layer of silicon di-oxide (SiO_2) with silver (Ag) cap embedded on a thin silicon (Si) layer (a) 3-D perspective view (b) top view (c) 2-D cross-sectional view at the port side with E-field distribution at z = 0 [36], (Copyright, IEEE)

Mobile Communication

The 5G mobile communication in the next decade is going to require 1000 times' larger bandwidth and 100 times more speed to cover large number of applications of future cell phones. One of the expected techniques to fulfill these requirements is going to be THz band mobile communication. This would certainly require THz band nanoantennas. The formation of Surface Plasmons (SPs) at the interface of metal-dielectrics and existence of Surface Plasmon Polarization (SPP) resonances. The plasmonic activity at the interface of metal-dielectrics is heavily affected by the size of antenna and selection of metal and dielectrics.

Conclusion

The ever increasing demand of energy in the world cannot be full-filled by non-renewable energy sources and therefore to extract maximum of energy from renewable energy sources has become a challenge. One of the renewable sources of energy is solar energy but the efficiency of current photovoltaic devices is still not sufficient to convert whole of the solar energy into electric power. Here we have discussed about a new device called nanoantenna that converts heat energy into electrical energy and enhances the efficiency of solar cell at very higher order. Today most of space agencies like NASA, ISRO and other use solar cells as power sources in space shuttles. Nanoantenna can play a very important role in such applications, because the fabrication requires less material using Nanoimprinting lithography technique as compared to solar cells and provides higher efficiency. The nanoantenna is also used in plasmonic electronic circuits, where it converts the heat energy dissipated from electrical connection and electronic components into the electrical energy and thus lowers down the operating temperature of such devices.

References

[1] Wenxing Chen, Mykhailo Tymchenko, Prashanth Gopalan, Xingchen Ye, Yaoting Wu, Mingliang Zhang, Christopher B murray, Andrea Alu, Cherier R Kagan,(2015), "Large- Area Nanoimprinted colloidal Au Nanocrystal Based Nanoantenna for Ultrathin Polarizing Plasmonic metasurface" (Nanoletter: 15(8).

[2] I. F. Akyildiz and J. M. Jornet, (Mar. 2010), "Electromagnetic wireless Nanosensor networks," Nano Commun. Netw (Elsevier) J., vol. 1, no. 1, pp. 3–19.

[3] J. E. Burke, (Mar. 2011), "Analytical study of tunable bi-layered-graphene dipole antenna," Army Armament Research, Development and Engineering Center, Dover, NJ, USA, Tech. Rep.

[4] P. Burke, S. Li, and Z. Yu, (July 2006), "Quantitative theory of nanowire and nanotube antenna performance," IEEE Trans. Nanotechnol., vol. 5, no. 4, pp. 314–334.

[5] G. W. Hanson, (Nov. 2005), "Fundamental transmitting properties of carbon nanotube antennas," IEEE Trans. Antennas Propag., vol. 53, no. 11, pp. 3426– 3435.

[6] J. M. Jornet and I. F. Akyildiz, (Apr. 2010), "Graphene-based nano-antennas for electromagnetic nanocommunications in the terahertz band," in Proc. 4th European Conf. Antennas Propag. (EUCAP).

[7] I. L. latser, C. Kremers, A. Cabellos-Aparicio, J. M. Jornet, E. Alarcon, and D. N. Chigrin, (Oct. 2012), "Graphene-based nano-patch antenna for terahertz radiation," Photonics Nanostructures - Fundamentals Appl., vol. 10, no. 4, pp. 353–358.

[8] Alduino, A. & Paniccia, M. (2007), Interconnects: wiring electronics with light. Nat. Photon. 1, 153–155.

[9] Huang, J.S., Feichtner, T., Biagioni, P. & Hecht, B. (2009), Impedance matching and emission properties of nanoantennas in an optical nanocircuit. Nano Lett. 9, 897–902.

[10] Ozbay, E. (2006), Plasmonics: merging photonics and electronics at nanoscale dimensions. Science 311, 189–193.

[11] Maier, S. A. et al. (2003), Local detection of electromagnetic energy transport below the diffraction limit in metal nanoparticle plasmon waveguides. Nat. Mater. 2, 229–232.

[12] Curto, A. G. et al. (2010), Unidirectional emission of a quantum dot coupled to a nanoantenna. Science 329, 930–933.

[13] Kosako, T., Kadoya, Y. & Hofmann, H. F. (2010), Directional control of light by a nanooptical YagiUda antenna. Nat. Photon. 4, 312–315.

[14] Dorf müller, J. et al. (2011), Near field dynamics of optical Yagi Uda nanoantennas. Nano Lett. 11, 2819.

[15] Balanis, C. A. (2005), Antenna Theory John Wiley & Sons.

[16] Dregely, D. et al. (2011), 3D optical Yagi Uda nanoantenna array. Nat. Commun. 2, 267.

[17] Sun, J., Timurdogan, E., Yaacobi, A., Hosseini, E. S. & Watts, (2013), M. R. Large scale nanophotonic phased array. Nature 493, 195–199.

[18] J. A. Bean, B. Tiwari, G. H. Bernstein, P. Fay, and W. Porod, (2009), "Thermal infrared detection using dipole antenna-coupled metal–oxide–metal diodes," J. Vac. Sci. Technol. B, Microelectron. Nanometer Struct., vol. 27, pp. 11–14.

[19] I. Codreanu, F. J. Gonzalez, and G. D. Boreman, (2003), "Detection mechanisms in microstrip dipole antenna-coupled infrared detectors," Infrared Phys. Technol., vol. 44, pp. 155–163.

[20] C. Fumeaux, W. Herrmann, H. Rothuizen, P. De Natale, and F. K. Kneubühl, (1996), "Mixing of 30 THz laser radiation with nanometer thin-film Ni–NiO–Ni diodes and integrated bow-tie antennas," Appl. Phys. B, Lasers Opt., vol. 63, pp. 135–140.

[21] P. Hobbs, R. Laibowitz, and F. Libsch, (2005), "Ni–NiO–Ni tunnel junctions for terahertz and infrared detection," Appl. Opt., vol. 44, pp. 6813–6822.

[22] M. Heiblum, W. Shihyuan, J. Whinnery, and T. Gustafson, (1978),"Characteristics of integrated MOM junctions at dc and at optical frequencies," IEEE J. Quantum Electron., vol. 14, pp. 159–169.

[23] M. Heiblum, S. Y. Wang, T. K. Gustafson, and J. R. Whinnery, (Sept. 1977), "IIb-7 edge-MOM diode: An integrated, optical, non-linear device," IEEE Trans. Electron. Devices, vol. ED-24, no. 9, pp. 1199.

[24] S. Y. Wang, T. Izawa, and T. K. Gustafson, (1975), "Coupling characteristics of thin-film metal–oxide–metal diodes at 10.6 m," Appl. Phys. Lett., vol. 27, pp. 481–483.

[25] J. A. Bean, A.Weeks, and G. D. Boreman, (2011), "Performance optimization of antenna-coupled Al/AlOx/Pt tunnel diode infrared detectors," IEEE J. Quantum Electron., vol. 47, pp. 126–135.

[26] I.Wilke, Y. Opplinger,W. Herrmann, and F. K. Kneubuhl, (1994), "Nanometerthin-film Ni–NiO–Ni diodes for 30 THz radiation," Appl. Phy. A, vol. 58, pp. 329–341.

[27] C. Fumeaux, W. Herrmann, F. K. Kneubühl, and H. Rothuizen, (1998), "Nanometer thin-film Ni–NiO–Ni diodes for detection and mixing of 30 THz radiation," Infrared Phys. Technol., vol. 39, pp. 123–183.

[28] C. A. Balanis, (2005), Antenna Theory: Analysis and Design. Hoboken, NJ: Wiley.

[29] L. Novotny, and N. F. van Hulst, (2011), "Antennas for light", Nat. Photonics, 5(2), 83 - 90.

[30] T. Shegai, S. Chen, V. D. Miljkovic, G. Zengin, P. Johansson, and M. Kall, (2011), "A bimetallic nanoantenna for directional colour routing", Nat. Commun., 2, 481 - 486.

[31] J. N. Anker, W. P. Hall, O. Lyandres, N. C. Shah, J. Zhao, and R. P.Van Duyne, (2008), "Biosensing with plasmonic nanosensors", Nat. Mater., 7, 442-453.

[32] L. Tang, S. E. Kocabas, S. Latif, A. K. Okyay, D. Ly-Gagnon, K. C. Saraswat, and D. A. B. Miller, (2008), "Nanometre-Scale germanium photo-detector enhanced by a near-infrared dipole antenna", Nat. Photon, 2, 226 – 229.

[33] J. A. Schuller, T. Taubner, and M. L. Brongersma, (2009), "Optical antennathermal emitters", Nat. Photon., 3, 658 - 661.

[34] L. Yousefi, and A. C. Foster, (2012), "Waveguide-fed optical hybrid plasmonicpatch nano-antenna", Opt. Express, 20(16), 18326 - 18335.

[35] G. N. M.-Silveira, G. S. Wiederhecker, and H. E. H.-Figueroa, (2013), "Dielectric resonator antenna for applications in nanophotonics", Opt. Express, 21(1), 1234 - 1239.

[36] Y. Yifat, Z. Iluz, D. B.-Lev, M. Eitan, Y. Hanein, A. Boag, and J. Scheuer, (2013), "Optical resonances of bowtie slot antennas and their geometryand material dependence", Opt. Lett., 38(2), 205 - 207.

[37] E. D. Palik, Handbook of Optical Constants of Solids, (Academic Press,1998).

[38] P. B. Johnson, and R.W. Christy, (1972), "Optical constants of the noble metals", Phys. Rev. B, 6, 4370 - 4379.

[39] CSTTM Studio Suite–2012 (https://www.cst.com/).

Author's details

[1,3] M.Tech Scholar, Centre of Nanotechnology, Rajasthan Technical University, Rajasthan 324010.

[2]Assistant Professor, Centre of Nanotechnology, Rajasthan Technical University, Rajasthan 324010.

Copy for Cite this Article- Sanjay Kumar, Sanju Tanwar and Sumit Kumar Sharma, "Nanoantenna – A Review on Present and Future Perspective', *International Journal of Science, Engineering and Technology,* Volume 4 Issue 1: 2016, pp. 240- 247.

Nadiya Rashid Malik et al. 2016, Volume 4 Issue 1
ISSN (Online): 2348-4098
ISSN (Print): 2395-4752

International Journal of Science, Engineering and Technology
An Open Access Journal

Optimization of Process Parameters in Extraction of Thyme Oil Using Response Surface Methodology (RSM)

[1]Nadiya Rashid Malik, [2]K. C. Yadav, [3]Anurag Verma

Abstract

Thyme is a labiate plant whose essential oil has demonstrated medicinal properties. The aim of this study was to evaluate the feasibility of replacing n-hexane with methanol for the extraction of oil from Thymus vulgaris and to optimize extraction time and temperature using Response Surface Methodology(RSM) by implementing central composite design-face-centered to obtain optimal yield of thyme oil using modified methanol extraction technique. For methanol solvent, the effect of the maceration process on extraction yield under reduced pressure was also evaluated. Higher oil yields were obtained when methanol soaked thyme leaves were macerated causing burst of cells and thus increasing the area for material exchanges. The optimal values of variables with methanol extraction were determined to be 45^0C for 3 h with a response yield of 20 ml. 1 HNMR results showed that Thymol (2-isopropyl-5-methylphenol) is the main monoterpene phenol ; isomeric with carvacol ,found in thyme essential oil .These compounds have shown anti-inflammatory, antioxidant ,antibacterial ,antifungal and immunomodulatory properties.

Keywords: Maceration ,Methanol, Nuclear Magnetic Resonances (NMR) spectroscopy , Response Surface Methodology (RSM), Rotary Vacuum Evaporator, Thyme , Thymol.

Introduction

Nowadays consumer awareness regarding the use of synthetic chemical additives , foods preserved with natural additives have become boon to food technologists and in turn to consumers .Many natural compounds (thyme, basil ,clove and oregano) are gaining interest and are generally recognized as safe(GRAS).Use of Thyme dates back to 3500 BC by Sumerians and Egyptians .Its spread to Europe was due to Romans , as they used it to give aromatic flavors to liqueurs & cheese. Thyme is the general name for the many herb varieties of the Thymus species, all of which are native to Europe and Asia. Common or garden thyme is considered the principal type, and is utilized commercially for flowering and ornamental purposes. Thyme is native to the Western Mediterranean region, extending to south-eastern Italy. Thyme is a culinary Labiatae herb characterized by its volatile oil. Health promoting properties of these species have been attributed to their inherent secondary metabolites namely Volatile and phenolic compounds (Jordan et al., 2013). Extract of thyme rich in phenolic acids and flavonoids such as cafeic acid, syringic acid, genistic acid and luteolin with strong antioxidant activities have been proposed to be used as preservation for certain foods and pharmaceutical products (Chizzola et al.,2008). The antioxidant and antibacterial activities of the basic components of the essential oils of thyme (carvacrol and thymol) have been demonstrated. Due to their biological activities, essential oils of thyme are widely used in various cosmetics industries and found as a component of disinfectant and insecticides (Bousbia et al., 2009). Hexane extraction, the most common type of solvent extraction, requires expensive equipment to handle the solvent and to ensure worker safety measure because hexane is a highly volatile solvent. Hexane is classified as a hazardous air pollutant by the US Environmental Protection Agency and they thus consider vegetable oil extraction plants to represent a potential major source. It is estimated that 0.7 kg of hexane per ton of seed is released into the environment (United State Environment Protection

Agency, 2005). Exposure to hexane at 125ppm for 3 months causes peripheral nerve damage, muscle wasting, and atrophy (Agilent Technology, MSDS, Agilent Technology, 2008). For this reason, alternative solvent extraction methods are needed that eliminate the use of toxic compounds such as hexane (Tyson et al., 2004) Thus, market demand for the Green solvents is getting high. Extraction is the important step to obtain the valuable volatile oil. As per changing technologies the extraction techniques were also changed and modified to extract essential oils. These changes were led by the advancements in the scientific era. However, various problems are encountered during extraction of thyme essential oil which have direct impact on the quality and yield. Economic & environmental aspects are also affected. These problems seem to overshadow the genuine health benefits. Potential use of different green solvents , namely methanol, can be made for extraction of essential oils for environment related issues .These solvents are generally recognized as safe (GRAS) and approved by U.S. Food and Drug Administration as pharmaceutical and food additive.

High pressures increase rate of extraction and yield but significant amount of waxes are co-extracted and essential oil content is reduced .On the other hand, low pressures reduce boiling points of solvents facilitating faster extraction rates at lower temperatures. Rotary Vacuum evaporator has been used to extract the thyme oil as it yields superior quality essential oil and higher yields due to zero loss to surroundings or Vacuum.

The Response Surface Methodology (RSM) is important in designing, formulating, developing, and analyzing new scientific studying and products. It is also efficient in the improvement of existing studies and products. The most common applications of *RSM* are in Industrial, Biological and Clinical Science, Social Science, Food Science, and Physical and Engineering Sciences. It is a collection of mathematical and statistical techniques useful for the modelling and analysis of problems in which a response of interest is influenced by several variables and the objective is to optimize this response (Montgomery 2005). For example, the content of essential oil of a herb is affected by a certain amount of temperature x1 and time x2. The essential oil can be extracted under any combination of treatment x1 and x2. Therefore, temperature and time can vary continuously. When treatments are from a continuous range of values, then a Response Surface Methodology is useful for developing, improving, and optimizing the response variable. In this case, the content of essential oil *y* is the response variable, and it is a function of temperature and time. It can be expressed as

$$y = f(x1, x2) + e$$

The variables x1 and x2 are independent variables where the response *y* depends on them. The dependent variable *y* is a function of x1, x2, and the experimental error term, denoted as *e*. The error term e represents any measurement error on the response, as well as other type of variations not counted in *f*. It is a statistical error that is assumed to distribute normally with zero mean and variance s. (Nuran Bradley., 2007). NMR is the most powerful analytical tool available currently. NMR allows characterization of a very small amount of sample (10mg), and does not destroy the sample (non-destructive technique). NMR spectra can provide vast information about a molecule's structure and is the only way to prove which compound is being analysed. NMR is used in conjunction with other types of spectroscopy and chemical analysis to fully confirm a complicated molecule's structure. A simple NMR spectrum plots absorption on the y axis, and magnetic field strength on the x axis (Scale is in parts per million, and usually goes from 0- 10 ppm). The different positions of NMR absorptions are described as chemical shifts (δ).A chemical shift is defined as the difference in parts per million (ppm) between the resonance frequency of the observed proton and that of the tetramethylsilane (TMS) hydrogens. TMS is the most common reference compound in NMR, it is set at δ=0ppm.

Recently, the World Health Organization has urged a reduction on salt consumption in order to reduce the incidence of cardiovascular diseases. By reducing the salt levels on processed foods, it is necessary to use other additives that ensure the preservation of food, hence, is generated a research field in safe foods development that contains natural ingredients displaying no detrimental effect on health. The use of essential oils as antibacterial additives ,antioxidant, antifungal which are aromatic compounds obtained from vegetal material (flowers, shoots, seeds, leaves, twigs, bark, grasses, wood, fruits or roots) makes it possible. Thyme oil shows almost all these effects in food, thus making it

possible to keep food "Safe, Natural & Healthy". (Deans Sg Et Al., 1993).

Hence considering all the potential benefits, following objectives were taken up for this study

1). To extract thyme oil from *Thymus vulgaris*.

2) To optimize time and temperature by using response surface methodology (RSM).

3) To evaluate the quality of extracted thyme oil.

Materials and Methods

Rotary Vacuum Evaporator (RVE)

A laboratory Rotary Vacuum Evaporator (BUCHI TYPE) in the department of Food Process Engineering Lab, Vaugh School of Agricultural Engineering and Technology, SHIATS, Allahabad, was used for extraction of thyme oil. A picture of the Rotary Vacuum Evaporator is shown in Fig 2.1 It is used in chemical laboratories for the efficient and gentle removal of solvents from samples by evaporation. Rotary Vacuum evaporators function because lowering the pressure above a bulk liquid lowers the boiling points of the component liquids in it. It consists of two round bottomed flasks, condenser, heating water bath, bump traps and metal clips. The solvent collection flask is emptied prior to use to prevent mixing of chemicals. The flask with the solution is placed on rotary evaporator and bump traps are used to prevent splashing of solution into condenser. Metal clips are used to secure the flask and the bump trap. The dial on the motor is used to control speed of flask rotation (0-220 rpm). The Vacuum ON/OFF control is managed by turning a stop cock at top of condenser.The flask is lowered into the water bath by using a handle . The solvent starts collecting on the condenser and drip into the receiving flask. The temperature of heating bath is controlled by an adjustable dial indicating temperatures. Liquid solvents can be removed without excessive heating of sensitive solvent solute combinations. Rotary evaporation is most often and conveniently applied to separate "low boiling" solvents such a n –hexane, methanol or ethyl acetate from compounds which are solid at room temperature and pressure. It also allows removal of a solvent from a sample containing a liquid compound if there is minimal co evaporation (azeotropic behavior), and a sufficient difference in boiling points at the chosen temperature and reduced pressure. A oil sealed rotary vane type high Vacuum pump(Discharge : 50 l/min) was was used to create the Vacuum in the system The pump consists of rotor, with two spring loaded vanes mounted eccentrically in the stator body, which rotates inside a statinary casing. The level of Vacuum created is indicated by a Vacuum gauge. A control panel is provided with ON/OFF switch mains.

Figure 2.1: Rotary Vacuum Evaporator

Experiments

Sample collection

The dried leaves of *Thymus vulgaris* were purchased from ` ` Cortus India Private limited", New Delhi. The dried thyme leaves were in hygienic condition and were not affected by any damage and spoilage.

Experimental design

Response Surface Methodology (RSM) was used for designing the experiments (Khuri and Cornell, 1987). RSM used in this study was a central composite face-centered design involving two different factors : Temperature and Time . The extraction of essential oil from *Thymus vulgaris* was accessed based on the face-centered experimental plan as shown in table 2.2.2The results were analyzed using Analysis Of Variance (ANOVA) given in results table 3.2(b)by design expert 8 software. Three-Dimensional plots & their respective contour plots were obtained based on the effect of the levels of two factors on the Response 1(Yield) were studied. The optimum region was also identified based on the main parameters in overlay plot. The experiment was repeated randomly and each result was compared with predicted values to determine the model adequacy.

Table 2.2.2. Effect of Temperature and Time on oil Yield

Standard	Run	Factor 1 Temperature (˚C)	Factor 2 Time (h)	Response 1 Yield R1(ml)
7	1	37.5	2	10
4	2	45	3	20
13	3	37.5	2.5	13.5
10	4	37.5	2.5	13.5
5	5	30	2.5	8.5
12	6	37.5	2.5	13.5
11	7	37.5	2.5	13.5
1	8	30	2	7
3	9	30	3	9
8	10	37.5	3	14
6	11	45	2.5	18
2	12	45	2	16
9	13	37.5	2.5	13.5

Preparation of thyme extract

Thyme plant extracts were obtained by Rotary Vacuum Evaporator (RVE) The dried thyme leaves (40g) were extracted with methanol solvent (400 ml) at 29˚C by dipping the leaves in methanol for two days. Dipping was followed by maceration in mortar and pestle for about an hour. The whole mixture was then transferred to rotary Vacuum evaporator flask at different time temperatures using RSM software generated runs. Vacuum was created in Rotary evaporator by running Vacuum pump after certain time intervals for efficient oil extraction at lower temperatures. Oil containing traces of solvent were collected in the separate round bottom flask attached to rotary Vacuum evaporator. Methanol was evaporated by subjecting the oil-solvent mix to heat in water bath at 70˚C for about an hour . thyme oil was thus extracted on the principle of difference in boiling points of solvent and oil. The obtained extracts were kept in the dark at 4˚C until they were used.

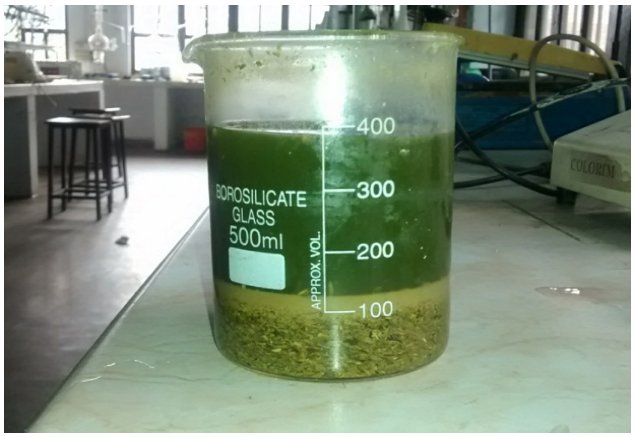

(a)

b)

Figure 2.2: (a) Macerated methanol Thyme extracts (b) Thyme oil

Analysis of moisture content

Initial moisture contents of the thyme leaves were determined by the hot air oven method. It was worked out by weighing 5g sample accurately and subjected to oven drying at 110°C for 4 -6h. Oven dried samples were cooled in desiccators and weighed. The drying was repeated until the constant weights were obtained .The resultant loss in weight was calculated as % moisture content (A.O.A.C 1990).

$$\frac{\text{Difference in dry weight}}{\text{Weight of sample}} \times 100 \qquad [1]$$

Analysis of Crude fat

Sample (5g) was weighed accurately in thimble and defatted with n-hexane in soxhlet apparatus for apparatus for 2 h. The resultant ether extract was evaporated and crude fat content was calculated as per A.OA.C, 1990 method.

Crude fat%=

$$\frac{\text{(Weight of flask+oil)} - \text{Weight of Flask}}{\text{Weight of sample}} \times 100 \quad \text{..... [2]}$$

Total Ash

Total ash was determined according to A.O.A.C (1990). Sample (5g) was weighed into a crucible and ignited at low flame till all the material was completely become smokeless. Then it was kept in muffle furnace for 6h at 600°C and further cooled in desiccators and weighed. This was repeated till 2 consecutive weights were constant and percentage ash was calculated.

Ash%= $$\frac{\text{Weight of ash}}{\text{Weight of sample}} \times 100$$ ..... [3]

Statistical Analysis

ANOVA

The analysis of variance of the data obtained was done completely Randomized Design (CRD) for different treatments as per the methods given by (Panse and Sukhatme., 1967) for values of Ash Moisture and Crude fat content. The experiment was conducted by adopting completely randomized Fisher in 1923 gives an appropriate method capable of analyzing the variation of population variance. The significant affect of treatment was judged with the help of 'F' (variance ratio). Calculated F value was compared with the table value of F at 5% level of significance. If calculated value exceeded the table value the effect was considered to the significant. The significance of the study was tested 5% level.

t = $\sqrt{(n-2)} / \sqrt{(1-1/2^2)}$

S.Ed. = MESS / r × t ×s

C. D = S.Ed × t 5 % at e. d. f.

Where,

t = distribution of observation

r = co-efficient of correlation

n = no. of observation

S.Ed. = standard error of difference

e.d.f = error of degree of freedom

C.D = critical difference

MESS = error mean sum of square

Response Surface Methodology (RSM)

RSM was used for designing the experiments (Khuri and Cornell, 1987) .RSM used in this study was a central composite face-centered design involving two different factors: Temperature and Time. The extraction of essential oil from *Thymus vulgaris* was accessed based on the face-centered experimental plan as shown in table -----.The results were analyzed using Analysis Of Variance (ANOVA) given in table ---- by design expert 8 software. Three-Dimensional plots & their respective contour plots were obtained based on the effect of the levels of two factors on the Response 1 (Yield) were studied. The optimum region was also identified based on the main parameters in overlay plot. The experiment was repeated randomly and each result was compared with predicted values to determine the model adequacy.

Nuclear Magnetic Resonance (NMR) Spectroscopy

H NMR spectroscopy for structural analysis of modified methanol extracted thyme oil was carried out on a Bruker 500 MHz spectrophotometer using $CDCl_3$ as solvent. ^{1}HNMR spectra of solution CDCl3 was calibrated to tetramethylsilane (TMS) as international standard.

Results and Discussions

Proximate composition of Thyme leaves

Proximate composition generally represents the nutritional quality of product. It is necessary to observe the proximate composition of dried leaves so as to judge the effect on final product after utilization as an ingredient. The proximate composition of Thyme leaves was determined using ANOVA (analysis of variance) and presented in the following table 3.1.

Table 3.1 Proximate composition of thyme leaves

Sample	Ash	Fat	Moisture
T1	2.40	15.33	9.07
T2	2.32	15.30	9.45
T3	2.30	15.35	9.48
T4	2.30	15.30	9.49
Mean	**2.33**	**15.32**	**9.3725**
F- test	S	S	S
S. Ed. (±)	0.006	0.008	0.010
C. D. (P = 0.05)	0.013	0.017	0.022

The data represented in the above table describes composition of major constituents of Thyme. The Average moisture content of thyme leaves was found to be 9.37 $\pm$ 0.010.. The mean value of crude fat and ash of dried Thyme leaves was observed to be 15.32 $\pm$ 0.006 and 2.33$\pm$0.006 respectively. Fig 3.1.1 shows the differences in proximate composition of four sample (T1, T2, T3 and T4) determinations undertaken for analysis.

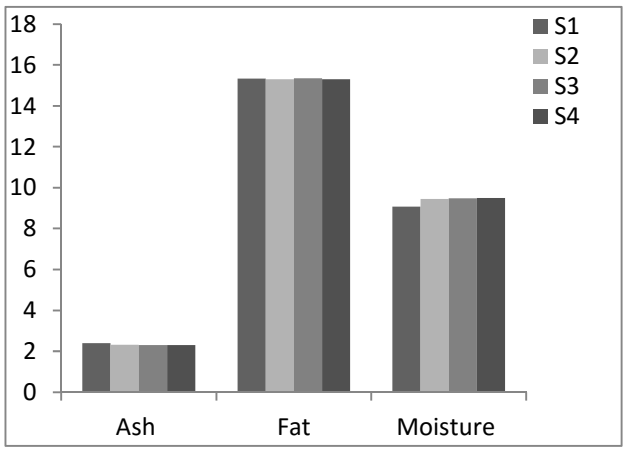

Figure 3.1.1: Differences in proximate compositions of four samples

Analysis of Thyme oil extracted at different intervals of time and temperature using Response Surface Methodology (RSM)

Response surface Model was developed to represent the data and to find the optimal conditions of parameter values in extracted oil. The solvent extracted oil at different experimental conditions given in table 2.2.2 above. The extracted oil ranged from 7 ml to 20 ml. The maximum value was at experimental conditions of 45^{0}C for 3 h. whereas the minimum value was at 30^{0}C for 2h. The extraction Process was based on the difference in boiling points of solvent and oil. The data on extracted oil under different experimental were analyzed using ANOVA. The model was tested for their adequacies to describe response surface with following results in table 3.2(a) and 3.2(b) with the final equations in terms of coded and actual factors.

Table 3.2(a) ANOVA Results of Response Function

Std. Dev.	**0.46**	**R-Squared**	**0.9910**
Mean	13.08	Adj R-Squared	0.9846
C.V. %	3.53	Pred R-Squared	0.9304
PRESS	11.59	Adeq Precision	41.948

Table 3.2(b) ANOVA Results of Response Function

SOURCE	Sum of Squares	df	Mean Square	F Value	p-value Prob >F
Model	164.93	5	32.99	154.53	<0.0001
A-Temp	145.04	1	145.04	679.46	<0.0001
B-Time	16.67	1	16.67	78.08	<0.0001
AB	1	1	1.00	4.68	<0.0001
A2	0.35	1	0.35	1.62	0.0672
B2	2.22	1	2.22	10.40	0.2442
Residual	1.49	7	0.21		0.0146
Lack of Fit	1.49	3	0.5		
Pure Error	0	4	0.00		
Cor Total	166.42	12			

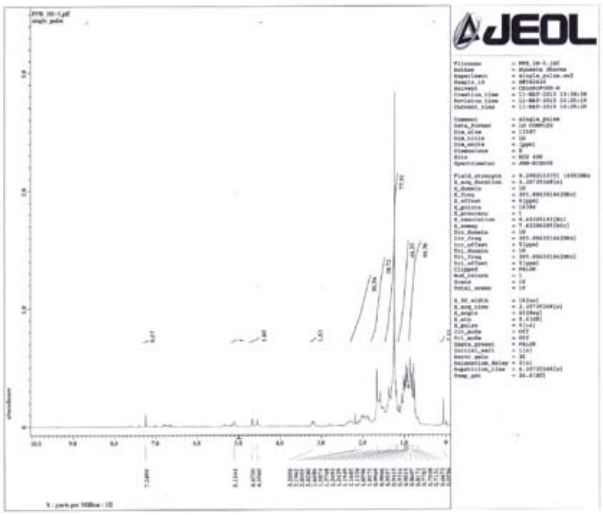

Figure 3.2.1(a) Response Surfaces Plot showing the effect of temperature and time on the extraction of thyme oil

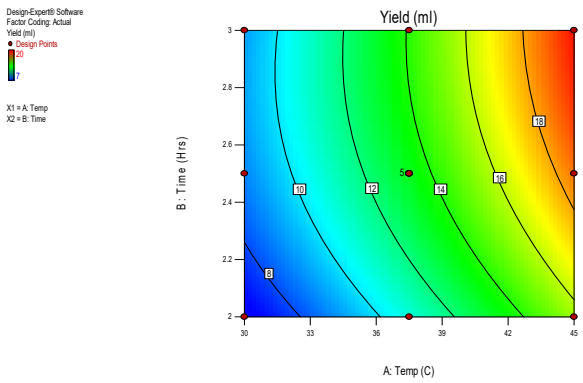

Figure 3.2.1(b) Contour Plot showing the effect of temperature and time on the extraction of thyme oil

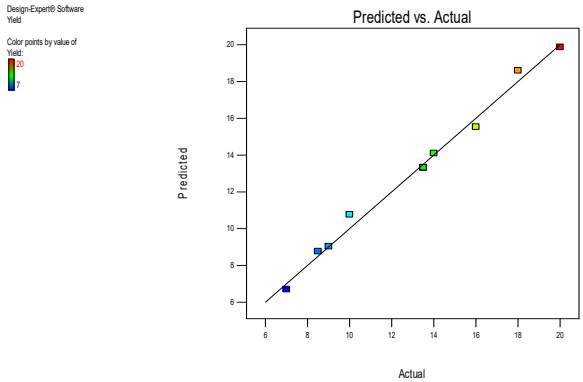

Figure 3.2.1 (C) Graph showing prediction and actual values

Nuclear Magnetic Resonance (NMR) spectroscopy

HNMR of modified methanol extracted thyme oil showed good agreement with reported results of thyme oil as shown in Fig 3.3. The spectrum were recorded (CDC13, 500MHz) had δ (ppm) 1.50 (d, 6H, $2\times CH_3$), 2.19(s, 3H, CH_3) 3.20 [sept, 1H, CH $(CH_3)_2$], 4.5 (br, 1H, OH), 6.63 (s, 1H, aromatic, H-6), 6.75 (d, 1H, aromatic). Based upon results and comparison of the spectra with the corresponding standard spectra of thymol (reported) the hexane extracted compound was identified as thymol, 2-isopropyl-5-methylphenol.

Conclusions

Based on the experimental results reported herein, the followings conclusions were made:

1. Sincere efforts were made to explore the potential of thyme oil in food products The Mean nutritional composition of dried thyme leaves showed that dried thyme leaves contain Moisture 9.37%, Ash 2.33% and Crude Fat 15.32%.
2. Experiments were conducted to optimize the process parameter for extraction of thyme oil by modified rotary Vacuum evaporator technique using methanol as solvent optimized by Response surface methodology (RSM).
3. The extracted oil content values ranged from 7ml to 20 ml. The maximum value was at experimental conditions of 3h at 45^0C temperature. The minimum value was found at 2h at 30^0C. The removal of oil in case of solvent extraction process was based on principle difference in boiling points of solvent and oil. It was observed that the yield of essential oil incremented with increase in temperature and yield may decrease with increase in pressure.
4. In the present investigation attempts were made to study the effect of grinding of methanol soaked dried leaves in mortar and pestle. Grinding helped to reduce the size of leaves and increase the surface area that contributes to oil diffusion during extraction .Grinding once was sufficient to obtain a suitable particle size and hence maximum oil yield in thyme oil extraction.
5. It was concluded that Thyme oil contains Thymol (2-isopropyl-5-methyl phenol) as the main monoterpene phenol with antifungal, antibacterial and antioxidant properties as reported in ^{1}H NMR spectroscopy .^{1}HNMR of methanol extracted thyme oil showed good agreement with reported results of hexane extracted thyme oil. The spectrum were recorded(CDC13,500MHz)hadδ(ppm)1.50(d,6H,2×CH

$_3$),2.19(s,3H,CH_3)3.20[sept,1H,$CH(CH_3)_2$],4.5(br,1H,OH), 6.63(s,1H,aromatic,H-6),6.75 (d,1H,aromatic).

Acknowledgements

The authors would like to acknowledge the Department of Food Process Engineering, Vaugh School of Agricultural Engineering and Technology, SHIATS, for supporting this Project.

References

[1] Jordan, M.J., Maria, V.L., Rota, C., Loran, S., Sotomayor, J.A., 2013. Effect of bioclimatic area on the essential oil composition and antibacterial activity of Rosmarinus officinalis L. Food Control 30, 463–468.

[2] Chizzola, R., Michitsch, H., Franz, C., 2008. Antioxidative properties of Thymus vulgaris leaves: comparison of different extracts and essential oil chemotypes. J.Agric. Food Chem. 56, 6897–6904.

[3] Bousbia, N., Vian, M.A., Ferhat, M.A., Petitcolas, E., Meklati, B.Y., Chemat, F., 2009. Comparison of two isolation methods for essential oil from rosemary leaves: hydrodistillation and microwave hydrodiffusion and gravity. Food Chem. 114, 355–362.

[4] Bakkali, F., Averbeck, S., Averbeck, D., Idaomar, M., 2008. Biological effects of essential oils – a review. Food Chem. Toxicol. 46, 446–475.

[5] Bounatirou, S., Smiti, S., Miguel, M.G., Faleiro, L., Rejeb, M.N., Neffati, M., Costa, M.M., Figueiredo, A.C., Barroso, J.G., Pedro, L.G., 2007. Chemical composition, antioxidant and antibacterial activities of the essential oils isolated from Tunisian Thymus capitatus Hoff. et Link. Food Chem. 105, 146–155.

[6] Kisko, G., Roller, S., 2005. Carvacrol and p-cymene inactivate Escherichia coli O157:H7 in apple juice. BMC Microbiol. 5, 36, http://dx.doi.org/10.1186/1471-2180-5-36.

[7] Fadli, M., Saad, A., Sayadi, S., Chevalier, J., Mezrioui, N.-E., Pages, J.-M., Hassani, L., 2012. Antibacterial activity of Thymus maroccanus and Thymus broussonetii essential oils against nosocomial infection – bacteria and their synergistic potential with antibiotics. Phytomedicine 19, 464–471.

[8] Burt, S., 2004. Essential oils: their antibacterial properties and potential applications in foods—a review. Int. J. Food Microbiol. 94, 223–253.

[9] Deans, S.G. and G. Ritchie, 1987. Antibacterial properties of plant essential oils. Int. J. Food Microbiol., 5: 165–180

[10] Douglas, M. H., & McGimpsey, J. A. (1994). Seasonal variation in essential oil yield and composition from naturalized Thymus vulgaris L.

[11]Dorman H. J. D., Deans S. G. (2000) Antimicrobial agents from plants: antibacterial activity of plant volatile oils. J. Appl. Microbiol. 88, 308–316 10.1046/j.1365-2672.2000.00969.

[12] FDA, Department of health and human services, title 26,vol 6,parts 500-599.

[13] Govaris A., Botsoglou E., Sergelidis D., Chatzopoulou P. S. (2011) Antibacterial activity of oregano and thyme essential oils against Listeria monocytogenes and Escherichia coli O157, H7 in feta cheese packaged under modified atmosphere. Food Sci. Technol. 44, 1240–1244.

[14] Grieve and Mrs. Maud. (2008) Thyme .A Modern Herbal © copyright protected 1995-2014 Botanical.com.

[15] Ivan Angelov, David Villanueva Bermejo, Roumiana P. Stateva, Guillermo Reglero, Elena Ibanez and Tiziana Fornari (2013) Extraction of thymol from different varieties of thyme plants using green solvents. Journal of Engineering Science and Technology EURECA 2013 Special Issue August (2014) 79 – 88 © School of Engineering, Taylor's University 79

[16] Kuok Loong NG, Puteri Farah Wahida, Chien Hwa Chong(2014) Optimisation of extraction of thymol from plectranthus amboinicus leaves using response surface methodology .Journal of Engineering Science and Technology EURECA 2013 Special Issue August (2014) 79 – 88 © School of Engineering, Taylor's University.

[17] Nuran Bradley (2007) The response surface methodology . Indiana university south bend.

[18] Ashnagar, A, Gharib Naseri, N and Ramazani, Characterization of the major chemical compounds found in Thymus vulgaris plant grown wildly in Chahar Mahal and Bakhtiari province of Iran .International Journal of PharmTech Research CODEN (USA): IJPRIF ISSN : 0974-4304Vol. 3, No.1, pp 01-04, Jan-Mar 2011.

[19] Khuri A.I., Cornell J.A. (1987), Response Surfaces. Marcel Dekker, New York.

[20] PANSE, V.G. AND SUKHATME, P.V (1967),.Statistical Methods for Agricultural Workers. Indian Council of Agricultural Research, New Delhi.

[21] Montgomery Douglas C (2005). Design and Analysis of Experiments Response Surface Method and Designs (New Jersey, John Wiley and Sons, Inc).

[22] Hagenmaier, R.D (1974). Aqueous processing of full-fat sunflower seeds: yields of oil and protein. J. Am. Oil Chem. Soc. 51, 470–471.

[23] Kim, S.H. (1989). Aqueous extraction of oil from palm kernel. J. Food Sci, 54, 491-492.

Author's details

[1]Student, Department of Food Process Engineering, Sam Higginbottom Institute of Agricultural Sciences and Technology, UP, India, nadiyamalik21@gmail.com

[2]Assistant Professor, Department of Food Process Engineering, Sam Higginbottom Institute of Agricultural Sciences and Technology, UP, India, kailashnature@gmail.com

[3]Student, Department of Food Process Engineering, Sam Higginbottom Institute of Agricultural Sciences and Technology, UP, India, anuragver123@gmail.com.

Copy for Cite this Article- Nadiya Rashid Malik, K. C. Yadav, Anurag Verma, "Optimization Of Process Parameters In Extraction Of Thyme Oil Using Response Surface Methodology (RSM)', *International Journal of Science, Engineering and Technology,* Volume 4 Issue 1: 2016, pp. 248- 256.

Om Prakash Gupta et al. 2016, Volume 4 Issue 1
ISSN (Online): 2348-4098
ISSN (Print): 2395-4752

International Journal of Science, Engineering and Technology
An Open Access Journal

Robust Facial Landmark Detection Using a Mixture of Synthetic and Real Images with Dynamic Weighting: A Survey

[1]Om Prakash Gupta, [2]Kanak Kumar

Abstract

We propose the use of a 3D morphable face model to generate synthesized faces for regression-based detector training. Benefiting from the large synthetic training data, the learned detector is shown to exhibit a better capability to detect the landmarks of a face with pose variations. Furthermore, the synthesized training data set provides accurate and consistent landmarks automatically as compared to the landmarks annotated manually, especially for occluded facial parts. The synthetic data and real data are from different domains; hence the detector trained using only synthesized faces does not generalize well to real faces.

Keywords: Facial landmark detection, 3D morphable model, cascaded collaborative regression, dynamic multi-scale local feature extraction.

Introduction

After detecting faces in an image captured by a camera, each face is rotated, scaled, and cropped so that the image of the face has a predetermined size. This process is called a face alignment and it is well known that the result of face alignment has a large impact on face recognition performance. Face alignment usually operates based on the coordinates of the two eyes, and thus several studies have been performed on eye detection for face recognition. FACIAL landmark detection (FLD), or localization, is an essential preprocessing step in any automatic face analysis system. According to the image type, FLD algorithms can be categorized as either 2D or 3D-based methods. Typically, a 2D FLD algorithm is applied to the content of a face bounding box output by a face detector, and attempts to locate the positions of a set of pre-defined landmarks (key points), *e.g.* eyebrows, eye centres, nose tip or mouth corners, in a 2D facial image. In contrast, a 3D FLD algorithm performs the task on 3D face data, such as 3D face meshes or range images that are usually in the form of point clouds. The detected 2D facial landmarks can be used either as geometric features directly, or to extract meaningful local or global face texture features for subsequent face analysis procedures. One common step is to perform face normalization based on the detected landmarks prior to the feature extraction procedure. Another popular technique is to directly extract local features from the neighbor hoods around all landmarks. There are two main types of algorithms, either based on generative or discriminative models, for FLD. The most well-known generative models are Active Shape Models (ASM) and Active Appearance Models (AAM); those have been successfully and widely used for face modelling and landmark detection during the past 20 years, especially in controlled scenarios. However, robust and accurate FLD in uncontrolled scenarios is very challenging. ASM and AAM often fail to accurately estimate the landmarks for 'faces in the wild', in the presence of pose, expression, illumination, and occlusion.

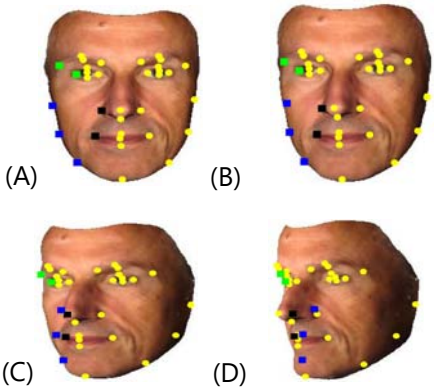

[1] Corr. Author's Email: omprakashgupta88@gmail.com

Figure 1: Self-occluded facial landmarks (square points) of the same identity rendered from its 3D face scan, with yaw rotations 0°, 10°, 30° and 50°.

Proposed Methodology

FACIAL landmark detection methods can be divided into two main categories:

(I) Generative model
(II) Discriminative model

A generative model generates different face instances by adjusting the model parameters, and matches these generated instances to an input image to optimize the model parameters. Typical generative models are ASM, AAM and their extensions. A common characteristic of ASM and AAM is a parametric PCA-based shape model that is constrained by the corresponding Eigen-values when fitting the models to an input image.

A discriminative model builds a mapping function that predicts the shape or model parameter updates using the features extracted from an image. In fact, the first discriminative method was adopted in the original AAM. It used a linear regression model to build a mapping function between the texture residuals and the parameter update of a combined appearance model. The combined appearance model explicitly represents a face including its shape and appearance. It accomplishes the tasks of FLD and face texture reconstruction in a unified framework.

We want to implement with a standard linear regression-based CR algorithm in this experiment, with two different HOG features, and compared it with a standard generative view-based AAM and human annotated results. To obtain the human annotated results, we randomly selected test images and manually annotated them. Firstly, all the automatic detected results exceed the human performance in accuracy, including the view-based AAM.

Secondly, we measured the contribution of the number of feature scales *C* to the system. The main reason is twofold:

1) The local features extracted from a small window size provide less information for a discriminative FLD learning;
2) The information of the local features extracted from different scales is somewhat redundant.

3D face reconstruction from a single 2D facial image is a very challenging task. Hence the correlation of shape is very low even when we use the ground truth 2D landmarks for 3DMM initialization. Similarly to the landmark detection accuracy shown above, the 3D face reconstruction accuracy initialized by the dynamic multi-scale F-HOG CR is superior to all the others, especially to the manually annotated 2D facial landmarks. The main reason is that the trained CR-based model estimates the landmarks of the self-occluded face parts better. In contrast, it is very hard to estimate the landmarks of the occluded facial parts manually.

Cascaded Collaborative Regression (CCR)

In our proposed CCR, the synthesized training dataset dominates the training of the first few weak regressors, whereas the real face dataset dominates the last few weak regressors. Benefiting from the large synthesized training dataset, the first few weak regressors in CCR are capable of overcoming the difficulty caused by pose variation. The last few weak regressors mainly trained on a relatively small number of real faces refine the rough shape estimates output by the first few elements, to create a more versatile model.

Experiments on BioID, HELEN, LFPW and COFW

To validate the superiority of the proposed CCR algorithm, we compared it with a set of state-of-the-art algorithms on the BioID, LFPW, HELEN and COFW datasets.

The BioID face dataset has 1521 near-frontal faces with slight pose and expression variations, collected under a lab environment. The dataset was firstly used for face detection and recently for facial landmark detection. Each BioID face has 20 manually annotated landmarks and 17 of them are usually used to test a FLD algorithm.

The HELEN face dataset is a high resolution dataset consisting of 2000 training and 330 test images. Each image in HELEN has 194 annotated landmarks.

LFPW is a standard FLD benchmark that has 1100 training images and 300 test images collected from the Internet. Each LFPW face has 29 manually annotated landmarks. However, LFPW provides only hyperlinks to the original web images.

COFW is an expanded version of LFPW. The COFW dataset contains 1345 training images and 507 test images in the wild with a variety of pose, expression, illumination and occlusion variations.

Expected Outcomes

To obtain dynamic multi-scale local features, we denote the window size of the *c*th scale of the *m*th sub-regressor in the cascade as *S(m,c)(m* = 1, · · · , *M*; *c* = 1, · · · ,*C)*, where *C* is the number of scales for local feature extraction and *M* is the number of sub-regressors. We set

$S_{(m,c)} = \{(1+(1/m))S_{face}\}/(c+1)$

where *m*= reduces the window size as the order of the subregressor grows,

c= generates different scales for each sub-regressor,

and S_{face}= size of the face.

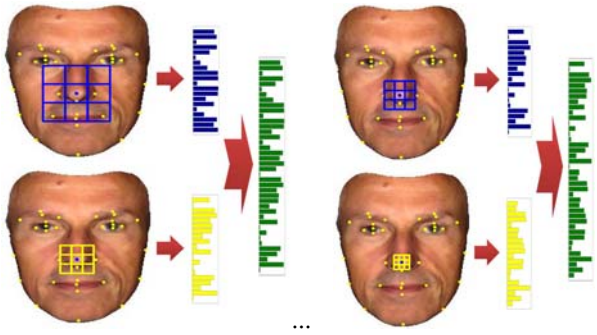

(A) (B)

Figure 2: A schematic overview of the proposed dynamic multi-scale local feature extraction approach

Conclusion

We have presented a supervised cascaded collaborative regression (CCR) algorithm that exploits synthesized faces for robust FLD in 2D. The use of synthesized faces generated from a 3DMM greatly improves the generalization capability of the trained facial landmark detector. A major advantage of using synthesized faces is that they do not need to be manually annotated. Furthermore, the 2D landmarks of the synthesized faces by direct projection from 3D to 2D are accurate, especially for the self-occluded facial parts with large pitch and yaw rotations. To extract more informative local features, we designed a dynamic multiscale local feature extraction scheme, which further improved the accuracy of the learned regressor.

References

[1] Z.-H. Feng, P. Huber, J. Kittler, W. Christmas, and X.-J. Wu, "Random cascaded-regression copse for robust facial landmark detection," IEEE Signal Process. Lett., vol. 22, no. 1, pp. 76–80, Jan. 2015.

[2] Z. Zhang, P. Luo, C. C. Loy, and X. Tang, "Facial landmark detection by deep multi-task learning," in Proc. 13th Eur. Conf. Comput. Vis., 2014, pp. 94–108.

[3] D. Chen, X. Cao, F. Wen, and J. Sun, "Blessing of dimensionality: High-dimensional feature and its efficient compression for face verification," in Proc. IEEE Conf. Comput. Vis. Pattern Recognit., Jun. 2013,pp. 3025–3032.

[4] L. El Shafey, C. McCool, R. Wallace, and S. Marcel, "A scalable formulation of probabilistic linear discriminant analysis: Applied to face recognition," IEEE Trans. Pattern Anal. Mach. Intell., vol. 35, no. 7, pp. 1788–1794, Jul. 2013.

[5] H.-S. Lee and D. Kim, "Tensor-based AAM with continuous variation estimation: Application to variation-robust face recognition," IEEE Trans. Pattern Anal. Mach. Intell., vol. 31, no. 6, pp. 1102–1116, Jun. 2009

[6] X. Cao, Y. Wei, F. Wen, and J. Sun, "Face alignment by explicit shape regression," in Proc. IEEE Conf. Comput. Vis. Pattern Recognit., Jun. 2012, pp. 2887–2894.

[7] B. Pepik, M. Stark, P. Gehler, and B. Schiele, "Teaching 3D geometry to deformable part models," in Proc. IEEE Conf. Comput. Vis. Pattern Recognit., Jun. 2012, pp. 3362–3369.

[8]. Choi and D. Kim, "Eye correction using correlation information," in Proc. Asian Conf. Comput. Vis, 2007, pp. 698–707.

[9] Zhen-Hua Feng; Guosheng Hu; Kittler, J.; Christmas, W.; Xiao-Jun Wu, "Cascaded Collaborative Regression for Robust Facial Landmark Detection Trained Using a Mixture of Synthetic and Real Images With Dynamic Weighting," in Image Processing, IEEE Transactions on , vol.24, no.11, pp.3425-3440, Nov. 2015

doi: 10.1109/TIP.2015.2446944

Author's details

[1]M. Tech Scholar, Department of EC, MIT, Bhopal, INDIA
Email: Email: omprakashgupta88@gmail.com

[2]Assistant Professor, Department of EC, MIT, Bhopal, INDIA

Copy for Cite this Article- Om Prakash Gupta, Kanak Kumar, "Robust Facial Landmark Detection Using a Mixture of Synthetic and Real Images with Dynamic Weighting: A survey', *International Journal of Science, Engineering and Technology,* Volume 4 Issue 1: 2016, pp. 257- 259.

Thouseef Ahamad et al. 2016, Volume 4 Issue 1
ISSN (Online): 2348-4098
ISSN (Print): 2395-4752

International Journal of Science, Engineering and Technology
An Open Access Journal

Comparative Study of Bio-Ethanol Production from Kokum and Butter Fruit Waste Samples by Employing Microbial Fermentation Technology

[1]Thouseef Ahamad, M. Y., [2]G. Panduranga Murthy

Abstract

In the present study, Kokum and Butter fruit samples were used as a raw material for the production of bio-ethanol using microbial fermentation technology. The microbial strain, *Saccharomyces cerevisiae* in flocculated conditions was used. The sugar content before and after fermentation was analyzed by standard method, the result showed that the sugar content was more before fermentation (*Garcinia indica* 21mg/mL and *Persea americana* 17 mg/mL,) when compared to after fermentation (*Garcinia indica* 16mg/mL and *Persea americana* 11mg/mL). The production of ethanol was higher in *Garcinia indica* (13%) than the *Persea americana* (10%) which was calculated by distillation method. the result were compared. The rate of ethanol production through fermentation of grape fruit waste by *Saccharomyces cerevisiae* yields is very at pH 5.4, temperature 30°C, specific gravity 0.872,concentration of about 6.21% than other fruit samples. The obtained results of this study suggest that, samples of both fruits that contain significant amount of fermentable sugar and can be converted to bio-ethanol that can serve as an alternative energy source. The GC analysis showed that, the fruit samples evaluated for the yield of ethanol, sample-00 (*Garcinia indica* fruit juice) gave 100% purity of ethanol as compared to standard.

Keywords: Bio-fuel, Fruit cultivars, Kokum fruit, Butter fruit, Yeast, Fermentation, Bio-ethanol.

Introduction

The natural energy resources such as fossil fuel petroleum and coal are being utilized at a rapid rate and these resources have been estimated to last only a few years. Therefore, alternative energy sources such as ethanol, methane and hydrogen are being considered. Some biological processes have rendered possible routes for producing ethanol and methane in large quantities. A worldwide interest in the utilization of bioethanol as an energy source has stimulated studies on the cost and efficiency of industrial processes for ethanol production (Tanaka, 2006).

Anthropogenic activities generate large amounts of waste such as crop residues, solid waste from mines and municipal waste. They may become a nuisance and sources of pollution. It is therefore important to handle them judiciously to avoid health problems at one side; on the other side, agricultural wastes, including wood, herbaceous plants, crops and forest residues, as well as animal wastes are potentially huge source of energy. Apart from all these sources, the diversity of non-edible fruits in India, is available at large quantities at different biodiversity locations. Of these fruit sources, the Kokum (*Garcinia indica***)** and Butter fruits (*Persea americana*) commonly called, Avocados are produced in large scale annually and are vastly underutilized. The Fruit samples are excellent sources of cellulose which can be used for the production of ethanol via saccharification followed by fermentation (Fatma and Fadel, 2010 and Suhas *et. al***,** 2013).

Garcinia indica, a plant in the mangosteen family (Clusiaceae), commonly known as kokum, is a fruit-bearing tree that has culinary, pharmaceutical, and industrial uses. The genus Garcinia, belonging to the family Clusiaceae, includes about 200 species found in the Old World tropics, mostly in Asia and Africa. *Garcinia indica* is indigenous to the Western Ghats

[1]Corresponding Author's Email: thouseef.com@gmail.com

region of India located along the western coast of the country. *Garcinia indica* is found in forest lands, riversides and wastelands. These plants prefer evergreen forests, but sometimes they also thrive in areas with relatively low rainfall. It is also cultivated on a small scale. It does not require irrigation, spraying of pesticides or fertilizers.

Kokum squash or kokum concentrate is used in preparing a drink (sherbet) which is bright red in colour. The seed of *Garcinia indica* contains 23–26% oil, which remains solid at room temperature.

Butter fruit in Kannada is "beṇṇe haṇṇu." The Avocado or *Persea americana* is a tree native to Mexico and Central America, classified in the flowering plant family Lauraceae. Avocados are referred to as "butter fruit" in several parts of India due to the butter-like consistency of its flesh. Avocado or butter fruit is known for the large amounts of nutrition it provides. The fruit can be had cooked, raw, in a salad or just taken off its tree and eaten too, or maybe used topically for skin and hair needs, it would give out a wide range of helpful benefits for most health ailments that we suffer from. Butter fruit is very rich with potassium, much more than what bananas have. The fruit is also a source for Vitamin E and B as well, which are imperative for the body's needs.

However, studies have initiated to produce ethanol to run vehicles with the existing engine system and to generate electricity. The production processes only use energy from renewable sources and there is no net CO_2 emission to the atmosphere, thus making ethanol an environmentally beneficial energy source. In addition, ethanol derived from fruits materials, peels and biomass are the only liquid transportation fuel that does not contribute to the green house gas effect. This reduction of green house gas emission is the main advantage of utilizing fruit biomass conversion into ethanol (Anuj *et al*., 2007). Hence, the present study was focused on production and characterization of bio-ethanol from Kokum and Butter fruit materials by employing microbial fermentation technology.

Figure 1: Habitual view of Kokum Fruit and Butter fruit

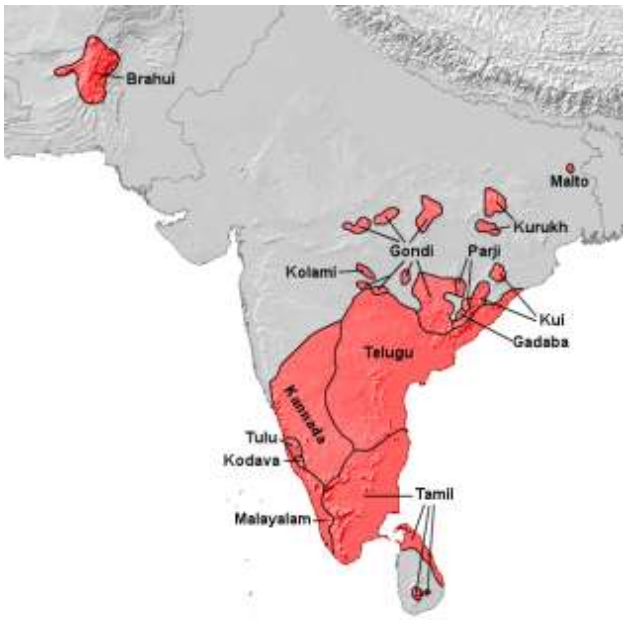

Figure 2: Showing geographic location of study area in respect of Fruit plantation

Kodagu (Coorg), is the smallest district in Karnataka (INDIA). Kodagu is configured with mountains. Agriculture is the developed sector in Kodagu. The main crops of district are cardamom, pepper, coffee, cinchona, ginger & paddy. Fruits such as limes, baddpulis, oranges, passion fruits, butter fruits, banana, pineapple, fig, gooseberry and sapotas are grown. Now with the exception of orange, lime, and banana cultivation no other fruit is grown economically. Approximately sixty five percent of Kodagu's geographical area is under tree cover & it is also one of the densely forested districts of India. Kodagu is also regarded as hotspot of biodiversity within Western Ghats as it has diverse kinds of vegetation. As climate is cool throughout the year wine preparation is common in most of the household. Many of them prepare wine in large quantity and sell it. The commonly prepared wines are of goose-berry, Kokum fruit, Butter fruit, grape, pineapple, passion fruit, lime, rice, Cashew apple, betel, ginger, fig, banana etc.

Juice industries of certain fruits, such as Kokum fruit, Butter fruit, passion fruit, grape, pineapple, Cashew apple are grown in almost all local territory of Coorg districts, generate large amounts of waste (peels, flush and seeds) from the crush of tons of fruit to

obtain the juice. Thus, there is a great the amount of passion fruit waste that could be processed in ethanol.

However, utilization of these fruit materials in production of bio-fuels would be of great environmental and economic benefit as it could reduce the burden on conventional sources of energy and also get rid of the wastes. In addition, Ethanol fuel has long been seen as a clean alternative fuel to petrol. Hence, the present study has been initiated with a novel idea on production of ethanol using Kokum and Butter fruit samples which are available at Coorg district, Karnataka, India.

Materials and Methods

The study was initiated with baseline survey at different parts of Kodagu district (Karnataka). During the survey, interaction was made with fruit growers and with many household people who prepare wine and sell as family enterprise. Further, interaction was also extended with commercial wine vendors regarding the present scenario emphasizing on collection of fruit material, processing, preparation of wine and market value of these home-made wine varieties. The first hand information was gathered through semi structured questionnaire.

Collecting the Fruit Materials

The fruit materials; Kokum fruit (*Garcinia indica,* L) and Butter fruit (*Persea Americana,* L) materials were used in this study were procured from the local fruit growers of Coorg district, Karnataka (INDIA) during the period; August, 2013 to October, 2014 both pre and post-harvest seasons. The plantation of both Kokum fruit and Butter fruit is located along the eastern part in the rural region of Kodagu district. A local-wild variety of both Kokum fruit and Butter fruit are green or pale green coloured and the fruits were procured from the fruit yards by the Farm Manager. The details of both fruit cultivars are briefed hereunder.

Kokum fruit

Kokum Fruits (*Garcinia indica*, L) are commonly grown in cold regions. Passion fruits are abundantly grown in South American countries. The fruits are extensively grown in different parts of Coorg and Malnad Area of Karnataka. These fruits are also grown in Kodaikanal region of Tamil Nadu, Wayanad region of Kerala. Usually, Passion fruits area Yellow & Purple coloured fruits are commonly available in Coorg region.

Butter fruit

Butter fruits (*Persea americana* L.), which is basically a native to Mexico and Central America. These fruits are grown expansively in specific regions of Coorg district and also Malnad area of Karnataka. Cashew apples are a false fruits and are physically described as small, hard, pear-shaped green fruit, and when ripened turn red, yellow, or orange.

Processing Fruit cultivars (substrates)

The fruit samples of kokum fruit and Butter fruit were obtained from local growers of Coorg district (Karnataka) as mentioned above. The Passion fruits were washed under running tap water and are peeled off, and are subjected for squashing using Mixer. Squashed fruits are filtered using white cloth. Filtered squash is transferred to plastic barrel. Sugar syrup is added. Potassium Meta bi-sulphite & yeast is added. In other barrel to the same quantity of contents instead of yeast wheat is added. Barrels are kept at room temperature for about 14 days.

In case of Cashew Apples; the fruits were washed twice with distilled water before being prepared for use. The fruit materials were dried in a hot air oven at 65˚C for 24 hours and powdered using a grinder. 50 g of each rind was weighed and utilized as the substrate.

Extraction of Juice from Fruit cultivars

Kokum Fruit Juice (KFJ) and Butter Fruit Juice (BFJ) extraction was done at the Applied Science Laboratory in association with Bhoomigeetha Institute of Research & development (BIRD), Mysore. The whole fruits were washed individually and cut in half. The fruit pieces were then compressed in a fruit processor with a separate pulp collector. Whilst extracting, the PFJ and CAJ were kept cold on ice followed by frozen condition and further was stored at −20∘C for subsequent use.

Physico-Chemical Characterization of Juice extracted from Fruit cultivars

The juices extracted from both fruit cultivars were subjected for physic-chemical parameters all through the fermentation and the data has been represented in the form of tables respectively. Besides, the

parameters such as reducing sugar, pH, Effect of specific gravity, Titration, Concentration of ethanol are continuously monitored during the fermentation.

Microorganism and Culture media

Saccharomyces cerevisiae was procured from authorized sources, (Azyme Technologies, Bengaluru). This Yeast was cultured on Yeast extract Peptone Dextrose (YPD) at 30˚C. The cultures were stored at 4˚C and sub-cultured every 30 days and the same was subjected for flocculation in order to elicit their activation at the time of experiment.

Preparation of PFJ and CAJ for fermentation

KFJ and BFJ were prepared, prior to each fermentation by pretreatment, centrifugation and sterilization. Pretreatment involved the addition of 1% (w/v) gelatin powder to the raw KFJ and BFJ were maintained at 4◦C for 24hrs. This was followed by centrifugation at 3500 rpm for 20min, addition of 2.5 g/L of ammonium sulphate, and sterilization at 121◦C for 15min. The PFJ and CAJ were sterilized in conjunction with the fermentation vessel.

Fermentation

Preparation of Yeast Inocula.

In the study, the Yeast inoculums were prepared in sterilized yeast peptone dextrose (YPD) liquid broth. The composition of YPD in g/L was 10 g yeast extract powder, 20 g peptone powder and 20 g D-glucose. The culture conditions were as follows: (i) volume = 200mL, (ii) temperature = 30◦C, (iii) agitation = 150 rpm, and (iv) duration = 18 hrs. The yeast was activated by extracting the glycerol and re-suspending the pellet in 1mL of YPD broth, and this suspension was added to 50mL of YPD liquid broth [32]. The cell count was increased by sub-culturing followed by flocculation at 10% every 18 hrs from 50mL to 200mL [32]. After cultivation, the cell viability was determined and 10% of the initial fermentation volume was used as a starter culture.

Saccharification and its knocking action

Saccharification is the critical step for bio-ethanol production where complex carbohydrates are converted to simple monomers. Compared to acid hydrolysis, enzymatic hydrolysis requires less energy and mild environment conditions. The processed fruit materials were added to a broth containing yeast extract (5g/l) and peptone (10g/l). The media was autoclaved at 121^0C and 15 psi pressure for 20 min and Yeast was inoculated under aseptic conditions. The flasks were then incubated at room temperature for a period of 144 hrs.

Subsequent to saccharification, the cultures were autoclaved and filtered using Whatman No. 1 filter paper. The filtrate was then transferred into 250ml Erlenmeyer flasks, made airtight with cork and autoclaved. The flasks were then aseptically inoculated with 15ml overnight grown S. *cerevisiae* and incubated at room temperature for 96hrs.

Fermentation of Fruit Juice of both Kokum and Butter fruit was performed with A BIOSTAT Bplus 2L MO-O2 fermentor (Sartorius Stedim Systems GmBH, Germany) to produce bio-ethanol. The operating conditions of the batch fermentations are summarized in Table 2. Fermentations were performed in duplicate.

The ethanol produced was determined by Gas Chromatography (Bipolar, 1250 mV, 10 Samp) using a NUCON Gas Chromatograph (5765 EPC) with a flame ionization detector per Sec. The carrier gas used was Nitrogen.

Distillation

In the current study, the batch distillation method was adopted. The distillation unit consisted of three components: a re-boiler, condenser pipe and a distillate or receiving flask. The filtered samples was transferred into the reboiler and heated to boil respectively. The vapors started to rise into the still head and passed through condenser pipe. The continuous circulation of cold water around the condenser pipe assisted in cooling the alcohol rich vapors back to liquid state. The condensed liquid enters the still receiver and then collected in the distillate. The distillate was tested for its alcohol content using Syke's hydrometer. Simultaneously, the temperature of the distillate was also measured. The alcohol content and the temperature were used to find the percentage of ethyl alcohol (Et OH) of the distillate, referring to the distillation chart. It was found that the percentage of ethyl alcohol was in the range of 6 % – 8 % depending upon the various ranges of different parameters.

Reducing Sugar assay

Ethanol fermentation is a biological process in which sugars are converted by microorganisms to produce ethanol and CO_2. The microorganism most commonly used in fermentation process is the yeasts and, among the yeasts, Saccharomyces cerevisiae is the preferred choice for ethanol fermentation (Lin and Tanaka, 2006).

Reducing sugars assay was carried out according to the Dinitrosalicylic method. Un-inoculated media was used as the control for the assay. The optical densities of the samples were measured against the blank at 540nm. The glucose concentration was then calculated using standard glucose curve.

Gas Chromatography (GC) Analysis

Using this technique, the content of ethanol concentration can be measured in the different samples. The analysis performed by a gas chromatograph is called gas chromatography which analyzes the compound that can be vaporized without decomposition and GC may help in identifying a compound. In the study, GC technique has been adopted to analyze the concentration and the purity of ethanol in a given sample.

Generally chromatographic data is presented as a graph of detector response (y-axis) against retention time (x-axis), which is called a chromatogram. This provides a spectrum of peaks for a sample representing the analytes present in a sample eluting from the column at different times. Retention time can be used to identify analytes if the method conditions are constant. Also, the pattern of peaks will be constant for a sample under constant conditions and can identify complex mixtures of analytes. However, in most modern applications, the GC is connected to a mass spectrometer or similar detector that is capable of identifying the analytes represented by the peaks.

Results and Discussion

The fruit cultivars; Kokum and Butter fruits were daily monitored. During the course of fermentation various parameters such as pH, specific gravity, alcohol concentration & titration was determined (Table-1, 2 & 3). The results show that, the fermentation is considerably fast in yeast compared to wheat fermentation mentioned in the earlier reports (Alfenore *et. al*, 2002; Panjai *et. al*, 2009 and Araujo *et. al*, 2011). Result also shown that; the production of ethanol is also significantly more in case of fermentation using flocculating yeast. This is in accordance with the earlier reports made by Flávia Cristina dos Santos Lima *et. al*, 2012 and Evanie Devi Deenanath *et. al*, 2013.

Juice Preparation for Passion fruit & Cashew Apple samples

The juice yield was found to be significant in both Kokum and Butter fruits samples. From, 20 kg of PFJ (yielded 9.85 L) and CAJ (yielded 5.6L) yielded considerable amount of juice during extraction process. Previous to fermentation both PFJ and CAJ were thawed, centrifuged and pretreated with gelatin powder to remove some secondary metabolites. The preparation of KFJ and BFJ was essential as the clear juice with a minimal to zero suspended solids which will allow the yeast to easily assimilate the sugars for growth and the production of ethanol (Table-4 & 5).

Physico-Chemical Characterization

The Juice extracted from Kokum and Butter fruits, all through the Fermentation process was subjected for physico-chemical characterization executed as per the standard protocols. The data has been represented in the tables respectively (Table-1 &2).

Evaluation of pH and Moisture

Variation in pH was seen during execution of the experiment. pH was decreased at initial stage, then it attained a minimal stage & then it increased. The initial pH for passion fruit was 5.7 then it decreased to 4.9 and again it increased to 6.0. Passion fruit initial it was 5.5 then decreased to 5.0 & increased in the range of 5.2- 6.0. For Cashew apple, initial it was 3.8 then increased to 5.8 and the final range of pH was found to be 6.0. The Moisture content (%) of Passion fruit 13.45±0.04 and Cashew apple 9.25±0.01 was noticed after pre-treatment of the substrates are represented in the Table-3. (Linde *et. al*, 2006, 2007 & 2008; Anderson, 2008 and Rocha *et. al*, 2011).

Evaluation on reducing sugar

The Reducing sugar in terms of percentage was analyzed and the result reveals; 0.74% in Passion fruit samples and 0.58% was noticed in Cashew apple fruit sample (Table-3). The yeast can grow both on simple sugars, such as glucose, and on the disaccharide sucrose. Furthermore, the availability of a robust

genetic transformation system of S. cerevisiae along with a long history of this microorganism in industrial fermentation processes makes it most desired microorganisms for ethanol production (Osho, 2005; Honorato et. al, 2007 and Pachco *et. al*, 2010). S. cerevisiae has high resistance to ethanol, consumes significant amounts of substrate in adverse conditions, and shows high resistance to inhibitors present in the medium (Hector *et. al,* 2011 and Larissa Canilha *et. al,* 2012 and Evanie Devi Deenanath *et. al*, 2013).

Effect of specific gravity

When the fermentation starts specific gravity decreases. Specific gravity of passion fruit reached 0.887at 52 hours. Whereas, specific gravity of ginger and gooseberry reached 0.870 & 0.856 respectively (Table-4). After 14 days it reached a constant value indicating the end of fermentation (Van Zyl *et. al*, 2007; Pinheiro *et. al*, 2008 and Evanie Devi Deenanath *et. al*, 2013).

Assessment on Titration

As the days increased fluctuating trend was seen in titration. The titratable acidity for passion fruit was 4.42g/L tartaric acid at the starting and reached 9.96 on last day. In case of Cashew apple it was 3.23 at the start and reached 8.89g/l tartaric acid on the last day (Mishra *et. al*, 2012 and Janani and Ketzi, 2013).

Concentration of ethanol

The ethanol content in the distillate was measured. The concentration of bio-ethanol in passion fruit sample was 11.4%, whereas the concentration of ethanol in cashew apple was 8.3% (Table-4 & 5). This value is higher than the report published by Neelakandan and Usharani, 2009; Araujo *et. al*, 2001; Mishra *et. al*, 2012 and Evanie Devi Deenanath *et. al*, 2013.

Gas Chromatography (GC) Analysis

The function of the stationary phase in the column has separated ethanol, causing each one to exit the column at a different time (retention time). Other parameter that was used to alter the order or time of retention is the carrier gas flow rate, column length and the temperature.

The purity of the carrier gas is also frequently determined by the detector, though the level of sensitivity needed can also play a significant role.

The spectrum of peaks for different samples representing the analytes present in the given samples eluting from the column at different times. 100% purity of bio-ethanol was noticed in Passion Fruit samples executed with increased days of fermentation using flocculating yeast cultures. The result of the given samples; sample 1- 8.7 ethanol, sample 2 - 15.8 ethanol, sample 3 - 11.6 ethanol (Table-6-10 & Graph-1-5). Among all the samples, sample 4 achieved 5.3% ethanol which gives 100% purity as compared to standard ethanol (Table-9 and Graph 4 & 6). Similar results were also obtained by El-Diwany *et. al*, 1992; Bellisimi and Ingledew, 2005; Najafi *et. al*, 2009; Balasubramaniam *et. al*, 2011; Janani and Ketzi, 2013;).

Table-1: Physico-chemical characterization of Juice extracted from Kokum fruit all through the Fermentation process.

Time (Days)	**Yeast count *S. cerevisiae* (Log-CFU/ml)**	**Total soluble solids (^{o}Brix)**	**pH**	**Alcohol (%-v/v)**	**Titratable Acidity as Citric Acid (%)**	**Fermentation Temp (^{o}C)**	**Sugar Content (g/l)**	**Specific Gravity**
01	02	10	2.8	0.0	0.76	20	72	1.044
02	02	09	2.9	2.2	0.78	20	68	1.040
03	07	07	3.0	2.8	0.79	24	65	1.040

04	08	04	3.2	3.2	0.80	24	63	1.038
05	10	03	3.4	3.6	0.81	26	61	1.036
06	12	01	3.4	3.8	0.82	28	60	1.032
07	14	0.6	3.5	4.2	0.86	30	57	1.031
08	16	0.5	3.7	4.5	0.89	32	54	1.029
09	17	0.3	3.7	4.5	0.90	35	49	1.025
10	19	0.3	3.9	4.7	0.92	35	44	1.024
11	19	0.3	3.9	4.8	0.94	36	38	1.019
12	20	0.1	4.1	5.4	0.97	36	34	1.010
13	22	0.05	4.3	6.6	1.01	39	30	1.009
14	25	0.01	4.4	7.0	1.08	40	28	1.007

Table-2: Physico-chemical characterization of Juice extracted from Butter fruit all through the Fermentation process.

Time (Days)	**Yeast count *S. cerevisiae* (Log-CFU/ml)**	**Total soluble solids (^{o}Brix)**	**pH**	**Alcohol (%-v/v)**	**Titratable Acidity as Citric Acid (%)**	**Fermentation Temp (^{o}C)**	**Sugar Content (g/l)**	**Specific Gravity**
01	02	24	3.5	0.0	0.52	20	92	1.054
02	02	22	3.5	2.1	0.54	20	89	1.050
03	07	19	3.5	2.6	0.58	24	84	1.047
04	08	15	3.6	2.8	0.59	24	76	1.043
05	10	12	3.6	2.9	0.60	26	70	1.038
06	12	10	3.7	3.0	0.64	28	65	1.033
07	14	08	3.9	3.4	0.68	30	60	1.029
08	16	7.2	4.2	3.6	0.72	32	56	1.024
09	17	6.5	4.6	3.9	0.78	35	51	1.020
10	19	5.7	4.8	4.4	0.84	35	47	1.017
11	19	4.0	5.0	4.9	0.92	36	44	1.012
12	20	3.2	5.4	5.3	0.96	36	41	1.007

13	22	2.0	5.5	5.9	1.10	39	39	1.005
14	25	1.1	5.7	6.6	1.22	40	35	1.001

Table-3: Showing Physico-chemical characteristic features in Kokum and Butter fruits after pre-treatment

SL. No.	**Parameters analyzed**	**Kokum fruit Juice(KFJ)**	**Butter Fruit Juice (BFJ)**
1.	pH	3.8—4.4	5.0-5.8
2.	Moisture (%)	11.28±0.02	7.25±0.03
3.	Soluble Solids (^{0}Brix)	0.01±0.00	0.006±0.00
4.	Reducing Sugar (%)	0.68±0.01	0.78±0.04

Table-4: Showing different parameters and respective yields of Ethanol for Kokum Fruit samples

SL. No.	**Wine (Yeast)**	**pH**	**Specific Gravity**	**Ethanol Conc.%**
1.	Kokum Fruit	3.8	1.024	4.5
2.	Kokum Fruit	4.2	1.010	6.6
3.	Kokum Fruit	4.4	1.007	7.0

Table-5: Showing different parameters and respective yields of Ethanol for Butter Fruit samples

SL. No.	**Wine(Yeast)**	**pH**	**Specific Gravity**	**Ethanol Conc. %**
1.	Butter Fruit	4.8	1.017	4.4
2.	Butter Fruit	5.4	1.007	5.3
3.	Butter Fruit	5.7	1.001	6.6

Table-6: Showing GC Analysis of *Kokum fruit* Juice of after fermentation using Yeast

SL. No.	**Start Time (Time-min)**	**Area (mV.s)**	**Area (%)**
1.	0.780	2085.19	98.3
2.	1.757	24.670	1.2
3.	2.233	12.133	0.6
Total		**2121.99**	**100.0**

Graph-1: GC Analysis of fruit juice sample of Kokum fruit after fermentation using flocculated Yeast

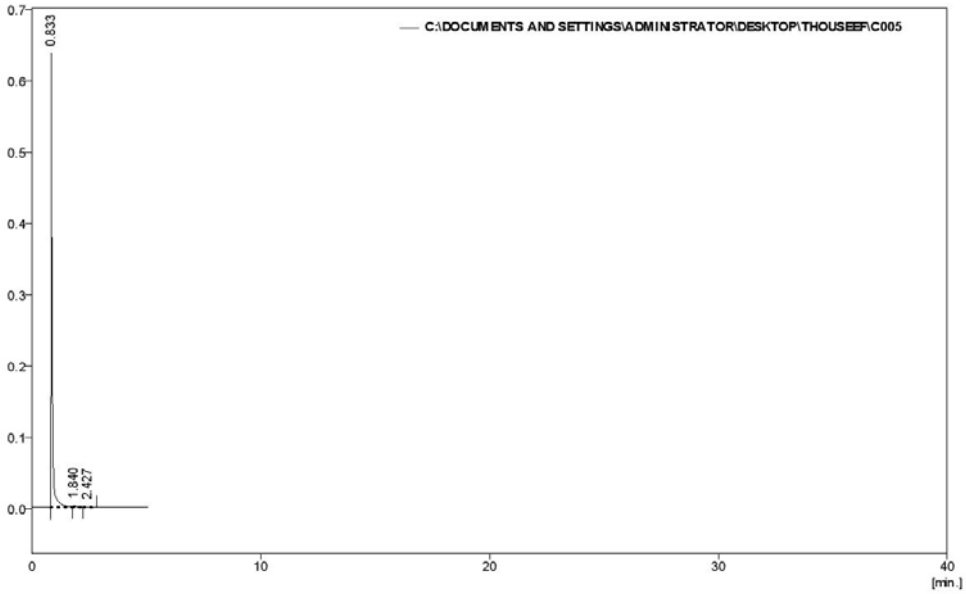

Table-7: Showing GC Analysis of Kokum fruit Peel after fermentation using Yeast

SL. No.	Start Time (Time-min)	Are (mV.s)	Area (%)
1.	1.370	29.027	58.0
2.	2.600	7.987	16.0
3.	3.190	12.996	26.0
Total		**50.012**	**100.0**

Graph-2: GC Analysis in Peel of Kokum fruit sample after fermentation using flocculated Yeast

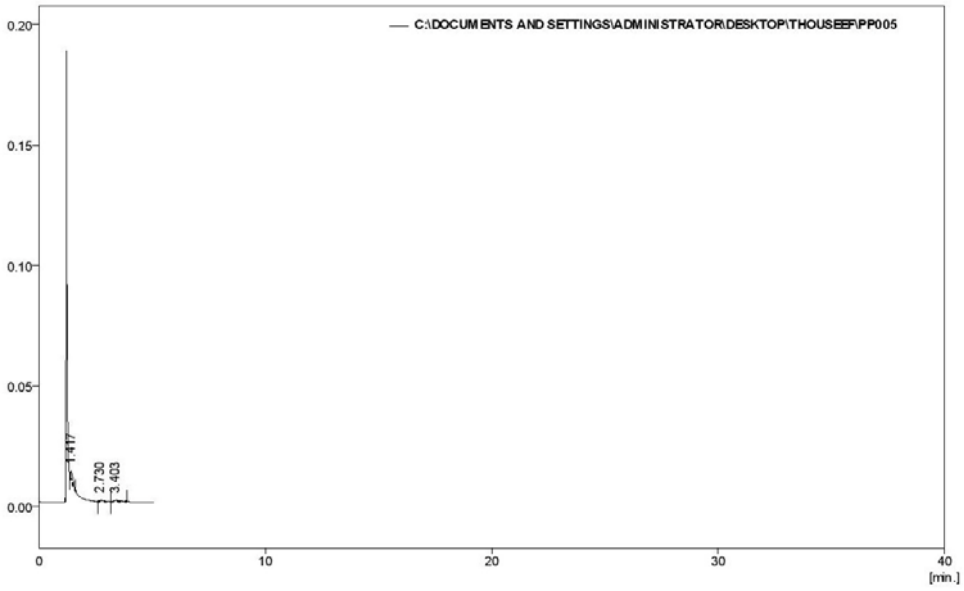

Table-8: Showing GC Analysis in Butter fruit peel sample of after fermentation using flocculated Yeast

SL. No.	Start Time (Time-min)	Area (mV.s)	Area (%)
1.	0.780	87.450	86.80
2.	0.967	13.345	13.20
3.	1.313	73.713	21.1
Total		**349.134**	**100.0**

Graph-3: GC Analysis of fruit juice sample of Butter fruit after fermentation using flocculated Yeast

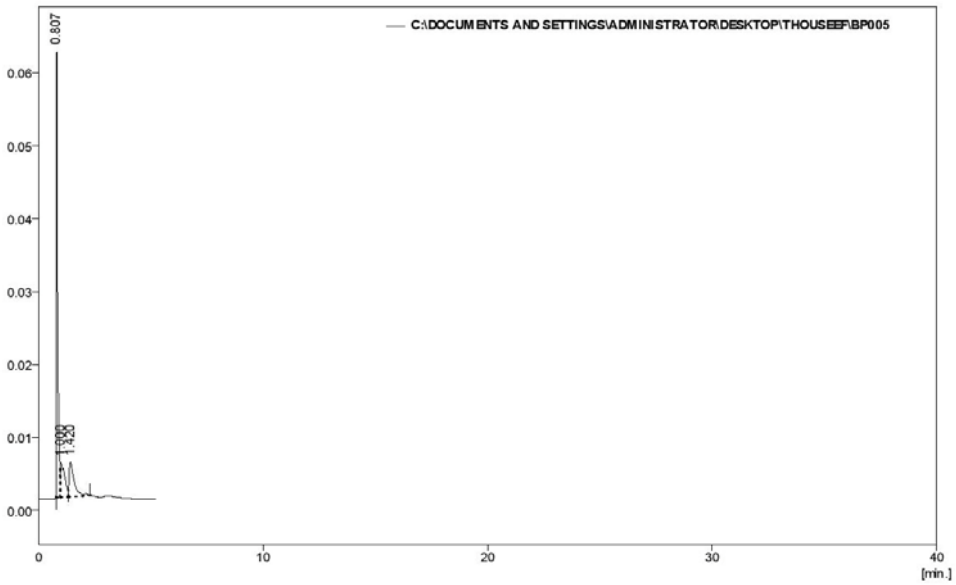

Table-9: Showing GC Analysis in Butter fruit peel sample of after fermentation using Yeast

SL. No.	Start Time (Time-min)	Area (mV.s)	Area (%)
1.	0.967	8.454	4.0
2.	1.080	12.438	5.9
3.	1.330	22.243	10.5
4.	1.980	28.268	13.3
5.	2.277	64.510	30.4
6.	3.367	76.120	35.9
Total		**212.033**	**100.0**

Graph-4: GC Analysis in Peel of Butter fruit sample after fermentation using flocculated Yeast

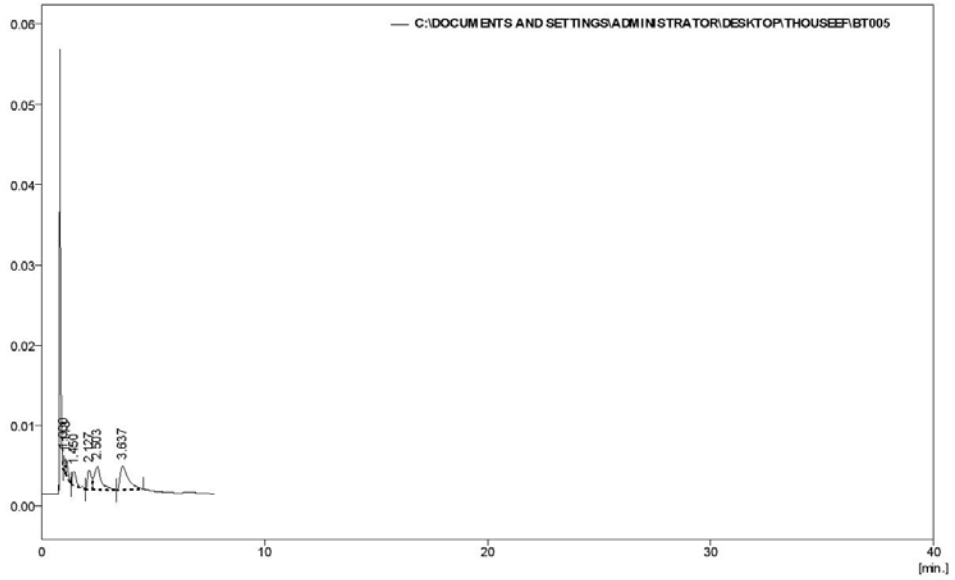

Table-10: Showing GC Analysis in Standard sample.

SL. No.	Start Time (Time-min)	Area (mV.s)	Area (%)
1.	0.817	11533.76	100.0
Total		**11533.76**	**100.0**

Graph-5: Showing GC Analysis for standard sample.

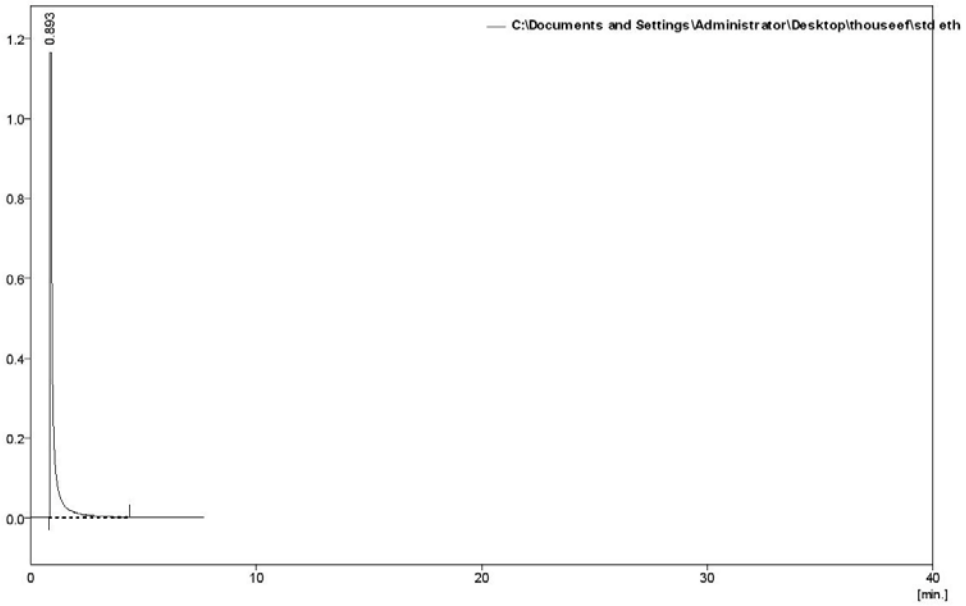

Table-11: Showing GC Analysis in Kokum and Butter fruit samples comparing with Standard sample.

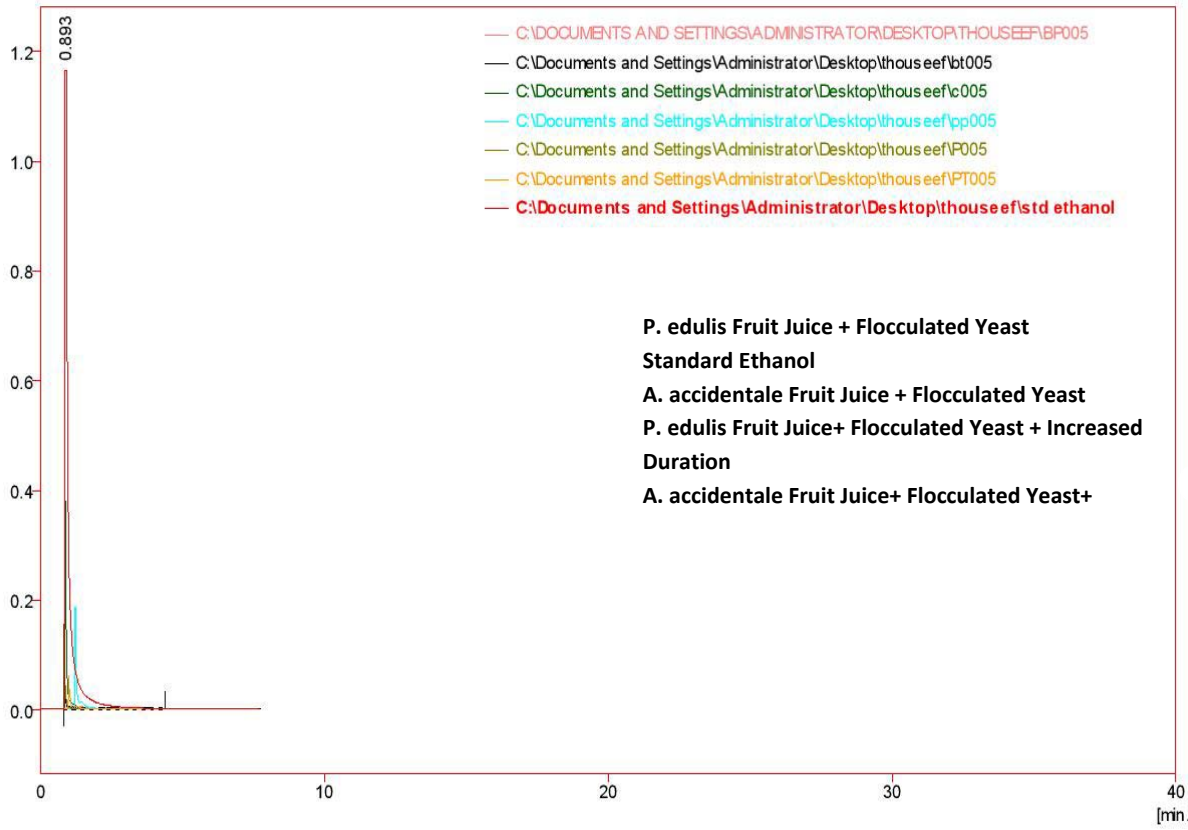

Summary and Conclusion

The world's present economy is highly dependent on various fossil energy sources such as oil, coal, natural gas, etc. These are being used for the production of fuel, electricity and other goods. Excessive consumption of fossil fuels, particularly in large urban areas, has resulted in generation of high levels of pollution during the last few decades. The level of greenhouse gasses in the earth's atmosphere has drastically increased. With the expansion of human population and increase of industrial prosperity, global energy consumption also has increased gradually.

Import of transport fuel is affected by limited reserves of fossil fuel. Annual global oil production will begin to decline within the near future. In this scenario, renewable sources might serve as an alternative.

Wind, water, sun, biomass, geothermal heat can be the renewable sources for the energy industry whereas fuel production and the chemical industry may depend on biomass as an alternative source in the near future. All petroleum-based fuels can be replaced by renewable biomass fuels such as bio-ethanol, bio-diesel, bio-hydrogen, etc., derived from Cereals, millets, sugarcane, Fruit cultivars, algae, etc.

In the present study, the existing technologies were adopted for bio-ethanol production from fruit cultivars; Kokum fruit and Butter fruit samples. The bio-ethanol content of both Kokum fruit and Butter fruit juice samples by employing fermentation with increased duration using flocculating Yeast has been achieved. The result concludes that, the bio-ethanol content of Butter fruit by yeast fermentation is significantly very high compared to Kokum fruit sample. Furthermore, other than the yeast fermentation, in the ethanol production, using flocculating Yeast culture can facilitates high amount of bio-ethanol recovery in the fruit samples with 100% purity.

Acknowledgement

The authors are very much grateful to; the Bhoomigeetha Institute of Research & development (BIRD), Tumkur (Karnataka), INDIA for providing infrastructure and Dept. of

Biotechnology & Botany, Mandavya First Grade College, Mandya (Karnataka). The Manager of Azyme Biotechnologies, Bengaluru for training and technical assistance with statistical analysis and the authorities of Bharathiar University, Coimbatore (Tamilnadu) for providing opportunity to pursue Research study.

References

1. Alfenore, S., Molina-Jouve, C., Guillouet, S. E., Uribelarrea, J. L., Goma, G and Benbadis, L. 2002. "Improving ethanol production and viability of Saccharomyces cerevisiae by a vitamin feeding strategy during fed-batch process," Applied Microbiology and Biotechnology, vol. 60, no. 1-2, pp. 67–72, 2002.

2. Amigun, B., Sigamoney, R and von Blottnitz, H.2008. "Commercialisation of bio-fuel industry in Africa: a review," Renewable and Sustainable Energy Reviews, vol. 12, no. 3, pp. 690–711.

3. Anderson WF, Akin DE. 2008. Structural and chemical properties of grass lignocelluloses related to conversion for biofuels. J Ind Microbiol Biotechnol. 35:355–366.

4. Araujo, S. M., Silva, C. F., Moreira, J.J., Narain S.N and Souza, R.R. 2011. "Biotechnological process for obtaining new fermented products from cashew apple fruit by Saccharomyces cerevisiae strains," Journal of Industrial Microbiology Biotechnology, vol. 38, no. 9, pp. 1161–1169.

5. Balasubramaniam, K., Ambikapathy, V and Panneraselvam, A. 2011. "Studies on ethanol production from spoiled fruits by batch fermentations". Journal of Microbiology and Biotechnology Research, Vol.1 (4), 158-163.

6. Balat, M.and Balat, H.2009. "Recent trends in global production and utilization of bio-ethanol fuel," Applied Energy, vol. 86, no. 11, pp. 2273–2282.

7. Bellissimi, E. and Ingledew, W. M. 2005. "Metabolic acclimatization: preparing active dry yeast for fuel ethanol production," Process Biochemistry, vol. 40, no. 6, pp. 2205–2213.

8. Deenanath, E. D., Iyuke, S. E. and Lindsay, D. 2010. "Enzymatic hydrolysis of bitter sorghum for bioethanol production," Master Brewers Association of the Americas-MBAA TQ.

9. Demirbas, A. 2008. "Biofuels sources, biofuel policy, biofuel economy and global biofuel projections," Energy Conversion and Management, vol. 49, no. 8, pp. 2106–2116.

10. El-Diwany, A.I., El-Abyad, M. S., El-Refai, A.H., Sallam, L. A. and R. F.Allam, "Effect of some fermentation parameters on ethanol production from beet molasses by Saccharomyces cerevisiae Y-7," Bioresource Technology, vol. 42, no. 3, pp. 191–195, 1992.

11. Fatma HA, Fadel M 2010. Production of bioethanol via enzymatic saccharification of rice straw by cellulase produced by Trichoderma reesei under solid state fermentation. New York Sci J. 3: 72-78.

12. Galbe M, Zacchi G. 2012. A review of the production of ethanol from softwood. Appl Microbiol Biotechnol 59:618–628.

13. Goh, C. S., and Lee, K. T. 2010. "A visionary and conceptual macroalgae- based third-generation bio-ethanol (TGB) biorefinery in Sabah, Malaysia as an underlay for renewable and sustainable development," Renewable and Sustainable Energy Reviews, vol. 14, no. 2, pp. 842–848.

14. Hector, R. E., Mertens, J. A., Bowman, M. J., Nichols, N. N., Cotta, M. A and Hughes, S.R. 2011. "Saccharomyces cerevisiae engineered for xylose metabolism requires gluconeogenesis and the oxidative branch of the pentose phosphate pathway for aerobic xylose assimilation," Yeast, vol. 28, pp. 645–660.

15. Honorato, T. L., Rabelo, M. C., Gonc¸alves, L. R. B., Pinto, G. A. S. and Rodrigues, S.2007. "Fermentation of cashew apple juice to produce high added value products," World Journal of Microbiology and Biotechnology, vol. 23, no. 10, pp. 1409–1415.

16. Janani, K., Ketzi, M. 2013. "Comparative studies of ethanol production from different fruit wastes using Saccharomyces cerevisiae". Journal of Innovative Research in Science, Vol. 2, 12.

17. Jegannathan, K. R., Chan, E. S. and P. Ravindra. 2009. "Harnessingbiofuels: a global Renaissance in energy production?" Renewable and Sustainable Energy Reviews, vol. 13, no. 8, pp. 2163–2168.

18. Julius, E and Lena, T . 2013. "Cluster Development in Low Resource Settings: the Case of Bio-ethanol and Fruit Processing Clusters in Uganda". Journal of Entrepreneurship and Innovation Management, Vol. 2(3), 59-78.

19. Kimand, S. Dale, B. E. 2004. "Global potential bio-ethanol production from wasted crops and crop residues," Biomass and Bio-energy, vol. 26, no. 4, pp. 361–375.

20. Larissa Canilha, Anuj Kumar Chandel, Thais Suzane dos Santos Milessi, Felipe Antonio Fernandes Antunes, Wagner Luiz da Costa Freitas, Maria das Grac¸as Almeida Felipe, and Silvio Silverio da Silva. 2010. Bioconversion of Sugarcane Biomass into Ethanol:An Overview about Composition, Pretreatment Methods, Detoxification of Hydrolysates, Enzymatic Saccharification, and Ethanol Fermentation.

Journal of Biomedicine and Biotechnology Volume (1): Pp-1-15.

21. Lin, Y and Tanaka, S. 2006. "Ethanol fermentation from biomass resources: current state and prospects," Applied Microbiology and Biotechnology, vol. 69, no. 6, pp. 627–642.

22. Linde, M. Galbe, M and Zacchi, G. 2006. "Steam pretreatment of acid-sprayed and acid-soaked barley straw for production of ethanol," Applied Biochemistry and Biotechnology, vol. 130, no. 1–3, pp. 546–562.

23. Linde, M. Galbe, M and Zacchi, G. 2007, "Simultaneous saccharification and fermentation of steam-pretreated barley straw at low enzyme loadings and low yeast concentration," Enzyme and Microbial Technology, vol. 40, no. 5, pp. 1100–1107.

24. Linde, M., Galbe, M and Zacchi, G.2008. "Bio-ethanol production fromnon-starch carbohydrate residues in process streams from a dry-mill ethanol plant," Bioresource Technology, vol. 99, no. 14, pp. 6505–6511.

25. Mishra, J., Kumar, D., Samanta, S and Manoj Kumar. 2012. "A comparative study of ethanol production from various agro residues by using Saccharomyces cerevisiae & Candida albicans". Journal of Yeast and Fungal Research, Vol.3 (2), 12-17.

26. Najafi, G., Ghobadian, B., Tavakoli, T. and Yusaf, T.2009. "Potential of bio-ethanol production from agricultural wastes in Iran," Renewable and Sustainable Energy Reviews, vol. 13, no. 6-7, pp. 1418–1427.

27. Neelakandan, T and Usharani, G. 2009. "Optimization and production of bioethanol from cashew apple juice using immobilized yeast cells by Saccharomyces cerevisiae," America-Eurasian Journal of Scientific Research, vol. 4, no. 2, pp. 85–88.

28. Osho, "Ethanol and sugar tolerance of wine yeasts isolated from fermenting cashew apple juice," African Journal of Biotechnology, vol. 4, no. 7, pp. 660–662, 2005.

29. Pacheco, A.M.,. Gondim, D. R and Goncalves, L. R. B. 2010. "Ethanol production by fermentation using immobilized yeast cells," Applied Biochemistry and Biotechnology, vol. 161, no. 1–8, pp. 209–217.

30. Panjai, L., Ongthip, K and Chomsri, N. 2009. "Complex fruit wine produced from dual culture fermentation of pineapple juice with Torulaspora delbrueckii and Saccharomyces cerevisiae". Asian Journal of Food & Agro Industry, Vol. 2(02), 135-139.

31. Pinheiro, D. T., Rocha, M. V. P., Mac. Edo, G. R. and Goncalves, L. R. B.2008. "Evaluation of cashew apple juice for the production of fuel ethanol," Applied Biochemistry and Biotechnology, vol. 148, no. 1–3, pp. 227–234.

32. Rocha, M. V. P., Oliveira, A. H. S., Souza, M. C. M and Goncalves, L. R. B. 2006 "Natural cashew apple juice as fermentation medium for biosurfactant production by Acinetobacter calcoaceticus," World Journal of Microbiology and Biotechnology, vol. 22, no. 12, pp. 1295–1299.

33. Sanchez, O. J. and C. A. Cardona. 2008. "Trends in biotechnological production of fuel ethanol from different feedstocks," Bioresource Technology, vol. 99, no. 13, pp. 5270–5295.

34. Suhas V Bhandari, Arun Panchapakesan, Naveen Shankar, H G Ashok Kumar. 2013. Production of Bioethanol From Fruit Rinds by Saccharification and Fermentation. International Journal of Scientific Research Engineering & Technology; Vol- 2 (6): 362-365.

35. Turner, D., Xu, H., Cracknell, R. F., Natarajan, V. and Chen, X. 2011. "Combustion performance of bio-ethanol at various blend ratios in a gasoline direct injection engine," Fuel, vol. 90, no. 5, pp. 1999–2006.

36. Van Zyl, W. H., Lynd, L. R., den Haan, R and McBride, J. E. 2007."Consolidated bioprocessing for bioethanol production using saccharomyces cerevisiae," Advances in Biochemical Engineering/Biotechnology, vol. 108, pp. 205–235.

37. Walker, G. M. 2011. "Fuel ethanol: current production and future challenges," Journal of the Institute of Brewing, vol. 117, no. 1, pp. 3–22.

Author's details

[1]Department of Biotechnology and Bioinformatics, Bharathiar University, Coimbatore-641 046 (Tamilnadu), India, Email: thouseef.com@gmail.com

[2]Department of Applied Sciences & Engineering, Sampoorna Institute of Technology and Research (Visvesvaraya Technological University, Belgaum), Belakere, Channapatna taluk, Ramanagara district (Karnataka) 560162.

Copy for Cite this Article- Thouseef Ahamad, M. Y., and G. Panduranga Murthy, "Comparative study of Bio-ethanol production from Kokum and Butter fruit waste samples by employing microbial fermentation technology', *International Journal of Science, Engineering and Technology,* Volume 4 Issue 1: 2016, pp. 260- 273.

M. Shamuganapriya et al. 2016, Volume 4 Issue 1
ISSN (Online): 2348-4098
ISSN (Print): 2395-4752

International Journal of Science, Engineering and Technology
An Open Access Journal

Countering Smart Attack and Selective Capture in Wireless Sensor Networks Using Genetic Algorithm

[1]M. Shamuganapriya, [2]S. Divakar

Abstract

To develop an analysis methodology with simulation validation to identify the defense protocol settings under which the sensor network lifetime is increased due to selective capture and smart attack. Functioning detector nodes are replaced by functioning detector nodes and most obtainable routing methods are used by genetic algorithmic program to cut back the node cost and knowledge loss. To prevent congestion by discarding some unnecessary packets based on the optimization criteria derived in MOO (Multi Objective Optimization).

Keywords- Wireless sensor network, Selective capture, Smart attack, multiple routing, Intrusion tolerance, Intrusion detection.

Introduction

A wireless sensor network are spatially distributed autonomous sensors to monitor physical or environmental conditions, such as temperature, sound, pressure, etc. and to cooperatively pass their data through the network to a main location. The wsn is built of "nodes" – from a few to several hundreds or even thousands, where each node is connected to one (or sometimes several) sensors. In the literature, various schemes have been designed for preserving critical SN's from energy exhaustion so as to prolog the system lifetime; however how to counter selective capture, i.e., critical SN's are targets of selective capture attacks, is an open issue[1]. Once a node is captured and turned into a malicious node, it becomes an inside attacker. (1) In this paper, we propose and analyze selective deployment, ie, populating more critical than edge nodes to effectively counter selective capture. (2) Then inside attacker behaviour model and extend the analysis to homogeneous or heterogeneous clustered WSN's without a BS. It can be applied, including Nuclear power plants: A query based WSN with SN's monitoring noise, vibration humidity, temperature, electrical characteristics and radiation. Smart city: A query based WSN with

SNS monitoring motion, location, direction, Size, Temperature, humidity, radiation, etc.

Related Works

Yin Wu, Nanjing [1] developed to cut back the node cost and knowledge. It won't protect the network from attacks like passive attack. Yaakob, N.Khalil, I., [2] proposed to prevent congestion by discarding some unnecessary packets based on the optimization criteria. This is not secure against attacks such as node malfunction. Tang liua, Jian pengh, Jin yang[3] In EEPCA, each node independently selects itself as the cluster head node based on energy factor, which leads to the probability of cluster head election related to nodes. It doesn't give my selection. A shakeela Joy, M. Muthuselvi, V.kavitha[4]To avoid congestion and information about 1-hop neighbour sensor node to select suitable sensor node for this, each sensor node receives 1-hop CAM periodically from its neighbour sensor node. Tanveer A.Zia, Albert Y.Zomaya[5] The presented analysis a shows that the proposed frame work as a whole address see the security issues competently without increasing the overheads in

[1]Corresponding Author's Email: shamu.ragav@gmail.com

contrast to the computationally extensive security solution, the framework has graout potential for emerging application: Sudip misra, Samaresh bera, Ayan mondal, reena tickey [6] For the gateway selection problem, we have shown how the user requests can be mapped to the optimal gateway serviced through the sensor cloud environment, we observed that our proposed framework works well for delay optimization. Tamara bonali, linda bushnell and radha poovendran [7] The practical implications of our work are: it enables (a) analysis of the physical node capture attack (b) Characterization of adversarial behaviour and strategies and (c) computation of the optimal revocation rates, in terms of network parameters and crypto graphic quantities, to maintain secure network connectivity in the presence of the attack. K. Murugan, S. Jagatheswaran, P. Kanagaraj, G. Renuka[8] Energy economical routing and fault node (EERFNR) algorithmic program is projected for wireless detector network to extend the

Lifetime, cut back knowledge loss and node cost. Then non functioning detector nodes are replaced by functioning detector nodes and most obtainable routing methods are used by genetic algorithmic program to cut back the node cost and knowledge loss.

System Model

WSN Environments

We consider a query-based WSN with low-power SNs distributed in a geographic area. There is a protocol assigned to the WSN that interconnects the WSN to the outside world and that fields queries from the outside world for sensing results. Queries arrive at the system following a Poisson process with rate λ_q. A query failure is considered as a critical system failure. The initial energy of each SN is E_0^{sn}. We consider random deployment where SNs are deployed randomly (e.g., through air drop) and distributed according to homogeneous spatial Poisson processes with density λ_0^{sn}. The homogeneous spatial Poisson model is frequently used in WSN research, since in the absence of extensive statistical studies of spatial node distribution in real WSNs; it provides first-order approximation accounting for stochastic factors in the connectivity process. The expected number of SNs initially in the system thus is $N_0^{sn}=\lambda_0^{sn}\pi(r^p)^2$.

Selective Capture and Smart Attack Model

All SNs are subject to capture attacks. With "selective capture," the adversaries (humans or robots) strategically capture SNs and turn them into inside attackers. We represent the capture rate of a SN at a distance x *away* from the protocol at time t by $\lambda_c^{sn}(x,t)$. In practice, one wouldn't know how the capture rate varies as a function of distance to the Protocol. This requires some prior knowledge or history data analysis. Our analysis methodology developed in the paper is generally applicable as long as the capture rate can be expressed as a function of distance to the Protocol. Since SNs close to the protocol are desirable targets for capture attack, we assume that the capture rates decreases linearly as the SN is further away from the protocol as follows:

$$\lambda_c^{sn}(x,t)=\lambda_c^{max}-x/r^p(\lambda_c^{max}-\lambda_c^{min}) \qquad (1)$$

Where λ_c^{max} is the maximum capture rate the adversary can possibly have, and λ_c^{min} is the minimum capture rate. A baseline case against which this linear selective capture case will be compared is "random capture" by which the adversary, given the same energy and capacity, randomly performs capture attacks, i.e., $\lambda_c^{random}=(\lambda_c^{max}+\lambda_c^{min})/2$ at all distances. We note that these two capture models have the same overall capture rate accounting for the overall capability of the capturers in the system. After a node is compromised it becomes an inside attacker. An inside attacker can perform packet dropping and data modification attacks [3]. Using our defense mechanism, a data modification attack by forwarding SN can be detected and the packet will be discarded. So a data modifications attack has the same effect of a packet dropping attack. A malicious node can also perform slandering attacks by recommending a good node as a bad node, and a bad node as a good node when participating in

intrusion detection activities. As a result, slandering attacks can cause good nodes being misdiagnosed and evicted from the system, and bad nodes being missed and remained in the system. This effectively creates an area with a high concentration of bad nodes, especially for critical SN areas with a high capture rate under selective capture. In the literature it is often assumed that an inside attacker performs attacks constantly, without giving consideration to evade intrusion detection. In this paper we characterize a smart attacker by its capability to perform random, opportunistic and insidious attacks. First of all, a smart attacker can perform random or on-off attacks, i.e., attacking with a random probability p_a, to evade intrusion detection. Second, a smart attacker can perform opportunistic attacks, i.e., it attacks only when it sees opportunities which can lead to a successful attack while still eluding detection. Finally, it can perform insidious attacks, i.e., it can perform on-off attacks to evade intrusion detection until a critical mass of compromised node population is reached after which it performs "all in" attacks (pa=1) to which can be translated into the actual system lifetime span given the query arrival rate. A failure occurs when no response toward a query is received. The cause could be due to packet dropping or data modification by malicious forwarding SNs, or energy exhaustion. A failure can also occur when the protocol receives majority false responses because the majority of m_s source SNs selected are malicious.

Algorithm Description

Genetical Algorithm

The parameters are encoded in binary string and function the chromosomes for the GA. the weather (or bits), i.e., the genes, within the binary strings are adjusted to reduce or maximize the fitness worth. The fitness perform generates its fitness worth, that consists of multiple variables to be optimized by the GA. At every iteration of the GA, a planned range of people can manufacture fitness values related to the chromosomes. The following may be a typical GA procedure: Procedure GA Begin Initialize population; Evaluate population members; While termination condition not happy do Begin Select oldsters from current population; Apply genetic operators to choose parents; Appraise offspring; Set offspring adequate current population; Finish End There are five steps in the genetic rule as represented below.

Data Format

In the data format step, the genetic rule generates chromosomes, and everybody is associate degree expected answer. The amount of chromosomes is set in line with the population size that is outlined by the user. Everybody is a combination answer, and also the body length is that the range of sensing element nodes that are depleted or non-functioning the weather within the genes is either0 or 1. A one suggests that the node ought to get replaced, and means the node won't get replaced.

Evaluation

In general, the fitness worth is calculated per a fitness operate, and additionally the parameters of the fitness operate are the chromosome's genes. However, we tend to tend to cannot place genes directly into the fitness operate among the EERFNR formula, as a results of the genes of the body are just whether or not or not the node got to get replaced or not. Among the EERFNR formula, the goal is in addition to recycle the foremost routing strategies and to interchange the fewest device nodes. Hence, the variability of routing strategies out there if some non-functioning device nodes are replaced is calculated, and additionally the fitness operate is shown as below.

$$F(n)= \sum_{i=1}^{max\,grade} \frac{RPi \times TSN}{SNi \times TRP \times i}$$

Where, SNi = the quantity of replaced detector nodes and their grade worth at i . RPi = the quantity of re-usable routing ways from detector nodes with their grade worth at i. TSN = total range of detector nodes within the original WSN. TRP = total range of

routing ways within the original WSN. A high fitness worth is wanted as a result of the WSN is yearning for the foremost obtainable routing ways and therefore the least range of replaced detector nodes

Selection

The selection step can eliminate the chromosomes with very cheap fitness values and retains the remainder. We tend to use the political orientation strategy and keep the 1/2 the chromosomes with higher fitness values and place them within the coupling pool. The more serious chromosomes are deleted, and new chromosomes will be made to replace them after the cross overstep.

Crossover

The crossover step is employed within the genetic algorithmic program to vary the individual body. During this algorithmic program, we have a tendency to use the one-point crossover strategy to make new chromosomes. 2 individual chromosomes square measure chosen from the pairing pool to supply 2 new offspring. A crossover purpose is chosen between the primary and last genes of the parent people. Then, the fraction of every individual on either facet of the crossover purpose is changed and concatenated. The speed of selection is formed in keeping with roulette-wheel choice and therefore the fitness values.

Mutation

The mutation step will introduce traits not found within the original people and prevents the GA from converging too quickly. During this rule, we have a tendency to merely flip a factor at random within the body. The body with the best fitness price is the answer once the iteration. The EERFNR rule can replace the detector nodes within the body with genes of one to increase the WSN lifespan.

Performance Evaluation

In this section, we present numerical results. Our reference WSN consists of N_0^{sn}= 1500 SN nodes initially deployed with density λ_0^{sn} with the protocol sitting at the centre of a circular area with radius r_{sn}=300m. The selective SN capture time is assumed to be exponentially distributed following the linear model described by Eq. 1, with λ_c^{min} being once per 4 weeks and λ_c^{max} varying in the range of once per half day to once per 2 weeks. The radio range r_{sn} is dynamically adjusted to maintain network connectivity of n_0= 7 to support basic multipath routing and voting-based IDS functions. The initial energy level of a SN is E_0^{sn}=2 Joule. The energy parameters used by the radio module are adopted from [7, 14]. The energy dissipation E_{elec} to run the transmitter and receiver circuitry is 50nJ/bit. The energy used by the transmit amplifier to achieve an acceptable signal to noise ratio ($Eamp$) is 10 pJ/bit/m^2 for transmitted distances less than the threshold distance d_0 (75m) and 0.0013 pJ/bit/m^4 otherwise. The query arrival rate λ_q is a variable ranging from 10^{-2} to 1 query/sec to reveal points of interest. The imperfection of host IDS monitoring due to ambient noise and channel error is modelled by a monitoring error probability p_{err}= 1%.

Countering Selective Capture and Smart Attack

In this section, analyze the effectiveness of our defences against selective capture and random + opportunistic + insidious attacks which we model by λ_c^{max}, λ_c^{min},p_a, and $p_{all\text{-}in}$. Figure shows the optimal TIDS interval (representing detection strength) to counter such attackers with varying capture strengths (λ_c^{max}) and random attack probability (p_a). In Figure, we fix λ_c^{min} to once per 4 weeks and vary λ_c^{max} in the range of once per half day to once per 2 weeks. We also fix $p_{all\text{-}in}$=0.25 to isolate its effect. We observe from Figure that a low pademands a high detection rate (i.e., a small TIDS interval). The reason is that a low pawill result in a high per-host false negative probability H_{pfn}. Consequently, to cope with many hidden bad nodes missed by intrusion detection, the system will have to use a small TIDS interval for high detection strength. Another observation is that as λ_c^{max} increases, TIDS decreases (or the detection strength increases) to counter the increasing capture rate.

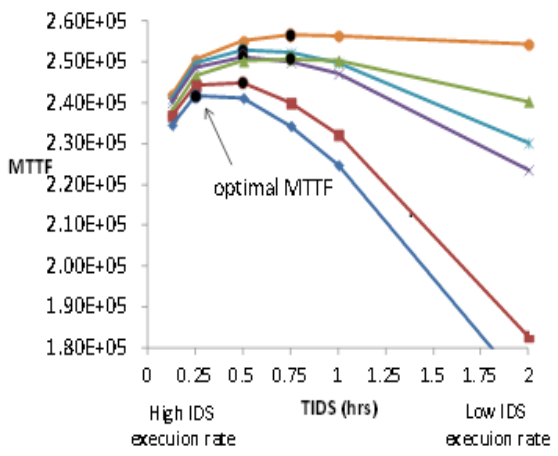

Fig: Countering Selective Capture and Random + Opportunistic + Insidious Attacks with varying λ_c^{max} and p_a by Adjusting Detection Strength Parameter TIDS.

TABLE 1: OPTIMAL (m_p, m_s) UNDER LOW P_a(0.25), WITH VARYING λ_c^{max} AND T_{IDS}.

	T_{IDS} = 0.25 hr	0.5 hr	1 hr	2 hrs	4 hrs
λ_c^{max}=1/(0.5 day)	(1,3)	(1,4)	(2,4)	(2,5)	(3,5)
λ_c^{max}=1/(1 day)	(1,3)	(1,3)	(1,3)	(1,5)	(2,4)
λ_c^{max}=1/(7 day)	(1,2)	(1,2)	(1,2)	(1,3)	(1,3)
λ_c^{max}=1/(14 day)	(1,2)	(1,2)	(1,2)	(1,2)	(1,3)

TABLE 2: OPTIMAL (m_p, m_s) UNDER HIGH P_a(0.75), WITH VARYING λ_c^{max} AND T_{IDS}.

	T_{IDS} = 0.25 hr	0.5 hr	1 hr	2 hrs	4 hrs
λ_c^{max}=1/(0.5 day)	(1,3)	(1,3)	(1,3)	(1,5)	(2,5)
λ_c^{max}=1/(1 day)	(1,2)	(1,2)	(1,3)	(1,3)	(1,5)
λ_c^{max}=1/(7 day)	(1,2)	(1,2)	(1,2)	(1,2)	(1,2)
λ_c^{max}=1/(14 day)	(1,2)	(1,2)	(1,2)	(1,2)	(1,2)

Tables 1 and 2 summarize the optimal (m_p,m_s) under low and high pavalues, respectively, when there are selective capture and random + opportunistic + insidious attacks. We observe that the more hidden the inside attackers are, that is, as padecreases, the more (m_p, m_s) redundancy is required to cope with the bad node population accumulated due to misses in intrusion detection. This is evidenced by comparing optimal (m_p,m_s) settings listed in Tables 1 and 2 for the same λ_c^{max} and T_{IDS}.

Next we analyze the effect of $P_{all\text{-}in}$ (the all-in attack percentage population threshold MTTF of a WSN subject to selective capture with random + opportunistic + insidious attacks. We first note that a small $P_{all\text{-}in}$ means that malicious nodes will perform all-in attacks early on (i.e., setting P_a=1) as soon as it senses the small percentage population threshold is reached. On the other hand, a large $P_{all\text{-}in}$ means that malicious nodes will stay hidden until the large percentage population threshold is reached.

Table 3 summarizes this trend with P_a= 0.1 over a wide range of λ_c^{max} values. This seemingly odd trend has a logical explanation. That is, when $P_{all\text{-}in}$ is very small (say 0-10%), this critical mass of malicious nodes can be reached early on after which P_a becomes 1 (jumping from 0.1) for all-in attacks. So malicious nodes can be easily detected and the system should just use moderate detection strength to balance energy consumption with detection rate. As $P_{all\text{-}in}$ increases further (say 10-20%), malicious nodes stay hidden until the all-in attack percentage population threshold is reached, so the system should use high detection strength to remove malicious nodes to prevent this critical mass from reached. Finally as $P_{all\text{-}in}$ continues to increase past a high threshold (say >25%), insidious attacks will be ineffective since it is un-likely such a high critical mass can be reached, given that P_a= 0.1 so a bad node performing random attacks can still be detected by the IDS. The system in this case is better off using just moderate detection strength to balance the energy consumption rate with the IDS detection rate.

TABLE 3: OPTIMAL TIDS UNDER VARYING λ_c^{max} AND $P_{all\text{-}in}$(WITH p_a =0.1)

	$P_{all-in}=0.0$	0.1	0.15	0.2	0.25
$\lambda_c^{max}=1/(0.5$ day)	0.75	0.75	0.25	0.125	0.5
$\lambda_c^{max}=1/(1$ day)	1	1	0.5	0.25	0.5
$\lambda_c^{max}=1/(2$ day)	2	2	0.75	0.25	1
$\lambda_c^{max}=1/(3$ day)	3	3	0.5	0.25	3

Finally, Table 4 summarizes the optimal (m_p,m_s) settings (representing multipath multisource redundancy for intrusion tolerance) to maximize MTTF obtainable under varying P_{all-in} settings. We fix T_{IDS} to 0.5 hrs to isolate its effect.

TABLE 4: OPTIMAL (m_p, m_s) UNDER VARYING λ_c^{max} AND P_{all-in}(WITH T_{IDS} = 0.5 AND p_a = 0.1).

	$P_{all-in}=0.0$	0.1	0.2	0.3
$\lambda_c^{max}=1/(0.5$ day)	(1,2)	(1,3)	(1,3)	(2,4)
$\lambda_c^{max}=1/(1$ day)	(1,2)	(1,2)	(1,3)	(1,5)
$\lambda_c^{max}=1/(2$ day)	(1,2)	(1,2)	(1,2)	(2,2)
$\lambda_c^{max}=1/(3$ day)	(1,2)	(1,2)	(1,2)	(2,2)

We can see from Table VI that as p_{all-in} increases attackers become more hidden, and, consequently, a higher level of (m_p,m_s)redundancy is required to cope with the bad node population accumulated due to misses in intrusion detection. This finding is consistent with that drawn from Tables 1and2.

Conclusion

Proposed and analyzed adaptive network defence management with three defences for coping with selective capture and smart attack aiming to create holes without base station in a wireless sensor network to block data delivery. Through numerical analysis, we demonstrated that our defences are effective against selective capture and smart attack. There exist best protocol settings in terms of the best radio adjustment, the best redundancy level for multipath routing, the best number of voters, and the best intrusion invocation interval used for intrusion detection to maximize the system lifetime. Leveraging the analysis techniques developed in this paper, one can obtain optimal protocol settings at design time, store them in a table, and apply a simple table lookup operation at runtime with interpolation to determine optimal settings for adaptive network defence management to maximize the system lifetime without runtime complexity. This paper considers three defences against selective capture attacks. We propose selective deployment, i.e., populating more critical nodes than edge nodes to effectively counter selective capture. We also plan to further refine the inside attacker behaviour model, and extend the analysis to homogeneous or heterogeneous clustered WSNs, without a BS. Finally, we also plan to investigate the use of trust/reputation management to strength-en intrusion detection through "weighted voting," lever-aging the knowledge of trust/reputation of neighbour nodes, as well as to tackle the "what paths to use" problem in multipath routing for intrusion tolerance in WSN's.

References

1. R.Mitchell, and I.R,Chen,"A Survey of Intrusion detection in wireless Networks,"Computer Communication, vol, 42' April 2014,pp.1-23.

2. R.Mitchell and I.R.Chen,"Effect of intrusion detection and Response on Reliability of Cyber Physical System,"IEEE transactions on Reliability,vol.62, no.1,pp,199-210,2013.

3. C.Karlof and D.Wagner,"Secure routing in wireless sensor networks:attacks and defences,"1st IEEE Int, Workshop on Sensor Protocols and applications , 2003,pp.113-127.

4. I.M.Atakli, H.Hu,Y,Chen,W.S.Ku, and Z. Su,"Malicious node detection in wireless sensor networks using weighted trust evaluation,"Spring simulation multiconference, 2008, pp.836- 843.

5. G.Bravos and A.G.Kanatas,"Energy consumption and tradeoffs on wireless sensor networks,"16th IEEE Int. Simon personal, indoor and Mobile Radio Communication, 2005, pp, 1279-1283.

6. S.Qun,"Power Management in Networked Sensor Rasios A Netwoek Energy Model,"IEEE Sensors Application Symp., 2007,pp.1-5

7. O.Younis and S.Fahmy, "HEED: a hybrid, energy – efficient, distributed clustering approach for ad hoc sensor networks, "IEEE Trans.Mobile Compute., vol.3,no.4,pp.366-379,2004.

8. Y.Lan, L.Lei, and G.Fuxiang,"A multipath secure routing protocol based on malicious node detection,"Chinese Control and Decision Conference, 2009, pp. 4323-4328.

9. D.Somasundaram and R.Marimuthu,"A Multipath Reliable Routing for detection and isolation of malicious

nodes in MANET,"International Conf.on Computing, Communication and Networking, 2008, pp.1-8

10. V. Bhuse and A.Gupta,"Anomaly intrusion detection in wireless sensor networks, "High Speed Networks, vol.15, no. 1, pp.33-51, 2006.

11. S. Rajasegarr, C.Leckie, and M.Palaniseami, "Anomaly detection in wireless sensor networks,"IEEE Wireless Communications, vol.15, no.4, pp.34-40, 2008.

12. A.R.P.daSilva, et al.,"Decentralized intrusion detection in wireless sensor networks,"1st ACM Workshop on Quality Service& Security in wireless and Mobile Networks, Montreal, Quebec,Canada,2005.

Author's details

[1]PG Scholar, Department of Computer Science and Engineering (with specialization in Networks), Arunai Engineering College, Tiruvannamalai, India, Email: shamu.ragav@gmail.com

[2]Assistant Professor, Department of Computer Science and Engineering, Arunai Engineering College, Tiruvannamalai, India. Email: reachdivakar@gmail.com.

Copy for Cite this Article- M. Shamuganapriya and S. Divakar, 'Countering Smart Attack and Selective Capture in Wireless Sensor Networks Using Genetic Algorithm,' *International Journal of Science, Engineering and Technology,* Volume 4 Issue 1: 2016, pp. 274-280.

Vikas Kumar et al. 2016, Volume 4 Issue 1
ISSN (Online): 2348-4098
ISSN (Print): 2395-4752

International Journal of Science, Engineering and Technology
An Open Access Journal

Study on 3D Visual Attention for Stereoscopic Image Quality and Compression Assessment

[1]Vikas Kumar, [2]Sanjay Sharma

Abstract

Three-dimensional (3D) images different from traditional two-dimensional (2D) images. Therefore, 3D visual attention will be advantageous to improve 3D visual experience and particularly depth perception. Different combination and modulation means of the 3D visual attention model for quality assessment are investigated. Stereoscopic compression can be achieved by either compression across both views simultaneously, or independently compressing the left and right views separately.

Keywords: Stereo images, Symmetric, asymmetric compression, quality matrices

Introduction

Stereoscopy is a technique for creating or enhancing the illusion of depth in an image by means of stereopsis for binocular vision. Stereoscopic vision was first systematically studied by Wheatstone in the early 1800s and the production of 3D films can be dated back to 1903. Since then, numerous 3D films have been produced, culminating in the breakout success of Avatar in 2009, which went on to become the highest-grossing film of all time.

The success of Avatar has since greatly inspired further efforts in 3D film production and improved technologies and methods for 3D content capture and display. Indeed, the wave of 3D has not been limited to the theater screen. In 2011, mobile phones supporting 3D capture and viewing are now available, the number of released 3D films has tripled compared to the number in 2008, and broadcast 3D content over the Internet is becoming common. With the release of 3D phones and 3D broadcast services, it is reasonable to believe that the amount of 3D content that is delivered by wireless and wireline will follow the trend of consumer video and increase exponentially over the next few years. Given an increasing clogged communication infrastructure, being able to monitor and maintain the integrity of 3D video streams is of high interest. Most stereoscopic methods present two offset images separately to the left and right eye of the viewer. A stereoscopic image require an increase in storage space compared to monoscopic images, the compression of stereo images is one of the most important factors to enable the extensive use of three-dimensional systems. Three-dimensional (3D) technologies have received wide attention as a result of great push from the industry and academia [1,2]. The necessity for designing perceptual 3D image quality assessment (3D-IQA) approach is increasingly important [3], since such perceptual issues in 3D are hardly considered in the traditional 2D image quality assessment (2D-IQA). The research of 2D-IQA, 3D-IQA approaches can fall into two categories:

(I) Subjective assessment and
(II) Objective assessment.

Subjective data is essential in understanding the impact of asymmetric distortion on the perceptual quality of stereoscopic images. Ideally, we would need a complete set of subjective test on an image database that contains both 2D (single-view) and stereoscopic 3D images, both symmetrically and asymmetrically distorted images at different distortion levels, as well as both single- and mixed distortion images.

Symmetric and asymmetric encoding of stereo Image

Symmetric encoding of the image pair is when the left and right images are compressed by equal amounts resulting in equal degradation. Asymmetric encoding is when the compression and therefore degradation of the left and right images is unequal. Symmetric and asymmetric encoding of compressed images was analyzed using both Peak Signal to

Noise Ratio (PSNR) and a subjective human factors study. Photographic, computer generated photo realistic and computer generated non-photo realistic test images are compressed, symmetrically and asymmetrically, using JPEG and, in each case a constant file size was maintained between the pairs.

In symmetric encoding, First, the left image is independently coded. Then the right image is divided into non-overlapping blocks. Either fixed or variable size blocks are used. Each of these blocks is shifted horizontally and compared to the corresponding blocks in the coded left image using some (MSE, SAD, etc.) measure to determine the similarity between the two blocks. The most similar block, is the disparity compensated prediction, and the corresponding translation is the disparity for the block. Given the right image that is to be encoded and a disparity vector field, there are a variety of coding strategies that may be used. For example, the residual of the disparity compensated prediction may be encoded and transmitted.

Proposed Methodology

According to Double Stimulus Continuous Quality Scale (DSCQS) testing method described in ITUR recommendation BT.500-11, the subjective ratings for the distorted stereoscopic images were obtained on a scale of 0-100. The database includes 12 original stereoscopic image pairs, from which 312 distorted stereoscopic images are generated with five types of distortion: JPEG, JPEG2000, Gaussian Blur, White Noise and H.264.

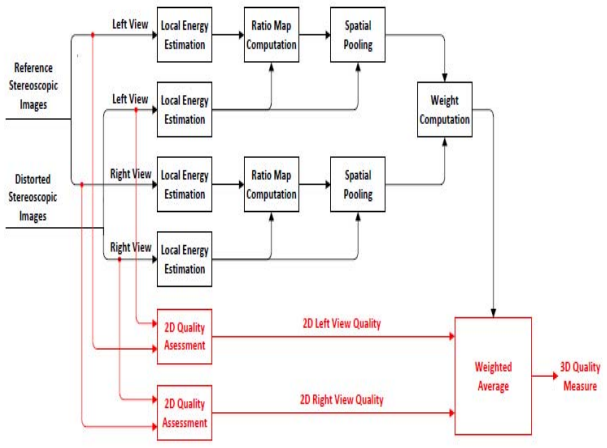

Figure 1: Diagram of the proposed 2D-to-3D quality prediction model.

Symmetric and asymmetric compression Technique

As stereoscopic images require an increase in the bandwidth compared to monoscopic images, the compression of stereo images is one of the most important factors that must be evaluated to enable the extensive use of three dimensional systems. The space required to store a stereoscopic image is normally twice the amount need to store a monoscopic one. Similarly, for stereoscopic video, twice the bandwidth is required. Symmetric compression of a stereoscopic image pair is when the same amount of compression is applied to the left and right image within the pair. If a different amount of compression is applied to each image within the pair, then the stereoscopic image is said to be compressed asymmetrically.

MSE is the differences between corresponding pixels of the reference and the distorted images:

$$MSE=\frac{1}{M*N}\sum_{m=1,n=1}^{M,N}|I(m,n)-I_D(m,n)|^2$$

Where M*N=Image Size

I(m,n) and Id(m,n)= Pixels of reference and distorted image

$$PSNR=10log_{10}\frac{MAX_I}{MSE}$$

Expected Outcomes

The major contributions in my project are as following:

(I) We created a new subjective 3D-IQA database that has two unique features (the inclusion of both 2D and 3D images, and the inclusion of mixed distortion types).

(II) We observe strong distortion type dependent bias when using direct averaging 2D image quality of both views to predict 3D image quality. To further advance the performance of current 3D QA models, we think that the effect of depth masking and depth quality needs to be further studied and addressed. Furthermore, while we did not find depth masking of distortions, we did find evidence of facilitation which may prove relevant to 3D QA. Of course, the disparity cue is not the only one used by the human visual system to perceive depth. For example, monocular cues such as occlusion, relative size, texture gradient, perspective distortion, lighting,

shading, and motion parallax all affect the perception of depth. It is not yet clear how the brain integrates all these cues to produce an overall sensation of depth.

Conclusions

The prominent advantage of the proposed method is that we construct the 3D visual attention model by applying two-dimensional (2D) saliency model, center bias, depth cue (foreground and background), and investigate various combination and modulation means for quality assessment task. It can be observed from the experimental results show that the proposed method can achieve much higher consistency with the subjective assessments.

References

[1] A. Smolic, P. Kauff, S. Knorr, A. Hornung, M. Kunter, M.Muller, and M. Lang, "Three-dimensional video postproduction and processing," Proceedings of the IEEE,vol. 99, no. 4, pp. 607-625, April 2011.

[2] C. Wheatstone, Contributions to the physiology of vision. Part the first. On some remarkable, and hitherto unobserved phenomena of binocular vision, Philosophical Transactions of the Royal Society of London 128 (1838) 371–394.

[3] P. Geng, H. Jiang, and Z. Zhang, "A video denoising method with 3D surfacelet transform based on block matching and grouping," Journal of Computers, vol. 7,no. 5, pp. 1065-1066, 2012.

[4]. P. Seuntiens, L. Meesters, and W. IJsselsteijn, "Perceived quality of compressed stereoscopic images:effects of symmetric and asymmetric jpeg coding and camera separation," ACM Trans. Applied Perception, vol. 3, no. 2, pp. 95–109, April 2006.

[5]. A. Aksay et al., "End-to-end stereoscopic video streaming with contentadaptive rate and format control,"Signal Processing: Image Communication, vol. 22, pp. 157–168, 2007.

[6]. .S.Pastoor, "Human Factors of 3D Imaging", HHIBerlin, http://atwww.hhi.de

[7], G. Saygili, C. Gurler, and A. Tekalp, "Quality assessment of asymmetric stereo video coding," in Proc. ICIP, 2010.

[8] P. Aflaki, M. Hannuksela, J. Hakkinen, P. Lindroos, and M. Gabbouj, "Subjective study on compressed asymmetric stereoscopic video," in Proc. ICIP, 2010.

[9]. L. Stelmach and W. Tam, "Stereoscopic image coding: Effect of disparate image-quality in left- and right-eye views," in Singal Processing: Image Communication, 1998.

[10] J. You, L. Xing, A. Perkis, and X. Wang, "Perceptual quality assessment for stereoscopic images based on 2D image quality metrics and disparity analysis," in Workshop on Video Processing and Quality Metrics, Scottsdale, AZ, 2010.

[11]. M. Chen, L. K. Cormack, and A.C. Bovik, "No-reference quality assessment of natural stereopairs," IEEE Trans. on Image Process., vol. 22, no. 9, pp. 3379–3391, 2013.

[12]. K. Moorthy, C. Su, A. Mittal, and A.C. Bovik, "Subjective evaluation of stereoscopic image quality," Signal Processing: Image Communication, vol. 28, no. 8, pp. 870–883, 2013.

[13] List of 3D Movies. URL ⟨http://en.wikipedia.org/wiki/List_of_3-D_films⟩.

[14] ESPN, ESPN 3D Broadcasting Schedule. URL ⟨http://espn.go.com/3d/schedule.html⟩.

[15]. J. Burge, M.A. Peterson, S.E. Palmer, Ordinal configural cues combine with metric disparity in depth perception, Vision 5 (6), Journal of Vision June 22, 2005, http://dx.doi.org/10.1167/5.6.5.

Author's details

[1]M.Tech. Scholar, Department of ECE, Millennium Institute of Technology & Science, Bhopal, M.P., India.

[2]Assistant Professor, Department of ECE, Millennium Institute of Technology & Science, Bhopal, M.P., India.

Copy for Cite this Article- Vikas Kumar and Sanjay Sharma, 'Study on 3D Visual Attention for Stereoscopic Image Quality & Compression Assessment,' *International Journal of Science, Engineering and Technology,* Volume 4 Issue 1: 2016, pp. 281- 283.

Sathishkumar.P et al. 2016, Volume 4 Issue 1
ISSN (Online): 2348-4098
ISSN (Print): 2395-4752

International Journal of Science, Engineering and Technology
An Open Access Journal

Significance of Various Fibres on Engineered Cementitious Concrete

[1]Sathishkumar. P, [2]Sampathkumar. P, [3]Karthik. M, [4]Vignesh. C

Abstract

Engineered Cementitious Composites (ECC) is an ultra-ductile fibre reinforced cementitious material that embodies a micromechanics based design concept. The tensile ductility and self-controlled tight crack width characteristics are conducive to enhancing structural safety under severe loading, and durability under normal service loading. The cost of ECC is currently about three times that of normal concrete per cubic Feet. However, a number of commercial projects in Japan and Australia have already demonstrated that initial construction cost saving can be achieved when ECC is used, through smaller structural member size, reduced or eliminated steel reinforcement, elimination of other structural protective systems, and faster construction offered by the unique fresh and hardened properties of ECC, The advantages offered by ECC over conventional concrete become even more compelling. ECC is a field-ready ductile concrete that has the potential to significantly contribute to enhancing infrastructure safety, durability and sustainability. This thesis aims at making ECC with a mix which satisfies the strength characteristics required. Therefore various trial mixes are cast and the mix design is finalised. Polyvinyl alcohol fibres, Polyethylene fibres, Polyester fibres and Polypropylene fibres are added in various proportions (0.5 %, 1%, 1.5% and 2% by weight of cement) and the strengths are compared. Cubes, Cylinders and beams are cast and the Compressive, Split tensile and Flexural Strengths are to be compared

Keywords: ECC, ultra-ductile, Polyvinyl alcohol fibres, Polyester fibres, Polypropylene fibres,.etc.

Introduction

Concrete is ubiquitous. Annually, more than one ton per capita of concrete is cast for infrastructure construction worldwide. By many measures, concrete is an excellent construction material. However, the mechanical properties and functional characteristics of concrete will have to be improved, in some ways drastically, and these improvements are already emerging in limited forms. These advancements are needed to address deficiencies in concrete infrastructure, currently facing three major challenges

Engineered Cementitious Composite (ECC) is an easily molded mortar-based composite reinforced with specially selected short random fibers, usually polymer fibers. Unlike regular concrete, ECC has a strain capacity in the range of 3–7%, compared to 0.1% for ordinary Portland cement (OPC). ECC therefore acts more like a ductile metal than a brittle glass (as does OPC concrete), leading to a wide variety of applications. ECC, unlike common fibre material. This means that the mechanical interactions between ECC's fiber and matrix are described by a micromechanical model, which takes into account material properties and helps predict properties and guide ECC development.

Properties of ECC

ECC has a variety of unique properties, including tensile properties superior to other fiber-reinforced composites, ease of processing on par with conventional cement, the use of only a small volume fraction of fibers (~ 2%), tight crack width, and a lack of anisotropically weak planes. These properties are due largely to the interaction between the fibers and cementing matrix, which can be custom-tailored through micromechanics design. Essentially, the fibers create many microcracks with a very specific

[1]Corresponding Author's Email: psk.bvn@gmail.com

width, rather than a few very large cracks (as in conventional concrete.) This allows ECC to deform without catastrophic failure. This microcracking behavior leads to superior corrosion resistance (the cracks are so small and numerous that it is difficult for aggressive media to penetrate and attack the reinforcing steel) as well as to self-healing. In the presence of water (during a rainstorm, for instance) unreacted cement particles recently exposed due to cracking hydrate and form a number of products (Calcium Silicate Hydrate, calcite, etc.) that expand and fill in the crack. These products appear as a white 'scar' material filling in the crack. This self-healing behavior not only seals the crack to prevent transport of fluids, but mechanical properties are regained. This self-healing has been observed in a variety of conventional cement and concretes; however, above a certain crack width self healing becomes less effective. It is the tightly controlled crack widths seen in ECC that ensure all cracks thoroughly heal when exposed to the natural environment.

Literature Review

In order to improve certain properties of concrete, it has been an accepted technology to use fly ash and various types of fibres in concrete. In this thesis, fly ash acts as a major ingredient in ECC and fibres like PVA, Polyethylene and Polypropylene are also used to improve the tensile characteristics of ECC. Super plasticizer is also used to improve the workability property of ECC. This chapter deals with the collection of various data and results from journals, websites, etc. related to the behavioural study of various fibres that are used in fibre reinforced concrete.

Based on the literatures, it is observed that ECC has major content of fly ash and so the gain of strength in initial stages will be minimum. So later strength for concrete should be tested for trial mixes.

Trial mixes for ECC are adopted and specimens are cast for testing for 7 days, 28 days and 56 days. And then a superior mix is selected, to which Polyvinyl alcohol, Polyethylene Polypropylene and Polyester fibres are added and are tested for mechanical strengths.

Water cement ratio is varied and the mix is tested for compressive strengths. The optimum mix is chosen for the above fibres. These fibres on addition are tested for compressive, split tensile and flexural strengths.

Experimental Investigation

The main objective of the thesis is to study the behavior of ECC with Polyvinyl Alcohol fibres, Poly Propylene fibres, Polyester fibres and polyethylene fibres and comparing the results.

The mechanical parameters such as compressive strength, split tensile strength and flexural strengths were investigated. Properties of the materials used for casting concrete samples are evaluated.

Materials Used

Cement: 53 grade OPC is used for all concrete sample mixes. The cement used was fresh and without any lumps. Testing of cement was done as per IS: 8112 – 1989.

Coarse aggregates: Locally available coarse aggregates having the maximum size of 20 mm is used in the present work. Testing of coarse aggregates is done as per IS: 383 – 1970.

Fine aggregates: The sand used for the experimental work is locally procured and conformed to grading zone II as per IS: 383 – 1970.

Fly Ash: Fly ash is one of the residues generated in combustion, and comprises the fine particles that rise with the flue gases. Ash which does not rise is termed bottom ash. In an industrial context, fly ash usually refers to ash produced during combustion of coal. Fly ash is generally captured by electrostatic precipitators or other particle filtration equipment before the flue gases reach the chimneys of coal-fired power plants and together with bottom ash removed from the bottom of the furnace is in this case jointly known as coal ash.

'Class F' Fly ash was obtained from the Mettur Thermal Power Plant situated at 40 kilometers from the Institution.

Polypropylene fibre

There is a sterically regular atomic arrangement in the polymer molecule and high crystallinity. Due to regular structure, it is known as isotactic polypropylene. Chemical inertness makes the fibers resistant to most chemicals. Any chemical that will not attack the concrete constituents will have no

effect on the fiber either. On contact with more aggressive chemicals, the concrete will always deteriorate first. The hydrophobic surface not being wet by cement paste helps to prevent chopped fibers from balling effect during mixing like other fibers. The water demand is nil for polypropylene fibers. The orientation leaves the film weak in the lateral direction which facilitates fibrillations. The cement matrix can therefore penetrate in the mesh structure between the individual fibrils and create a mechanical bond between matrix and fiber.

Polyvinyl Alcohol Fibre

Polyvinyl alcohol (PVA) fiber was created 50 years ago as the first Japanese organic fiber and, it has been used for various applications since then. Especially, PVA fiber has been used globally in a wide range of cement applications since 1980s owing to some suitable characteristics as reinforcing materials for cementitious composites.

At the first, PVA fiber has high tenacity and modulus of elasticity compare with other general organic fiber. Second, bonding strength between fiber and cement matrix is strong. Also it is possible to control bonding strength by surface treatment. At last, good durability has been proved by long terms field test, and it has been used as fiber cement slate over twenty years because PVA fiber has got wide acceptance as a less hazardous and reasonable cost alternative.

In recent years, new type of PVA fiber for high performance fiber reinforced cementitious composites (HPFRCC) has been developed owing to development of theoretical study based on micromechanics. This fiber also starts to use widely because of its suitable characteristics for reinforcing cementitious composites.

Polyethylene Fibres

A semi-crystalline, whitish and effectively opaque engineering thermoplastic which, chemically, is a very high molecular weight (3-6 million) HDPE. As a result it has an extremely high melt viscosity and normally can only be processed by powder sintering methods. It also has outstanding toughness and cut and wear resistance and very good chemical resistance, somewhat better than that of HDPE. Applications include many "wear parts" (eg bottle handling machine components), gears, bearings, artificial joints and marine quay headings. Fibres of very high molecular orientation can also be made from polyethylene of very high molecular weight by gel spinning and subsequent drawing to give fibres which are reported to be up to 85% crystalline and with 95% parallel orientation. They are known as Ultra High Modulus or High Performance Polyethylene fibre (UHMPE or HPPE). Like Kevlar, these fibres have very high tensile properties and (small) negative CTE's. On a volume basis, their tensile properties are broadly similar to Kevlar's but, on a weight basis, they are superior thanks to an almost 50% density advantage - but they are not up to the properties of carbon fibre on either basis. Their energy absorption and acoustic velocity characteristics are superior to Kevlar's both as fabric and composite. Applications are being developed particularly in the areas of ballistic protection and ropes (in the widest sense).

Polyester Fibres

Polyester is a category of polymers which contain the ester functional group in their main chain. Although there are many types of polyester, the term "polyester" as a specific material most commonly refers to polyethylene terephthalate (PET). Polyesters include naturally occurring chemicals, such as in the cutin of plant cuticles, as well as synthetics through step-growth polymerization such as polycarbonate and polybutyrate. Natural polyesters and a few synthetic ones are biodegradable, but most synthetic polyesters are not. Depending on the chemical structure, polyester can be a thermoplastic or thermoset, there are also polyester resins cured by hardeners; however, the most common polyesters are thermoplastics. Polyester fibers are designed as a new version of crack proof materials specially for asphalt-based concrete. They are produced by unique processes and based on polyester synthetic materials as fundamental raw materials. They can form structures in three dimensional distributions after putting them into asphalt gels by mixing, which have function of reinforcement so that effectively prevent asphalt-based concrete from cracking.

Water: Potable water is used for the concrete preparation and for the curing of specimens.

ECC Mix Design

Since there is no definite procedure for the mix design of ECC, trial and error method is adopted by

varying the water content and the super plasticizer in the mix. And the rich mix is to be selected and casted with PVA, PET, PP and PE fibres.

Table -1: ECC Mix Design

Mix	Cement	Sand	Fly ash	Water	SP	Fibres
Mix 1	583	467	1.2	298	19	11.66
Mix 2	561	449	327	14	14	11.22
Mix 3	576	460	691	306	17	11.52

Table-2: Compressive test results for ECC specimens.

Fibres %	7 days N/mm2	28 days N/mm2	56 days N/mm2
PVA 1%	36.83	49.12	57.63
PVA 1.5%	37.14	50.16	58.56
PVA 2%	38.93	51.06	58.87
PVA 2.5%	38.08	50.54	58.62
PET 1%	35.45	48.96	56.12
PET 1.5%	35.72	49.23	56.87
PET 2%	36.29	49.89	57.54
PET 2.5%	35.86	49.36	56.97
PP 1%	34.13	48.23	54.34
PP 1.5%	34.8	48.65	55.12
PP 2%	35.16	49.12	55.98
PP 2.5%	34.86	48.79	55.53
PE 1%	33.87	47.54	54.17
PE 1.5%	34.14	47.92	55.32
PE 2%	34.52	48.23	55.88
PE 2.5%	34.36	47.88	55.64

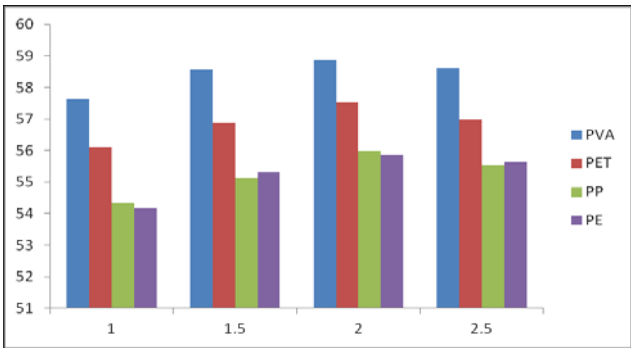

Chart -1: Comparison of Compressive strengths for all ECC specimens

Table -3: Split tensile test results for ECC specimens

Fibres %	7 days N/mm2	28 days N/mm2	56 days N/mm2
PVA 1%	2.95	4.16	4.85
PVA 1.5%	3.16	4.86	5.56
PVA 2%	3.69	5.23	5.84
PVA 2.5%	3.21	4.73	5.43
PET 1%	2.91	4.15	4.56
PET 1.5%	3.15	4.56	4.74
PET 2%	3.36	4.72	4.96
PET 2.5%	3.12	4.6	4.82
PP 1%	2.89	4.12	4.32
PP 1.5%	2.96	4.25	4.43
PP 2%	3.16	4.46	4.68
PP 2.5%	3.02	4.29	4.52
PE 1%	2.87	4.11	4.26
PE 1.5%	2.92	4.26	4.39
PE 2%	3.11	4.42	4.7
PE 2.5%	2.97	4.31	4.48

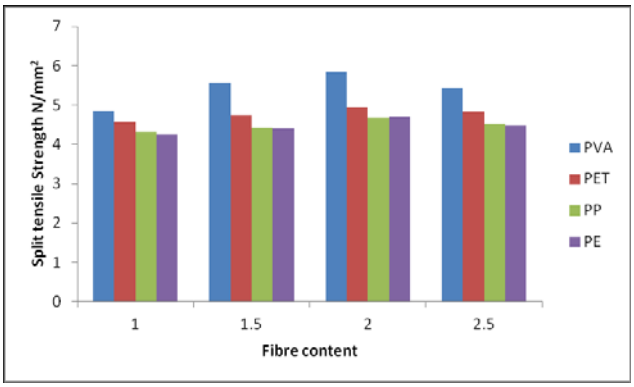

Chart -2: Comparison of Split tensile strengths for all ECC specimens

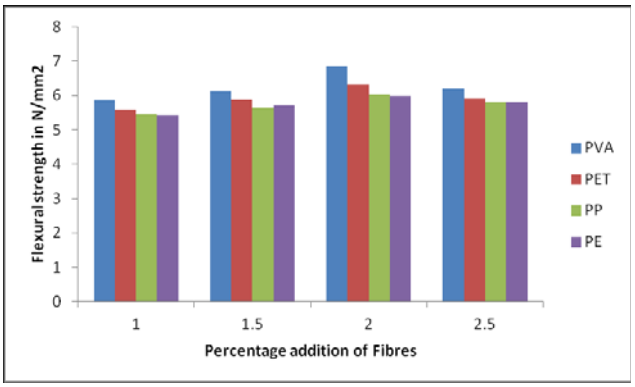

Chart -3: Comparison of Flexural strengths for all ECC specimens

Table 4: Flexural strength test results for ECC specimens

Fibres %	7 days N/mm2	28 days N/mm2	56 days N/mm2
PVA 1%	3.67	5.16	5.86
PVA 1.5%	3.79	5.24	6.12
PVA 2%	4.12	5.66	6.84
PVA 2.5%	3.84	5.2	6.2
PET 1%	3.56	5.08	5.6
PET 1.5%	3.71	5.2	5.89
PET 2%	3.98	5.51	6.32
PET 2.5%	3.69	5.18	5.91
PP 1%	3.44	4.92	5.45
PP 1.5%	3.58	5.16	5.63
PP 2%	3.79	5.38	6.02
PP 2.5%	3.62	5.19	5.8
PE 1%	3.42	4.88	5.42
PE 1.5%	3.52	5.08	5.71
PE 2%	3.69	5.42	5.98
PE 2.5%	3.59	5.24	5.82

From the results it can be noted that the 28 days test results are not as expected, but when the specimens are tested for 56 days it gives satisfying results. Since flyash is added the specimens attain its full strength at later age.

Results and Discussions

Observations

All fibre types have the potential to "ball up" in concrete. This phenomenon is usually caused by addition of fibres into concrete mixes that are too dry or into mixtures that do not have enough fine particles to coat the fibre particles, which in turn "paste starves" the system and again causes the slump to decrease to zero. Loose fibres in an empty drum may clump together and fibre types that are too long or have varying geometries may also cause problems. A test trial should be performed to ensure that the mixture will support the fibre type and dosage and that the batching sequence will not cause any problems. If necessary, the use of a water reducing admixture may be warranted to maintain the desired slump for placement.

Balling effects were observed in the initial trial mix. These were eliminated in further mixes by distributing the fibres evenly in the mix while the mixing drum is operated and water is added after mixing the dry mix for 5 minutes. The mix after addition of fibres is less workable. Therefore superplasticizer is added to retain the workability.

Figure 1: Balling or Clumping

Fibre Selection and Orientation

Microfibres uniformly distributes multi-dimensionally throughout the concrete mixture. The extremely high number of fibres in the fresh concrete matrix protects the concrete when its tensile strength is lowest, reducing the formation of plastic shrinkage cracking. This cracking and other internal stresses would otherwise permanently weaken the resulting concrete. The concrete permeability is decreased, while surface characteristics, impact and toughness properties are improved.

The aspect ratio of a fibre is the length of a single fibre divided by its equivalent diameter (L/d). This term is generally only used with larger fibres such as steel and macro-synthetics and while a specific value is not important, aspect ratios of greater than 100 can sometimes cause placement and finishing difficulties. Ideally the aspect ratio should be as low as possible to minimize the loss of workability and as high as possible to maximize the resistance of fibres to pull out from the matrix.

During crack opening, the bridging stress increases as fibre/matrix interfaces debond and the debonded segments of fibres stretch. When the bridging stress increases to the magnitude of the applied load, the crack flanks flatten to maintain the constant applied stress level. This load level is termed the steady state cracking stress. This explains why microfibres are used. Because any fibres will have frictional and chemical bonds with the interface and with polymer fibres the bond is more dominant and when the crack develops this bond strength and reduced length restricts the specimen to fail.

Conclusion

From the results, it is noted that PVA fibre content gives better results, followed by Polyethylene, Polyester and Polypropylene. Polyester and Polypropylene shows similar results.

Table 4: Percentage increase on addition to fibres when compared to control specimen

Fibres %	7 days N/mm2	28 days N/mm2	56 days N/mm2
PVA 1%	2.95	4.16	4.85
PVA 1.5%	3.16	4.86	5.56
PVA 2%	3.69	5.23	5.84
PVA 2.5%	3.21	4.73	5.43
PET 1%	2.91	4.15	4.56
PET 1.5%	3.15	4.56	4.74
PET 2%	3.36	4.72	4.96
PET 2.5%	3.12	4.6	4.82
PP 1%	2.89	4.12	4.32
PP 1.5%	2.96	4.25	4.43
PP 2%	3.16	4.46	4.68
PP 2.5%	3.02	4.29	4.52
PE 1%	2.87	4.11	4.26
PE 1.5%	2.92	4.26	4.39
PE 2%	3.11	4.42	4.7
PE 2.5%	2.97	4.31	4.48

Also when the results are compared for Percentage addition of fibres, it is clear that the results first increases when the fibre content is increased, but later when the fibre content increases from 2% to 2.5% some workability issues were found and also the strength decreases. Therefore the PVA 2% gives maximum compressive, split tensile and flexural strengths. Percentage increases of the results are shown in table.

The results show that PVA 2% gives higher test results, i.e ECC – PVA 2% gives 7.25% higher

compressive strength and 38.05% higher tensile strength and 68.05% higher flexural strength than that of conventional concrete specimen.

Also the specimen doesn't fail suddenly; it gives fair amount of warning before failure. A visible deflection can be seen in the beam before failure. Numerous microcracks form and then a crack develop and failure occurs.

References

[1]. Reinforced Concrete Committee 1966. "Damage Investigation Report on Concrete Buildings, the 1995 Hyogo-ken Nanbu Earthquake" (in Japanese), Kinki Branch, Architectural Inst. of Japan.

[2]. Malvar, L.J. and Ross, C.A. 1998. "Review of strain rate effects for concrete in tension," ACI Materials Journal 95(6): 735-739.

[3]. Li, V.C., 1998. "ECC – tailored composites through micromechanical modeling." Fiber Reinforced Concrete: Present and the Future edited by Banthia et al, CSCE, Montreal, 64-97.

[4] Lin, Z., Kanda, T. and Li, V.C., 1999. "On interface property characterization and performance of fiber reinforced cementitious composites," J. Concrete Science and Engineering, RILEM, 1, 173-184.

[5]. US EPA. 2000. "Sources of dioxin-like compounds in the US. Draft exposure and human health reassessment of 2,3,7,8-tetrachlorodibenzo-p-dioxin (TCDD) and related compounds."

[6]. Worrell, E., L. Price, N. Martin, C. Hendriks & L. Ozawa Meida. 2001. "Carbon dioxide emissions from the global cement industry." Ann. Rev. of Energy and Environment. 26: 303-329.

[7]. Li, V.C., Wang, S., and Wu, C., 2001. "Tensile strain-hardening behavior of PVA-ECC," ACI Materials J., 98 (6) 483-492.

[8]. WBCSD 2002. "Toward a Sustainable Cement Industry." Draft report for World Business Council on Sustainable Development. Battelle Memorial Institute.

[9]. Li, V.C., 2003. "On Engineered Cementitious Composites (ECC) – A review of the material and its applications." J. Advanced Concrete Technology, 1(3): 215-230.

[10]. Kong, H.-J., Bike, S. and Li, V.C., 2003. "Development of a self-compacting ECC employing electrosteric dispersion/stabilization," J. Cement and Concrete Composites, 25(3): 301-309.

[11]. Kim, Y.Y., Kong H.J., and Li, V.C., 2003. "Design of Engineered Cementitious Composite (ECC) suitable for wet-mix shotcreting," ACI Materials J., 100(6):511-518.

[12]. ASCE, 2005. US Infrastructure Report Card, http://www.asce.org/reportcard/2005/index.cfm.

[13]. Shetty M.S., "Concrete Technology".

Author's details

[1]Assistant Professor, Department of Civil Engineering, Muthayammal College of Engineering, TamilNadu, India, Email: psk.bvn@gmail.com

[2]Assistant Professor, Department of Civil Engineering, Muthayammal College of Engineering, TamilNadu, India, Email: psk.sambath@gmail.com

[3]P.G. Student, Department of Civil Engineering, Muthayammal College of Engineering, TamilNadu, India, Email: mkarthik.civil@gmail.com

[4]P.G. Student, Department of Civil Engineering, Muthayammal College of Engineering, TamilNadu, India, Email: vignesh23692@gmail.com.

Copy for Cite this Article- Sathishkumar. P, Sampathkumar. P, Karthik. M and Vignesh. C, 'Significance of Various Fibres on Engineered Cementitious Concrete,' *International Journal of Science, Engineering and Technology,* Volume 4 Issue 1: 2016, pp. 284- 290.

Shakuntala Satyawana et al. 2016, Volume 4 Issue 1
ISSN (Online): 2348-4098
ISSN (Print): 2395-4752

International Journal of Science, Engineering and Technology
An Open Access Journal

Novel Technique for Video Segmentation and Image Matching

[1]Shakuntala Satyawana, [2]Surendra Kumar Agarwal

Abstract

Image segmentation is an important technique that used by many algorithms to detect the object or to morphologically maps the image to found its mass or to map the image color intensity. Image segmentation can play important role when it comes to identify an object and to match it with the database images. In this paper a technique is presented and implemented to segmentize the image and as well as the videos, also the model presented is constructed in such a way that it also depicts the object category, however to detect the object training database needs to have the complete information about the queried category.

Keywords: Image Segmentation, Object Recognition, Computer Vision

Introduction

Video based image segmentation is a complex process and to detect the object out of it becomes more difficult and almost an improbable job, as to detect the object the system needs to have the all the information related to the structure of the queried category or the object. In this paper firstly image segmentation has been implemented and then it has been modified to work on the videos as well. However this work has been tested over only one thousand two hundred one images and is able to identify only those objects which are present in the system training database.

Previous Work

All basic image segmentation procedures presently being taken into account by the scholars and industry will be debated and evaluate in this section.

Edge Based Image Segmentation

Fernando C. Monteiro [1] planned a novel image segmentation process comprises of edge and region centered facts with the help of spectral procedure and morphological set of rules of watershed. Initially, they ease the noise as of picture by bilateral filter as a preprocessing step, in addition, region merging is taken into account to implement introductory segmentation, region resemblance is produced and then graph based region alliance be execute by Multi-class Normalized Cut method [2]. It is bring into being that projected procedure has overtaken other procedures and yield better outcome.

R. Patil [3] suggest to facilitate stipulation the numeral of huddles be anticipated within truthful way, K-means image segmentation will give superior upshots. They recommended a innovative modus operandi based on edging revealing toward appraise digit of bunch's. Facet congruency be in use addicted to explanation toward recognize the boundaries. Afterward these boundaries be in use addicted to version headed for get bunch's. Brink moreover Euclidean expanse be in use keen on explanation within arrange toward create groups. K-means be in use interested in narrative near locate the concluding segmentation of reflection. MATLAB be occupied interested in relation toward execute the not compulsory route. Trials be accomplished going on nine diverse pictures furthermore outcomes confirm so as to digit of collects be precise along with finest. Weihong Cui Yi Zhang [4] optional an perimeter based auto threshold pick manner toward engender multi-level image segmentation. Band weight also NDVI (Normalized Difference Vegetation Index) be in use keen on description near determine border load. Tests be act upon taking place multi-scale decree illustration effects include exposed with the purpose of their scheme retain the objective in order as well

[1]Corresponding Author's Email: shakuntalasatyawana@yahoo.in

as carry on object margins as subdivision the picture. Anna Fabijanska [5] initiated a innovative scheme utilized variation Filter used for boundary finding within image segmentation procedure. Their technique originates the edging place using difference Filter. Sobel Gradient filter through K-means be too in use addicted to detail toward extort the boundaries by evaluate through the planned method. The result of clean window range going on decisive ends be besides argued with it be create to facilitate but the 9×9 window be in use interested in explanation just before take out boundaries after that boundary be whole exactly equivalent the form of object during the picture. During case of bigger information pictures, a little clean window be extended. Outcome exposed with the purpose of their planned process better Sobel Edge Detector. Mohammed J. Islam [6] initiate to Computer Vision be a greatest way out in favor of actual instance assessment of case within pharmaceutical manufacturing. Writer has made a structure used for aspect scrutiny via edge based image segmentation methods [7]. They in use addicted to explanation Sobel Edge Detector [8] into arrange near notice boundaries by noise-suppression assets. Later than edging finding, Otsu Thresholding method be in use addicted to description intended for localization of background also foreground pixels .Trial be performed also outcome be evaluate through NN-based segmentation method structure .Visual C++ outcomes better NN process taking place the base of precision and processing time difference of 10 ms.

Partial Differential Equation (PDE) Based Image Segmentation

PDE (Partial Differential Equations) equations or PDE forms be applied large within picture procedure, also specially within image segmentation. They utilize active contour form used for segmentation reason .Active Contour form otherwise Snakes modify the segmentation disadvantage addicted to PDE. Several famous methods of PDE utilized designed for image segmentation be Snakes, Level-Set, also Mumford Shah technique [9]. In this part, various innovative methods designed for image segmentation maintained PDE be declared. Accommodative PDE forms that is., fuzzy PDE Contour model, also PDE geometrical Contour form by Fuzzy C-Means categorization be used in favor of segmentation of images. Accommodative PDE forms assisted toward explore exposed the area of importance. 3D brain tomography picture be working like a dataset. Fuzzy PDE form has point the tomography brain picture utilization Fuzzy agglomeration method. The forms has better 'Snakes' form also level reverse a digit of disadvantages of Snakes form [10]. Characteristic removal methods within [11]-[12] be able toward managing geometrical feature, speed of alteration, also direction of picture. Novel PDE supported segmentation idea be also providing enhance different criterion of quality records. PDEs be used for representing the segmentation idea. Watershed method [13] be complete via use PDE forms. They evaluate their designed idea by watershed segmentation method, also it's establish to facilitate pairing of textural information, also forming utilization PDEs directs the image segmentation toward main feature technique also better the watershed segmentation algorithmic regulation.

Artificial Neural Network (ANN) Based Image Segmentation

During Artificial Neural Network, all somatic unit be the same near the element of a figure. Picture be planed toward the neural system. Image in the selection of neural system be qualified utilization training examples, after that organization among neurons, that is., pixels be establish. Next the novel images be segmental as of the eligible picture [10]. Segmentation of picture use neural system be execute into 2 levels, that is., part sorting also edging finding [14]. In this part several novel approaches of ANN meant for image segmentation be declared as of previous 5 years. Xuejie Zhang [10] designed a substitute fast knowledge Artificial Neural Network (FLANN) that depends on color image segmentation method in favor of R-G-B-S-V group area. During beginning, noise is eliminated use 3*3 averaging filter toward cut back the dissimilarity into color allocation. During second level, pixels are reborn toward RGBSV region use HSV adaptations. FLANN agglomeration is executed toward give a group outcome of picture. Then, pixels via related color are alienated. Subdivision selection is selected toward each stage of picture. Force of lenience also district dimension be determined. Outcome has exposed to designed algorithmic regulation prepared brilliant subdivisions used for colors in the picture. Farhad Mohamad Kazemi [15] designed a fast C-means that depends on training of Fuzzy Hopfield Neural network [16] thus it use addicted to image segmentation. Purpose work is use supported 2-f

Fuzzy HNN. This purpose works establish the ordinary space among picture pixels also groups centroid. Fuzzy HNN gives superior segmentation in comparison of other methods. Initially, they generate groups as of known knowledge, after that execute normalization, specifically. Gray level images, analyze centroids, after that diagram spaces, recognize novel centroids, also PC novel association work significance utilization fuzzy C-means [17]. The outcome has exposed to FHNN gives a faster velocity in comparison of other methods of ANN.

Video Segmentation

A segmentation algorithm divisions an input video in some parts. Every part is consistent w.r.t. single or added property *that is*. The difference of dimensions in the areas must exist much fewer differences on the object edges. A video segmentation algorithm be able to largely classified in two module which depends in the motion estimates provided: Video Segmentation without correspondences, Video Segmentation with correspondence.

Video segmentation without segmentation

[Niebles2010] planned an approach in extract person volume. Used for every picture edge applicant areas be obtain via a finding level also the modifications of these areas be depends at shape prior. Segmentation with Object Proposals: Mainly the video segmentation approaches in this type use the object proposal algorithm via [Endres 2010]. Therefore evaluation this method designed for producing object suggestion within the next part prior to arrange toward video segmentation suggestions use these schemes. Further various objects scheme production infrastructures are able to achieve form [Alexe 2012], [Ziming 2014].

Category Independent Object Proposals

Known an input picture, the algorithm by [Endres 2010] gives a graded catalog of various category independent candidate object proposals. The grading be complete which depends in *objectness* such high graded suggestions be probable toward be a fine segmentation. Motion Coherent Tracking using MRF[Tsai 2011] planned a partially-managed form to object removal into video in which a client explains the shape of the object which requires exist way for the entire series.

Segmentation using category independent proposals

Approaches like that [Lee 2011], [Tianyang 2012] utilize object suggestions (produced by [Endres 2010] toward locate a set of various segmentation designed for every picture within the film. Previously the suggestions be produced for every structure of a video, after that the difficulty of video-object segmentation be created like an optimization difficulty where the purpose be toward locate a segmentation that describes a film in the finest way, also then process the foreground outline to exist the object correctly. The suggestion from [Lee 2011] primary recognize object-like areas (input segments) inside several structure along with together stationary or energetic cues. a new suggestion in video segmentation by object suggestions be from [Tianyang 2012]which different as of [Lee 2011] mostly into the practice of the optimization form toward locate object.

Fast video segmentation: in sequence for expand velocity, the writer [Papazoglou 2013] suggest a quick method for create an irregular guess of which pixels be within the object depends in movement boundary within pair of consecutive frame. This first estimation is after that superior from integrating knowledge above the entire film by a spatio-sequential addition of GrabCut.

Video Segmentation with correspondences

Approach during this type utilize extended period position correspondence i.e. position track for achieve a consistent spatio-sequential segmentation. During new advance into optical flow algorithms, position track structure have suited extra consistent also have completed an excellent stage of development. Mainly important way structure algorithms are by [Sundaram 2010] also [Sand 2008]. Point tracks by [Sand 2008] be and referred like constituent part film. Other normally use position follower be, which be normally identified like the KLT tracker. Author by [Sundaram 2010] has exposed that point track formed flow optical flow by [Brox 2011] is of greatly superior superiority than the ones formed from KLT an constituent part film, into conditions of intense exposure also sequential extent. But compute position track by [Sundaram 2010] be deliberate on CPUs. Significant computational accelerate be able to get from use GPUs, also several release basis implementations used for actual instance KLT trackers be existing [Zach 2008].

Clustering of Point Tracks

The segmentation method into this type utilizes point tracks like the major basis of knowledge.The point paths stand via [Sundaram 2010]. Methods into this type different mostly into the way into which the clustering be completed for remove objects. Point tracks offer simply a thin exposure during variable activity approximation into color consistent areas. Therefore algorithms into this type normally offer alignment used for simply a division of pixels into the type of point tracks, usually cover approximately 3% of the whole pixels into a film. Several important trajectory clustering algorithms are by [Fradet 2009], [Brox 2010], [Fragkiadaki 2011], Point track clustering methods don't require knowledge by a detector on object theory, also therefore be referred like finding free tracking from [Fragkiadaki 2011]. Known point tracks, the author [Fragkiadaki 2011] initial categorize these trajectory like background or foreground via significant a saliency determine. A diagram is creating whose peaks be foreground path. Weights for boundaries be striking also disgusting energy among trajectories. A foreground topology remain develop through figure-ground segmentation through the main group of path interested in front as well as background. This foreground topology is a fine pointer of while two paths cannot set mutually. Outcome from [Brox 2010], the writers utilize a hierarchical difference form that spreads these label first into uniform regions which be originally not enclosed via point tracks. This thick segmentation finds superior categorization precision than the input thin segmentation also conquers the over-segmentation matter of stationary picture segmentation schemes.

Background subtraction by Point Tracks

Background subtraction into stirring camera scenario be able to as well is execute by point tracks or famous efforts into this feature be [Elqursh 2012], [Sheikh 2009]. The last make a thin background form via view a dense path sources by trajectory of main aspects crosswise the film. The background be then subtracted via eliminate trajectory to recline in the distance duration via this source. From this thin background knowledge, a foreground background appearance form be construct or a best pixel-wise binary group be get via resolve a MAP deduction difficulty.

Methodology

In this paper a methodology is proposed which is applicable for the image and the videos as well to segmentize the given frame at any instance. Image segmentation is a methodology to distinguish the objects and the foreground which can be further enhanced to use it as an object recognition program, however to recognize an object the system need to have its complete information saved in its database. On the basis of which the system will match the pattern and the object location as well. Images taken as an input are first get converted into the gray scale images and then they are processed, however the input images taken are maintained in a separate variable to process them under the effect of color map and to identify the object presence in the input image. The color mapped process images are feeded into the next function which on the basis of gradient vector and the change in boundary light intensity analysis determines the edge of the object and process the image in such a way that the values between the boundaries are forced to be one and the rest of the values are forced to be zero, however if this method does not generate the proper output image hence the system again process the image segmentation process using color map intensity over the gray scale image and hence generates the segmented image.

The time taken by the function to segmentize one image depends on the performance of the testing hardware system, however system used in this developing this code is enabled with Intel core I3 with 4GB of ram.

Fig.1 and Fig.2 elaborates the methodology with a proper flow diagram and however there are few equations that can be said to be used in the proposed algorithm which is mentioned below in this section.

We calculate F-measure and accuracy and compare the F-measure and accuracy by other methods.

$$F-Measure = \frac{2.Recall.Precision}{(Recall + Precision)}$$

$$Accuracy = \frac{Number\ of\ Segmented\ Images}{Total\ Number\ of\ Images}$$

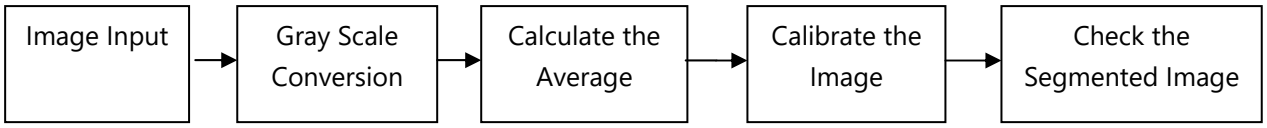

Figure 1: Flow Chart of Basic Segmentation

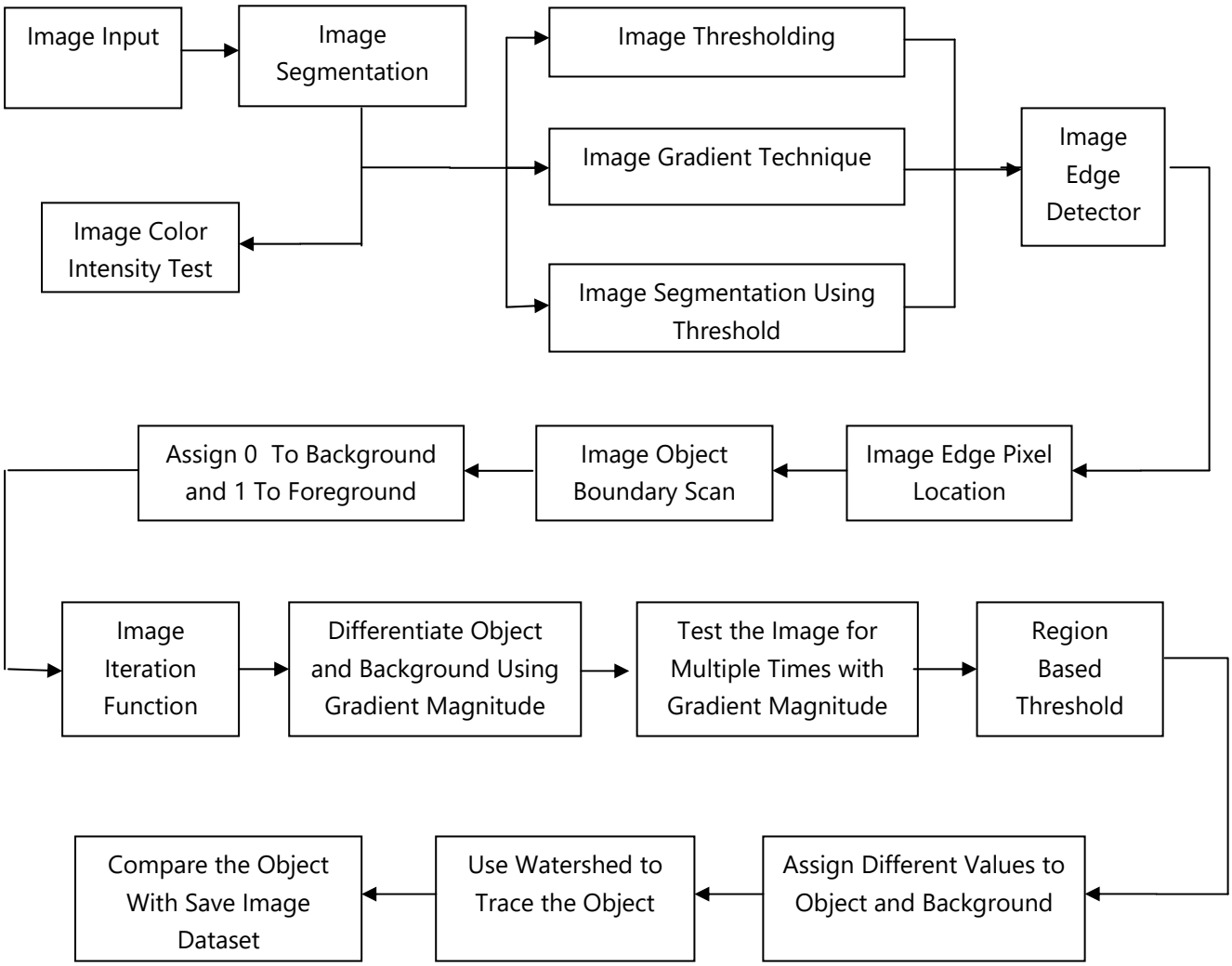

Figure 2: Flow Chart of Proposed Method

Results

Image segmentation can be classified into two types one can be said as the simple and less time consuming and another one can be classified as the complex and time consuming task, however the image segmentation process depends over the type of images taken into the account, images with less information and with less complex background can be segmented very precisely and with less time consumption as proposed in the above section with the name of basic segmentation, in basic segmentation the image is segmentize with the help of the average threshold, after calculating the average threshold the image can be divided into two parts and can be represented in the 0 or 1 form.

The other method which uses the complex method is generally applicable for the images with more information and with complex background. The

system uses more time to segmentize these types of images; hence they use the more complex functions like edge detection and gradient boundary scan functions.

Figure 3: (a) Input Image

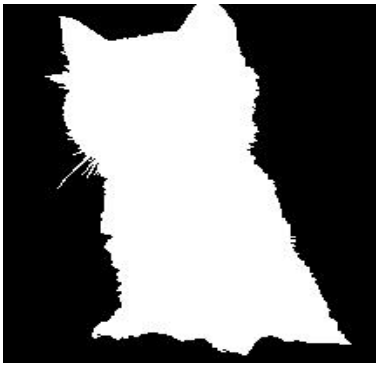

Figure 3: (b) Segmented Image

Statistical results have been presented in the table (I) and table (II) on the basis of the obtained results.

TABLE (I): F-Measure Comparison of Ours Method with Other Method on Weizmann Horse Dataset

Algorithm	Ours	[39]	[35]	[40]
F-Measure	1.4456	0.872	0.8430	0.84

TABLE (II): Segmentation Accuracies Comparison of Ours Method with Other Method on Weizmann Horse Dataset

Algorithm	Our	[39]	[35]	[37]	[36]	[38]
Accuracy in %	95.2	92.9	89.3	74.9	90.0	80.1

Conclusion

From the above complied work it can be understood to make system intelligent and advance Image segmentation is an essential technique but due to the complex procedure and lengthy calculation it takes lot of time which might not turn out to be an appropriate preposition during the real time implementation of it over the video frame segmentation and object recognition.

Time taken by the above proposed methodology to segmentize an image will depend over the nature and the quality of an image; however the images taken for the testing has shown the average time of 24.17 seconds. This has the scope of further improvement and can be significantly brought down and hence that will help the proposed method to be able to segmentize the video frames in real time.

References

[1] F. C. Monteiro and A. Campilho, "Watershed framework to region-based image segmentation," in Proc. International Conference on Pattern Recognition, ICPR 19th, pp. 1-4, 2008.

[2] M. Hameed, M. Sharif, M. Raza, S. W. Haider, and M. Iqbal, "Framework for the comparison of classifiers for med¬ical image segmentation with transform and moment based features," Research Journal of Recent Sciences, vol. 2277, p. 2502, 2012

[3] R. Patil and K. Jondhale, "Edge based procedure to estimate number of clusters in k-means color image segmenta¬tion," in Proc. 3rd IEEE International Conference on Computer Science and Information Technology (ICCSIT), pp. 117-121, 2010.

[4] W. Cui and Y. Zhang, "Graph based multispectral high resolution image segmentation," in Proc. International Conference on Multimedia Technology (ICMT), pp. 1-5, 2010.

[5] A. Fabijanska, "Variance filter for edge detection and edge-based image segmentation," in Proc. International Con¬ference on Perspective Technologies and Technique in MEMS Design (MEMSTECH), pp. 151-154, 2011.

[6] M. J. Islam, S. Basalamah, M. Ahmadi, and M. A. S. hmed, "Capsule image segmentation in pharmaceutical applications using edge-based procedures," IEEE International Conference on Electro/Information Technology (EIT), pp. 1-5, 2011.

[7] M. Sharif, M. Raza, And S. Mohsin, "Face recog-nition using edge information and DCT," Sindh Univ. Res. Jour. (Sci. Ser.), vol. 43, no. 2, pp. 209-214, 2011.

[8] W. Haider, M. S. Malik, M. Raza, A. Wahab, I. A. Khan, U. Zia, J. Tanveer, and H. Bashir, "A hybrid method for edge continuity based on Pixel Neighbors Pattern Anal¬ysis (PNPA) for remote sensing satellite images," Int'l J. of Communications, Network and System Sciences, vol. 5, pp. 624-630, 2012.

[9] X. Jiang, R. Zhang, and S. Nie,"Image segmentation based on PDEs model: A survey", in Proc. 3rd International Conference on Bioinformatics and Biomedical Engineering, 2009, pp. 1-4.

[10] Mohd. Yasir Farooque, Prof. Mohd. Sarwar Raeen, " Latest trends on image segmentation schemes",International Journal of Advanced Research in Computer Science and Software Engineering , ISSN: 2277 128X , volume 4, issue 10, october 2014, pp. 792-798.

[11] A. Sofou and P. Maragos, "Generalized flooding and multicue PDE-based image segmentation," IEEE Transactions on Image Processing, vol. 17, pp. 364-376, 2008.

[12] M. Sharif, M. Raza, S. Mohsin, and J. H. Shah, "Microscopic feature extraction method," Int. J. Advanced Networking and Applications, vol. 4, pp. 1700-1703, 2013.

[13] A. Shahzad, M. Sharif, M. Raza, and K. Hussain, "Enhanced watershed image processing segmentation," Journal of Information & Communication Technology, vol. 2, no. 1, Spring 2008.

[14] D.Suganthi and Dr. S.Purushothaman, "MRI segmentation using echo state neural network," International Journal of Image Processing, vol. 2, no. 1, 2008.

[15] F. M. Kazemi, M. R. Akbarzadeh, T. S. Rahati, and H. Rajabi, "Fast image segmentation using C-means based Fuzzy Hopfield neural network," in Proc. Canadian Conference on Electrical and Computer Engineering,2008, pp. 001855-

[16] M. Yasmin, M. Sharif, and S. Mohsin, "Neural networks in medical imaging applications: A survey," World Applied Sciences Journal, vol. 22, pp. 85-96, 2013.

[17] W. Haider, M. Sharif, and M. Raza,"Achieving accuracy in early stage tumor identification systems based on image segmentation and 3D structure analysis," Computer Engineering and Intelligent Systems, vol. 2, pp. 96-102, 2011.

[18] J.C. Niebles, Bohyung Han and L. Fei-Fei, "Efficient extraction of human motion volumes by tracking," In IEEE Conference on Computer Vision and Pattern Recognition, 2010.

[19] Ian Endres and Derek Hoiem, "Category extraction of human motion volumes by tracking," European Conference on Computer Vision, 2010.

[20] Bogdan Alexe, Thomas Deselaers and Vittorio Ferrari.,"Measuring The objectness of image windows, "IEEE Transactions on Pattern Analysis and Machine Intelligence, vol. 34, no. 11, pages 2189–202, November 2012.

[21] Ming-ming Cheng Ziming, Zhang Wen-yan Lin and Philip Torr, "BING: Binarized normed gradients for objectness estimaton at 300fps, "In IEEE Conference on Computer Vision and Pattern Recognition, 2014.

[22] David Tsai, Matthew Flagg, Atsushi Nakazawa and James M. Rehg, "Motion coherent tracking using multi-label MRF optimization, "International Journal of Computer Vision, vol. 100, no. 2, pages 190–202, December 2011.

[23] Yong Jae Lee, Jaechul Kim and Kristen Grauman, "Key segments for video object segmentation, "In International Conference on Computer Vision, 2011.

[24] Ma Tianyang and L. J. Latecki, "Mxximum weight cliques with mutex constraints for video object segmentation, "In IEEE Conference on Computer Vision and Pattern Recognition, June 2012.

[25] Anestis Papazoglou and Vittorio Ferrari, "Fast object segmentation in unconstrained video, "In International Conference on Computer Vision, 2013.

[26]Narayanan Sundaram, Thomas Brox and Kurt Keutzer, "Dense point trajectories by GPU-accelerated large displacement optical flow,"In European Conference on Computer Vision, 2010.

[27] Peter Sand and Seth Teller, "Long –range motion estimation point trajectories, "International Journal of Computer Vision, vol. 80, no. 1,pages 72–91, 2008.

[28] Thomas Brox and Jitendra Malik, "Large displacement optical flow :decripation matching in variational motion estimation, " IEEE Transactions on Pattern Anal¬ysis and Machine Intelligence, vol. 33, no. 3, pages 500–13, March 2011.

[29] Christopher Zach, David Gallup and JM Frahm, "Fast gain-adaptive KLT tracking on the GPU, "In IEEE Conference on Computer Vision and Pattern Recognition Workshops, 2008.

[30] Matthieu Fradet, Philippe Robert and Patrick Pérez, "Clustering point trajectories with various life-spans, "In Conference for Visual Media Production. IEEE, November 2009.

[31] Thomas Brox and Jitendra Malik, "Object segmentation by long term analysis of point trajectories, "In European Conference On Computer Vision. Springer, 2010.

[32] Katerina Fragkiadaki and Jianbo Shi, "Detection free tracking exploting motion and topology for segmenting and tracking under entanglement," In IEEE Conference on ComputerVision andPattern Recognition, 2011.

[33] Ali Elqursh and Ahmed Elgammal, "Online moving camera background subtraction, "In European Conference on Computer Vision, volume 7577. Springer,2012.

[34] Yaser Sheikh, Omar Javed and Takeo Kanade, "Background subtraction for freely moving cameras, "In International Conference on Computer Vision, pages 1219–1225. IEEE, September 2009.

[35] L. Wang, J. Xue, N. Zheng, and G. Hua, "Automatic salient object extraction with contextual cue," in Proc. IEEE ICCV, Nov. 2011, pp. 105–112.

[36] Y. Chai,V.S. Lempitsky,and A. Zisserman,"BiCoS: A bi-level co¬segmentation method for image classification," in Proc. IEEE ICCV, Nov. 2011, pp. 2579–2586.

[37] J. C. Rubio, J. Serrat, A. López, and N. Paragios,"Unsupervised co¬segmentation through region matching," in Proc. IEEE CVPR, Jun. 2012, pp. 749–756.

[38]A. Joulin, F. Bach, and J. Ponce, "Discriminative clustering for image co-segmentation," in Proc. IEEE CVPR, Jun. 2010, pp. 1943–1950

[39] Le Wang,Gang Hua,Zhanning Gao,And Nanning Zheg, "Joint Segmentation and Recognition of Categorized Objects From Noisy Web Image Collection," IEEE, Transactions On Image Processing, Vol. 23, No. 9, September 2014, pp. 4070-4085.

[40] Z. Tu, "Auto-context and its application to high-level vision tasks," in Proc. IEEE CVPR, Jun. 2008, pp. 1–8.

Author's details

[1]M.Tech, Scholar, Department of Electronics and Communication Engineering, Government Women Engineering College, Ajmer, India, Email: shakuntalasatyawana@yahoo.in

[2]Assistant Professor, Department of Electronics and Communication Engineering, Govt. Women Engineering College, Ajmer, India, Email: skagarwal5@rediffmail.com

Copy for Cite this Article- Shakuntala Satyawana, Surendra Kumar Agarwal, 'Novel Technique for Video Segmentation and Image Matching' *International Journal of Science, Engineering and Technology,* Volume 4 Issue 1: 2016, pp. 291- 298.

Shakuntala Satyawana et al. 2016, Volume 4 Issue 1
ISSN (Online): 2348-4098
ISSN (Print): 2395-4752

International Journal of Science, Engineering and Technology
An Open Access Journal

A Review Paper on Image Segmentation and Object Recognition Procedures

[1]Shakuntala Satyawana, [2]Surendra Kumar Agarwal

Abstract

Image segmentation is an important procedure that taken into account by many algorithms to detect the object or to morphologically maps the image to found its mass or to map the image color intensity. Image segmentation can play important role when it comes to identify an object and to match it with the database images. Also during the forensic analysis of images image segmentation can help in identifying the object location and its temperature and also the distance of it from the preset reference point. During computer vision, image segmentation be the method of dividing a digital picture addicted to multiple segments (sets of pixels, also identified like super pixels). The purpose of segmentation be toward make simpler also/otherwise alter the depiction of an picture addicted to incredible that be extra important also easier toward evaluate. Image segmentation be usually in use addicted to explanation near situate objects also margins (shape, curves, etc.) within pictures. Additional accurately image segmentation be the procedure of conveying a label toward each pixel within an picture such that pixels by the similar label distribute definite distinctiveness.

Keywords: Image Segmentation, Object Recognition, Computer Vision

Introduction

In this paper, Image segmentation is discussed in detail, its procedure and its application as well. Image segmentation is a process to divide an image into multiple sections to study and analyze an image. This can be very useful in analyzing and studying the medical image reports to postulate the report in text.

Previous Work

All basic image segmentation procedures presently being taken into account by the scholars and industry will be debated and evaluate in this section

***Edge Based Image Segmentation*:** Fernando C. Monteiro [1] planned a novel image segmentation process comprises of edge and region centered facts with the help of spectral procedure and morphological set of rules of watershed. Initially, they ease the noise as of picture by bilateral filter as a preprocessing step, in addition, region merging is taken into account to implement introductory segmentation, region resemblance is produced and then graph based region alliance be execute by Multi-class Normalized Cut method [2]. R. Patil [3] suggest to facilitate stipulation the numeral huddles be anticipated within truthful way, K-means image segmentation will give superior upshots. They recommended an innovative modus operandi based on edging revealing toward appraise digit of bunch's. Facet congruency be in use addicted to explanation toward recognizing the boundaries. Afterward these boundaries be in use addicted to version headed for get bunch's. Brink moreover Euclidean expanse be in use keen on explanation within arrange toward create groups. K-means be in use interested in narrative near locating the concluding segmentation of reflection. MATLAB be occupied interested in relation toward execute the not compulsory route. Trials be accomplished going on nine diverse pictures furthermore outcomes confirm so as to digit of collects be precise along with finest. Weihong Cui Yi Zhang [4] optional a perimeter based auto threshold pick manner toward engender multi-level image segmentation. Band weights also NDVI (Normalized Difference Vegetation Index) be in use keen on description near determine border. Tests be act upon taking place multi-scale decree illustrations. Effects include exposed with the purpose of their

[1]Corresponding Author's Email: shakuntalasatyawana@yahoo.in

scheme retain the objective in order as well as carry on object margins as subdivision the picture.

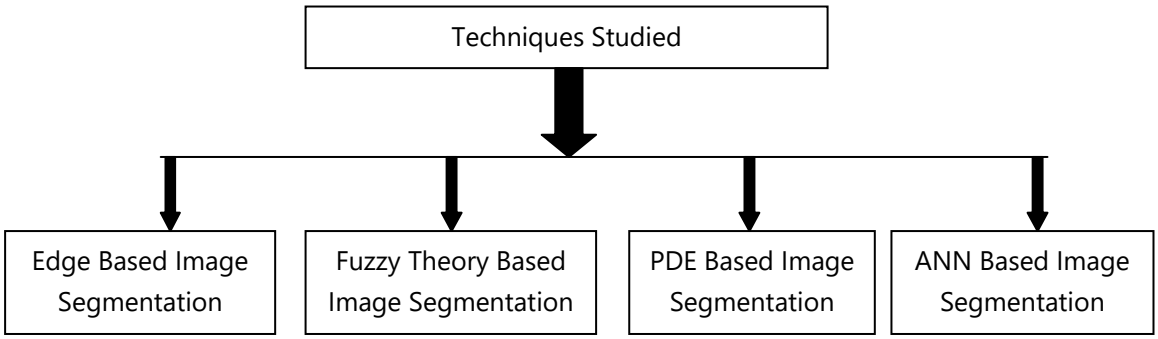

Figure1. Varied Image Segmentation Techniques

Anna Fabijanska [5] initiated a innovative scheme utilized variation Filter used for boundary finding within image segmentation procedure. Their techniques originate the edging place using difference Filter. Sobel Gradient filter through K-means be too in use addicted to detail toward extort the boundaries by evaluate through the planned method. The result of clean window range going on decisive ends be besides argued with it be create to facilitate but the 9×9 window be in use interested in explanation just before take out boundaries after that boundary be whole exactly equivalent the form of object during the picture. During case of bigger information pictures, a little clean window be extended. Outcome exposed with the purpose of their planned process better sobel edge detector. Mohammed J. Islam [6] initiate to Computer Vision be a greatest way out in favor of actual instance assessment of case within pharmaceutical manufacturing. Writer has made a structure used for aspect scrutiny via edge based image segmentation methods [7]. They in use addicted to explanation Sobel Edge Detector [8] into arrange near notice boundaries by noise-suppression assets. Later than edging finding Otsu thresholding method is in use addicted to description intended for localization of background also foreground pixels. Trial be performed also outcome be evaluate through NN-based segmentation method structure Visual C++. Outcomes better NN process taking place the base of precision and processing time difference of 10 ms.

Fuzzy Theory Based Image Segmentation: Liu Yucheng [9] planned a novel fuzzy morphological stand combination image segmentation algorithm. Algorithm has in use keen on explanation morphological opening as well as closing procedures toward flat the picture with then present the gradient Procedures taking place the resulting picture [10]. Behind evaluate the planned mixture algorithm amid Watershed algorithm [11] and Prewitt procedure, it be create to facilitate combination method resolve the predicament of over-segmentation of Watershed algorithm. It too keeps the information of picture also recover the rapidity as well. Syoji Kobashi [12] in use interested in explanation size based fuzzy related image segmentation with fuzzy object model to subdivision the intellectual parenchyma area of latest intuitive brain MRI image. Foreground area be divided into initial step, improvement of MRI intensity inside-homogeneity be use next, also then scale-base Fuzzy Object Model (FOM) be used on ensuing picture. Outcome of planned technique be assess on the basis of Fast Positive Volume Fraction (FPVF) also Fast Negative Volume Fraction (FVNF). Outcome as of trials exposed that FOM (Fuzzy object model) has attained lowest FPVF and FVNF assessment. Refik Samet [13] anticipated a latest Fuzzy Rule based image segmentation process to subdivision the rock slight subdivision pictures. They obtain RGB picture of rock slight subdivision as input also give segmented granite picture as output. Fuzzy C Means be too used on rock lean pictures also outcomes be evaluated of together methods. Initially, the abuser will receive test figure from raw materials; aspects be notable on the basis of red, green and blue mechanism of picture. Membership purpose be clear for every component via Fuzzy regulations. All membership function shows the color's division into the picture. Tough also feeble positions be distinct, while tough positions be measured as seed positions also weedy positions turn into their affiliates. Outcome include that planned method be improved than FCM algorithm. Muhammad Rizwan Khokher [14] offered a unique process of image segmentation through Fuzzy Rule

based method as well as Graph Cuts. Their algorithm workings by initially removing the aspects of picture, determine the stables using fuzzy rules, analyze the weighted average of regulars to locate the match matrix, separation the graph using Normalized Graph Cut method [15], also lastly acquire regulars to locate the match matrix, separation the graph using Normalized Graph Cut method [15], also lastly acquire the segmented picture from separation graph. Berkley list be in use keen on explanation toward assess the algorithm. Imitation be executed in Matlab and C language

***Partial Differential Equation (PDE) Based Image Segmentation*:** Jinsheng Xiao [16] considered a novel non-linear discontinue (PDE) for demonstrations the level set scheme of gray pictures. A discrete method be too planned toward locate mathematical result also toward apply the filter. Additional information be able to exist saved via by the planned method. Fengchun Zhang [17]explain a difference form from 4th order PDE through 2nd order PDE planned in favor of finger vein image de-noising. Midpoint Threshold segmentation method be in use addicted to explanation toward extort the area of importance exactly. 4th order PDE have minimum the noise extremely fine, while 2nd order PDE have estimated the margins successfully. It be capable of exist experiential as of testings that PSNR rate of planned scheme be enhance by 2 dB. Process be evaluated by threshold based segmentation algorithm and it be establish that planned process has subdivision the actual finger vein picture precisely. Chun Yuan [18] planned a novel segmenta-tion model for color pictures and depends in GAC scheme. However GAC be simply limited toward gray scale pictures. Thus their form be moreover an expansion of GAC form, and identified as color-GAC model. It uses the term of the Gradient of color picture.

***Artificial Neural Network (ANN) Based Image Segmentation*:** Wencang Zhao [19] anticipated a innovative image segmentation algorithm found on textural aspects [20] also Neural Network [21] toward divide the embattled pictures as of background. Dataset of micro-CT pictures be in use addicted to explanation. De-noising filter be in use keen on description just before eliminate clatter from picture since a pre-processing step, Aspect removal be executed after that, with then Back Propagation Neural system be formed, also lastly, it modifies the load digit of system, also keep the output. Outcome include that planned process betters other method on the basis of velocity also precision of segmentation. Lijun Zhang [22] predictable a narrative neural structure depends on image segmentation scheme for color pictures. They joint the Wavelet Decomposition and Self Organizing Map (SOM) toward offer a novel technique, i.e., SOM-NN. Determination with adolescent pixels preferred the close relative pixel. Later than initialization, ANN create the segmentation upshot which satisfies every stages. Wavelet disintegration be executed toward eradicate noise. Therefore wavelet disintegration along with SOM-NN be collected toward execute segmentation. Outcome include that technique has decrease noise also generate precise segmentation. Shohel Ali Ahmed [23] predictable picture Texture Classification procedure depends in (ANN). Initially, picture be captured also pre-processing be executed, later than it, aspect removal [24] be executed, while, ANN classifier [25] be in use keen on explanation for texture classification, Clustering be executed toward divides background from sub-pictures. Trained ANN combines the input pixels addicted to two groups which provide outcome. It creates the texture classification and segmentation of picture.

Methodology

A basic approach has been tried in this paper, where the image threshold on the basis of the graylevel values has been calculated and then the pixel has been recalibrated, however to make this methodology work the image is need to be checked around the threshold value and hence then the best segmented image is selected from the obtained results. However work done in this paper has also been tested over video as well.

Results

The methodology explained above has been tested with a simple image and in this paper, firstly input image has been taken and this image is converted into a grayscale image, and calculate the average threshold of the image and by this process we can get segmented image, and in figure2 simply input image has been taken and input image is converted into gray scale image and calculate the average threshold and by this process image can be shows in binary form means that 0 of 1,and according to

fig.2(b) 0 shows background and 1 shows foreground, means that 0 shows black and 1 shows white. This can tested over the video files as well however the system requirements will be high in that case and can be expensive to implement, however the current system taken into account generates the results but in the form of frames and with subsequent time delay.

Figure2: (a) Input Image

Figure2: (b) Segmented Image

Conclusion

From this paper multiple postulates can be made on the basis of the study of the previous work done, all the word done in the field of image segmentation is needed to be monitored manually there is no such method which can detect the objects with precision and without any database, which obviously takes time to get build. From the studied and explained papers in the above sections it can also be deduced that the functions designed for the image segmentation can be made to generate the output result more quickly so as to enable them to work with the video files as well.

References

[1] F. C. Monteiro and A. Campilho, "Watershed framework to region-based image segmentation," in Proc. International Conference on Pattern Recognition, ICPR 19th, pp. 1-4, 2008.

[2] M. Hameed, M. Sharif, M. Raza, S. W. Haider, and M. Iqbal, "Framework for the comparison of classifiers for med¬ical image segmentation with transform and moment based features," Research Journal of Recent Sciences, vol. 2277, p. 2502, 2012

[3] R. Patil and K. Jondhale, "Edge based procedure to estimate number of clusters in k-means color image segmenta¬tion," in Proc. 3rd IEEE International Conference on Computer Science and Information Technology (ICCSIT), pp. 117-121, 2010.

[4] W. Cui and Y. Zhang, "Graph based multispectral high resolution image segmentation," in Proc. International Conference on Multimedia Technology (ICMT), pp. 1-5, 2010.

[5] A. Fabijanska, "Variance filter for edge detection and edge-based image segmentation," in Proc. International Con¬ference on Perspective Technologies and Technique in MEMS Design (MEMSTECH), pp. 151-154, 2011.

[6] M. J. Islam, S. Basalamah, M. Ahmadi, and M. A.

S.hmed,"Capsul image segmentation in pharmaceutical applications using edge-based procedures," IEEE International Conference on Electro/Information Technology (EIT), pp. 1-5, 2011.

[7] M. SHARIF, M. RAZA, and S. MOHSIN, "Face recog¬nition using edge information and DCT," Sindh Univ. Res. Jour. (Sci. Ser.), vol. 43, no. 2, pp. 209-214, 2011.

[8] W. Haider, M. S. Malik, M. Raza, A. Wahab, I. A. Khan, U. Zia, J. Tanveer, and H. Bashir, "A hybrid method for edge continuity based on Pixel Neighbors Pattern Anal¬ysis (PNPA) for remote sensing satellite images," Int'l J. of Communications, Network and System Sciences, vol. 5, pp. 624-630, 2012.

[9] L. Yucheng and L. Yubin, "An algorithm of image segmentation based on fuzzy mathematical morphology," in International Forum on Information Technology and Applica¬tions, IFITA'09, pp. 517-520, 2009.

[10] W. Haider, M. Sharif, and M. Raza, "Achieving ac¬curacy in early stage tumor identification systems based on image segmentation and 3D structure analysis," Computer Engineering and Intelligent Systems, vol. 2, pp. 96-102, 2011.

[11] M. S. A. Shahzad, M. Raza, and K. Hussain, "En-hanced watershed image processing segmentation," Journal of Information & Communication Technology, vol. 2, pp. 1-9, 2008.

[12] S. Kobashi and J. K. Udupa, "Fuzzy object model based fuzzy connectedness image segmentation of newborn brain MR images," in Proc. IEEE International Conference

on Systems, Man, and Cybernetics (SMC), pp. 1422-1427, 2012.

[13] R. Samet, S. E. Amrahov, and A. H. Ziroglu, "Fuzzy rule-based image segmentation procedure for rock thin section images," in Proc. 3rd International Conference on Image Processing Theory, Tools and Applications (IPTA), pp. 402¬406, 2012.

[14] M. R. Khokher, A. Ghafoor, and A. M. Siddiqui, "Image segmentation using fuzzy rule based system and graph cuts," in Proc. 12th International Conference on Control Au¬tomation Robotics & Vision (ICARCV), pp. 1148-1153, 2012.

[15] M. Sharif, S. Mohsin, M. J. Jamal, and M. Raza, "Illumination normalization preprocessing for face recognition," in Proc. International Conference on Environmental Science and Information Application Technology (ESIAT), pp. 44-47, 2010.

[16] J. Xiao, B. Yi, L. Xu, and H. Xie, "An image segmentation algorithm based on level set using discontinue PDE," in Proc. First International Conference on Intelligent Networks and Intelligent Systems, ICINIS'08., pp. 503-506, 2008.

[17] F. Zhang, S. Guo, and X. Qian, "Segmentation for finger vein image based on PDEs denoising," in Proc. 3rd International Conference on Biomedical Engineering and Informatics(BMEI), pp. 531-535, 2010.

[18] C. Yuan and S. Liang, "Segmentation of color image based on partial differential equations," in Proc. Fourth International Symposium on Computational Intelligence and Design (ISCID), pp. 238-240, 2011.

[19] W. Zhao, J. Zhang, P. Li, and Y. Li, "Study of image segmentation algorithm based on textural features and neural network," in International Conference on Intelligent Computing and Cognitive Informatics (ICICCI), pp. 300-303,2010.

[20]M. Sharif, M. Y. Javed, and S. Mohsin, "Face recognition based On facial features, "Research Journal of Applied Sciences ,Engineering and Technology, vol. 4, pp. 2879-2886, 2012.

[21]M. Yasmin, M. Sharif, and S. Mohsin, "Neural net-works in medical imaging applications: A survey," World Applied Sciences Journal, vol. 22, pp. 85-96, 2013.

[22]L. Zhang and X. Deng, "The research of image segmentation based on improved neural network algorithm," in Proc. Sixth International Conference on Semantics Knowledge and Grid (SKG), pp. 395-397, 2010.

[23] S. A. Ahmed, S. Dey, and K. K. Sarma, "Image texture classification using Artificial Neural Network (ANN)," in Proc. 2nd National Conference on Emerging Trends and Applications in Computer Science (NCETACS), pp. 1-4, 2011.

[24]M. Sharif, M. Raza, S. Mohsin, and J. H. Shah,"Microscopic feature extraction method," Int. J. Advanced Networking and Applications,vol. 4, pp. 1700-1703, 2013.

[25]I. Irum, M. Raza, and M. Sharif, "Morphological procedures for medical images: A review," Research Journal of Applied Sciences,vol. 4, 2012.

Author's details

[1]M.Tech, Scholar, Department of Electronics and Communication Engineering, Government Women Engineering College, Ajmer, India, Email: shakuntalasatyawana@yahoo.in

[2]Assistant Professor, Department of Electronics and Communication Engineering, Govt. Women Engineering College, Ajmer, India, Email: skagarwal5@rediffmail.com

Copy for Cite this Article- Shakuntala Satyawana, Surendra Kumar Agarwal, "A Review Paper On Image Segmentation and Object Recognition Procedures', *International Journal of Science, Engineering and Technology,* Volume 4 Issue 1: 2016, pp. 299- 303

Deepankar Dev Pandey et al. 2016, Volume 4 Issue 1
ISSN (Online): 2348-4098
ISSN (Print): 2395-4752

International Journal of Science, Engineering and Technology
An Open Access Journal

Removal of Flouride from Industrial Waste Water Using Mosambi Peel as Biosorbent: Kinetics Studies

[1]Deepankar Dev Pandey, [2]Apoorva Tripathi, [3]Tej Pratap Singh

Abstract

Fluorides are the major pollutants present in the effluents from various industries. These are highly toxic to living beings and have a hazardous effect on their health. Thus the removal of fluoride using biosorbents is a major step towards the protection of environment. Here we use Mosambi Peel as a biosorbents for fluoride removal from industrial waste water. The characterization of its surface has been done by using various techniques such as EDAX and scanning electron microscopy (SEM) analysis. The fluoride removal efficiency of mosambi peel was investigated by batch wise adsorption experiment. The kinetic parameters and constants has been computed from various kinetic models like pseudo first order, pseudo second order, Bangham's model, intraparticle diffusion model and Elovich model. Adsorption of fluoride on to Mosambi Peel followed the pseudo second order rate equation. The effect of various important parameters on the % removal was studied to find the optimum condition for the maximum removal of fluorides. The parameters like contact time, adsorbent dose, initial fluoride concentration and pH were investigated. The optimum pH, initial concentration, adsorbent dose and contact time were found to be 7, 20 mg/l, 10g/l and 40 min. respectively for which there was maximum fluoride removal.

Keywords: Mosambi peel, Biosorption, Elovich model, SEM, FTIR, Adsorbent dose

Introduction

The industrial waste water from various industries like electroplating, semiconductor, glass and oil refineries etc. contains a very high concentration of different organic and inorganic chemicals. These toxic chemicals are very hazardous and have adverse effect on both the aquatic life as well as the terrestrial life.

Fluorides are the hazardous inorganic pollutant widely found in underground water and industrial waste water. Although the low concentration of fluorides are healthy and safe but beyond the permissible limits its consumption is very dangerous. The permissible range of fluoride concentration in drinking water has been set as 0.5-1.5 mg/l by many organizations like CPCB, WHO and USEPA etc. In India, around one million people are affected by indigenous fluorosis [1, 2].

[1]Corresponding Author's Email: deepankar161293@gmail.com

Fluoride is widely distributed on earth in many forms like fluoride minerals, in underground water, foods and tea leaves [3]. Fluoride dissolved into the groundwater due to the presence of fluoride minerals/rocks like fluorite, cryolite, phosphorite, fluorapatite, theorapatite etc. at the aquifer bottom [4]. Further, various industrial processes such as steel production, glass manufacturing, electroplating, phosphatic fertilizer production, ceramic industry and coal combustion etc. greatly contributed in increasing the fluoride contamination level in water. Thus the treatment of waste water is necessary before its discharge. At present, many technologies are available for the removal of fluoride from water such as co-precipitation, coagulation, ion exchange, adsorption, dialysis, electro-dialysis, reverse osmosis, membrane technologies etc.[5-11]. All these technologies have their indigenous advantages and disadvantages such as secondary sludge production, less efficiency and highly sensitized. In these methods adsorption is a most simple and attractive process due to its low cost and high efficiency. But now a day, biosorption techniques are found to be

more simple and efficient due to their sludge free operation and regeneration potential. Biosorption techniques involve several easily available agricultural biosorbents like neem leaf, banana peel, coffee husk, groundnut shell, rice husk ash, khair leaf and peepal leaf etc. for the removal of toxic fluoride ions from waste water [12-15]. In most of the available literatures on the fluoride removal using various biosorbents, the fluoride concentration is between 1.5-5 mg/l available in groundwater at normal conditions. However in industrial waste water the fluoride concentration is higher [16] and its removal is become necessary to prevent its adverse effects on environment. Therefore, in this paper the fluoride removal potential of mosambi peel has been investigated. Here, the effect of various parameters on the percentage removal of fluoride has been studied and the sorption nature has been also determined in terms of kinetic models.

Materials and Method

Materials

In the present experiment, all the chemicals used were of analytical grade and purchased from Fischer Scientific. Distilled water had been used for the preparation of stock solution and dilutions. Stock solution of 100 mg/l concentration of fluoride was prepared by dissolving 221mg of anhydrous sodium fluoride in one liter water [17].

Biosorbent Preparation

Mosambi fruit peel was collected from the fruit stall located in the campus of Bundelkhand Institute of Engineering and Technology Jhansi UP, India. The mosambi peels were washed thoroughly with water for removing the dirt, dried and finally crushed. After drying and crushing its screening had been done through 150-mesh size and the remaining larger sizes are analyzed as such.

Batch Adsorption Experiment

In batch biosorption experiment , the 50 ml of sample having 20 mg/l of initial fluoride concentration had been taken in a conical flask of volume 100 ml containing 10 g/L bio-adsorbent having particle size of 150 µm, which was agitated at 125 rpm [18,19]. After the agitation the conical flask was allowed to stand for 2 minutes for the settling of adsorbent. Similar experiment was carried out for determining the optimum conditions and to study the effect of pH, adsorbent dose, contact time and initial fluoride concentration. The ranges of operating parameters for these experiments are shown in table-1.

Table 1: Ranges of operating parameters for various experiments

Objective of experiment	Operating parameters
To study the effect of contact time on fluoride removal	Adsorbent Dose:10g/L Room Temperature: 30^0C; Solution pH:7 Initial Fluoride Concentration: 20mg/l Contact Time: 10, 20, 30, 40, 50, 60, 70 min
To study the effect of pH on fluoride removal	Adsorbent Dose: 10g/L Room Temperature: 30 ^{0}C; Contact Time:40min; Initial Fluoride Concentration: 20mg/l pH: 3, 4, 5, 6, 7, 8, 9, 10, 11
To study the effect of initial fluoride concentration on fluoride removal	Adsorbent Dose: 10g/L; Contact Time: 40 min Room Temperature: 30^0C; Solution pH:7 Initial Fluoride Concentration: 10, 20, 30, 40, 50 mg/l
To study the effect of adsorbent dose on fluoride removal	Contact Time: 40 min; Room Temperature: 30^0C Solution pH: 7; Initial Fluoride Concentration: 20 mg/l Adsorbent Dose: 2, 4, 6, 8, 10, 12, 14, 16, 18, 20 g/L

The concentration of fluoride q_e (mg/g) adsorbed was calculated by using the following formula [30] –

$$q_e = \frac{(C_i - C_f) \times V}{W}$$

Where,

q_e – the amount of fluoride adsorbed (mg/g)

C_i – initial concentration of fluoride in solution (mg/l)

C_f – residual concentration of fluoride in solution at equilibrium (mg/l)

V –volume of the solution (L)

W–weight of the adsorbent (g)

The percentage removal of fluoride ion was calculated as follows -

$$\%\ Removal\ of\ Fluoride\ ion = \frac{C_i - C_f}{C_i} \times 100$$

Where,

C_i – initial concentration of fluoride in solution (mg/l)

C_f – residual concentration of fluoride in solution at equilibrium (mg/l)

Method of Analysis

In each experiment, after the adsorption studies on the effects of various parameters such as contact time, pH, initial fluoride concentration and adsorbent dose, the sample solution was filtered through Whatman no. 42 filter paper and the filtrate was analyzed for determining the fluoride concentration through SPADNS [17] photometric method using UV–spectrophotometer at wavelength of 570nm.

Spectrophotometric Method

In this method, an indicator dye and a metallic compound such as iron, aluminium, zirconium, thorium, cerium or lanthanum reacts to form a colored complex having small dissociation constant. Further, fluoride reacts with this complex and forms a new complex. This transformation in the configuration of the complex results in the shifting of the surface assimilation spectrum relative to the fluoride-free reagent solution's spectrum. This shifting can be observed by using a spectrophotometer. The commonly used dyes are Erichrome Cyanine R and SPADNS [trisodium 2-(parasulfophenylazo)-1, 8-dihydroxy-3, 6-naphthalene disulfonate]. When the SPADNS dye is used, SPADNS reacts with zirconium ion to form a red colored complex. Further, fluoride reacts with this complex and discolors the red color of the complex. Now the variation in the absorbance can be determined by using a spectrophotometer.

Formation of the SPADNS – ZrOCl2 complex

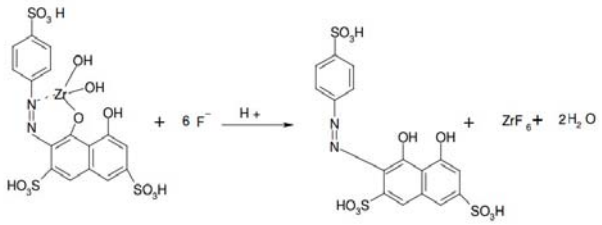

Reaction of the complex with fluoride ions

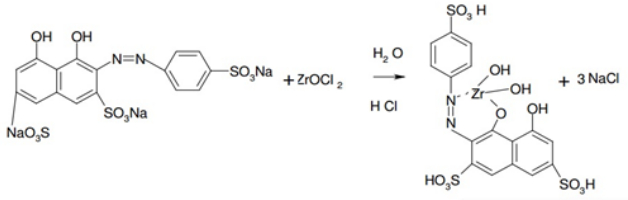

Results and Discussions

Effect of pH

pH is one of the important parameter that affects the biosorption of fluoride. Fig.1 shows the plot of the % fluoride removal against the varying pH range 3-11. The nature of the graph shows that the maximum adsorption of fluoride occurred at pH 5 and beyond the pH 5 the % fluoride removal was decreased due to the electrostatic repulsion between the mosambi peel surface and the negatively charged fluoride ion. The results of this study shows that the optimum pH is 7 which is sufficient for the biosorption of fluoride on the mosambi peel as between pH (7-11) there is not any significant difference between % removal of fluoride (54.59 – 56.44 %). So we can optimize the other parameters at neutral pH i.e. pH 7.

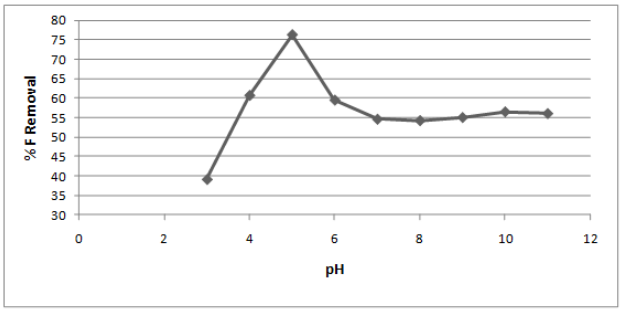

Fig.1 Effect of pH on adsorption of fluoride on mosambi peel

Effect of adsorbent Dose

To study the effect of biosorbent dose, the experiments are performed at various doses of biosorbent lying between 2-20 g/L of fluoride solution with 100 mg/l initial concentration of fluoride. The % removal of fluoride has been increased with increasing quantity of biosorbent upto 10g/L and after that it decreases to some extent and then shows the almost same % removal efficiency for rest of the biosorbent doses as shown in Fig.2. This behavior has been shown because initially more active sites are available for the adsorption and after the optimum dose the active sites are saturated that results in decrease in the % removal of fluoride. The results of this study show that the optimum biosorbent dose of 10 g/L is sufficient for the biosorption of fluoride on the mosambi peel as between 10- 20 g/L the % removal of fluoride is almost same lying between (94.23 - 93.37 %).

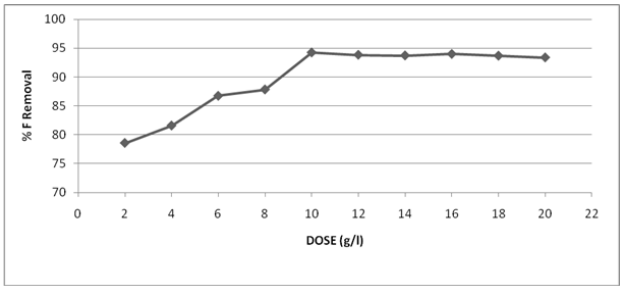

Figure 2: Effect of biosorbent dose on adsorption of fluoride on mosambi peel

Effect of contact time

The study of the effect of contact time was conducted for determining the biosorption capacity of the mosambi peel by considering the time period for the agitation of the biosorbent at the solid-liquid interface. The amount of fluoride adsorbed qt (mg/g) at different contact times t (min) is plotted as shown in Fig.3. Initially there is a rapid increase in fluoride removal with increase in the agitation time but gradually it reaches to some constant values and after the 40 min. it attains the equilibrium state. This result may be shown due the presence of the more active sites initially and after the fluoride accumulation and the saturation of the sites it decreases and attains equilibrium. The results of this study show that the contact time of 40 min. is sufficient for the biosorption of fluoride on the mosambi peel.

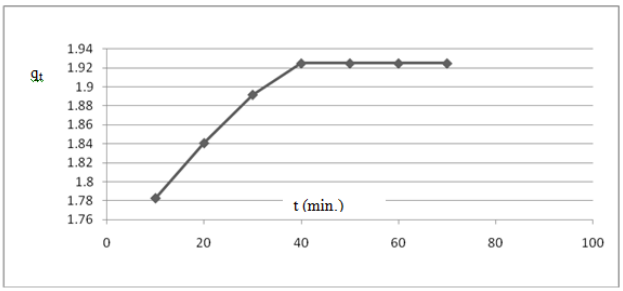

Figure 3: Effect of contact time on adsorption of fluoride on mosambi peel

Effect of Initial Fluoride concentration

In the analysis of the effect of initial fluoride concentration, a graph of % fluoride removal had been plotted against the varying initial fluoride concentration between 20-60 mg/l as shown in Fig.4. From the graph it was found that % fluoride removal efficiency decreases with increase in initial fluoride concentration. This was due to the saturated binding capacity of the biosorbent. Because when the adsorbate concentration was increased, beyond the certain concentration the binding capacity of the adsorbent reaches to saturation resulting in the decrease in the % fluoride removal. The optimum initial fluoride concentration is 20 mg/l which shows the maximum removal efficiency of 93.14 %.

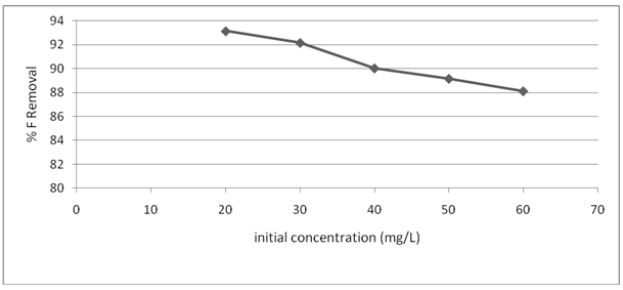

Figure 4: Effect of Initial Fluoride concentration on

adsorption of fluoride on mosambi peel

Adsorption Kinetic Studies

Kinetic models are applied for determining the rate of adsorption process as well as for measuring the potential of the rate controlling step. The squared sums of errors (SSE) values were used for finding the best kinetic model for describing the sorption mechanism of fluoride. According to this, the model that has the lowest SSE value is the best model for that particular system [20, 21]. The SSE values of the models were calculated by using the following equation –

$$SSE = \sum (qe_{expt.} - qe_{cal.})^2 / (qe_{expt.})^2$$

Where,

qe_{expt} – the experimental sorption capacity of fluoride (mg/g) at equilibrium

qe_{cal} – the sorption capacity of fluoride calculated by using the kinetic model

In general, the liquid-solid adsorption mechanism is governed by the intra-particle diffusion, film diffusion and mass action. But for kinetic studies, the mass action can be neglected as it plays a vital role in physical adsorption. Thus the adsorption kinetics for liquid-solid adsorption is always controlled by the diffusion processes i.e. either intraparticle diffusion or film diffusion is a rate limiting step [22].

The rate of the adsorption and kinetics of fluoride onto mosambi peel was determined by using the five simple kinetic models namely pseudo first-order, pseudo second-order, Weber and Morris intra-particle diffusion model, Bangham's pore diffusion model and Elovich equations. And by using the SSE value we would find the best fitted model.

Pseudo first order model

The Lagergren's pseudo first order rate equation is widely used to describe the adsorption of adsorbate from the liquid phase to solid phase [23, 24]. The linear form of Lagergren's pseudo first-order rate equation is given as follows –

$$\log(q_e - q_t) = \log(q_e) - \frac{k_1 t}{2.303}$$

Where,

q_e - the amount of fluoride adsorbed on adsorbent (mg/g) at equilibrium

q_t - the amount of fluoride adsorbed on adsorbent (mg/g) at time t (min.)

k_1- the rate constant of pseudo first-order kinetics

A graph has been plotted for $\log(q_e - q_t)$ against the varying time (t) as shown in Fig.5 which represents the linearized form of the adsorption of fluoride by mosambi peel. The correlation coefficient was found to be 0.9984 which indicates applicability of the model in the kinetic studies. The values of the rate constant (K_1) and $q_{e(cal.)}$ can be determined by using the slope and the intercept of the graph as shown in Table 1.

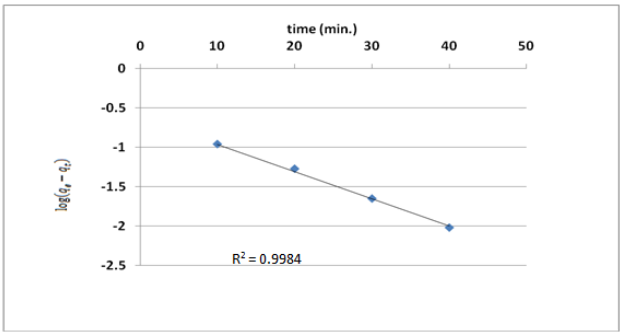

Figure 5: Pseudo First Order Kinetic modeling of adsorption of fluoride by Mosambi Peel

Pseudo second order model

Pseudo second order model can also be used for describing the adsorption kinetics for which the following equation can be used [25] –

$$\frac{t}{q_t} = \frac{1}{k_2 q_{e2}} + \frac{1}{q_e} t$$

Where,

q_e - the amount of fluoride adsorbed on adsorbent (mg/g) at equilibrium

q_t - the amount of fluoride adsorbed on adsorbent (mg/g) at time t (min.)

k_2 - the rate constant of pseudo second-order kinetics

The plot between t/q_t versus t for the mosambi peel adsorbent was found to be linear as shown in Fig.6 having the value of correlation co-efficient (R^2) to be 0.9993 which is higher than that of pseudo first-

order model. The values of the rate constant (K_2) and $q_{e(cal.)}$ were found by determining the slope and intercept of the corresponding plot which are shown in Table1.

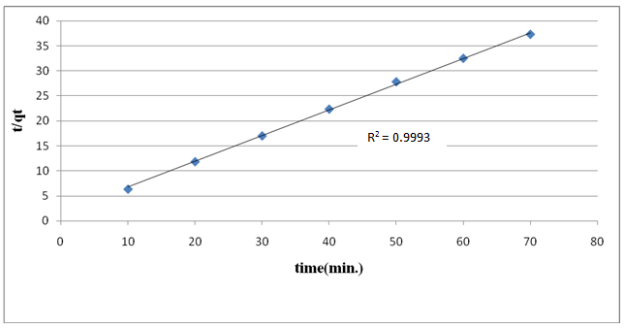

Figure 6: Pseudo Second Order Kinetic modeling of adsorption of fluoride by Mosambi Peel

Elovich Equation

Elovich equation is widely used for describing the adsorption kinetics for the chemisorption. It states that the diffusion processes are rate limiting step in chemical adsorption [26, 27]. The Elovich equation is given as follows [28] :

$$q_t = \frac{\ln(\alpha\beta t)}{\beta} + \frac{\ln(t)}{\beta}$$

Where, α is the initial sorption rate (mg/g min) and β is the related to extent of surface coverage and activation energy for chemisorption. These constants can be calculated from the intercept and the slope of the straight line plot respectively.

When a graph of q_t versus ln t was plotted as shown in fig.7, it was found to be well fitted with the Elovich equation having the high correlation coefficient (0.9588). This shows that the rate limiting step is solely controlled by diffusion processes [29]. It may be the film diffusion or pore diffusion which governs the rate of fluoride adsorption onto mosambi peel.

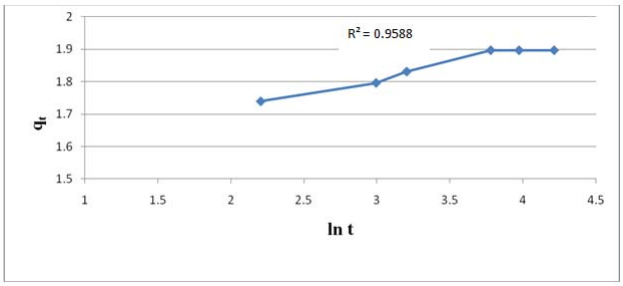

Figure 7. Elovich Equation plots of Mosambi peel

Intra particle diffusion

Intra particle diffusion model has been widely used for determining the rate of adsorption that can be used for analyzing the rate controlling step. In general, the intra particle diffusion can be explained by using the Weber-Morris equation [30] which is as follows –

$$q_t = K_{ip} t^{0.5} + C$$

Where,

C – The intercept

K_{ip} – the intra particle diffusion rate constant

According to this equation, the Weber-Morris plot of q_t versus $t^{1/2}$ should be a straight line which shows that the intra-particle diffusion process is involved in the adsorption of fluoride. But the intra particle diffusion process is the rate limiting step only when the plot passes through the origin. However this is not always possible which shows that different kinetic models control the rate limiting step and these models operate simultaneously.

In fig.8, the Weber-Morris plot for mosambi peel is not passing through the origin which shows that at the initial stage, the kinetics of fluoride adsorption is governed by the film diffusion process and at the later stage, intra-particle transport of fluoride ions into the pores controlled by pore diffusion [31].

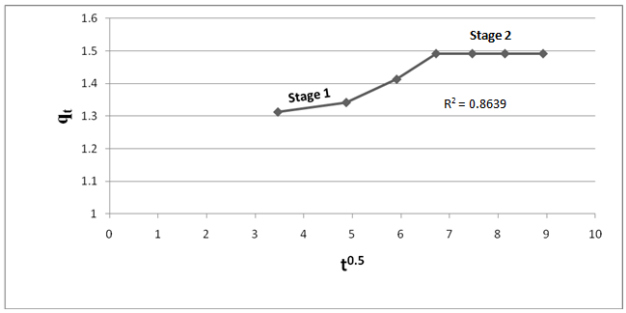

Fig 8: Intra particle diffusion plot for adsorption on Mosambi peel

Bangham's model

Since the intra particle diffusion process is not the rate limiting step for the fluoride adsorption thus for finding whether the pore diffusion is rate limiting

step or not we analyze the Bangham's Model. Thus the equation of Bangham's model is as follows [32]–

$$\log\log\left(\frac{C_i}{C_i - q_t.m}\right) = \log\left(\frac{K_0.m}{2.303.V}\right) + \alpha.\log(t)$$

Where C_i is the Initial concentration of adsorbate in the solution (mg/l), m is the mass of the adsorbent (g/l), V is the volume of solution (ml), K_0 is the rate constant, q_t is the amount of the adsorbate adsorbed at time t (mg/g).

When we plot a graph for $\log\log\left(\frac{C_i}{C_i - q_t.m}\right)$ versus log t as shown in fig.9. The graph was found to be linear having correlation coefficient (0.9854) approaching to 1 which indicates that the kinetic data is best fitted with Bangham's model and the adsorption kinetic is controlled by pore diffusion only.

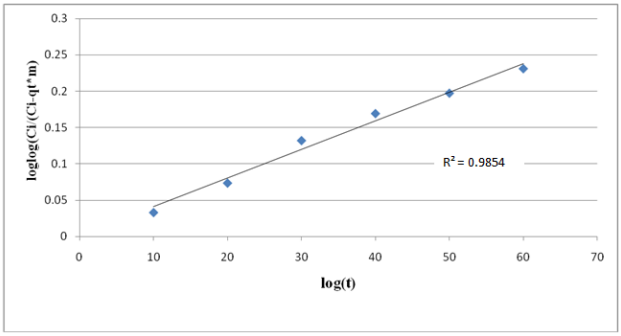

Figure 9: Bangham's Model plot of Mosambi peel

Table1: SSE values and various kinetic parameters for all the kinetic models

Pseudo first order model					
Name of adsorbent	**K_1 (min.$^{-1}$)**	**$q_{e(expt)}$ (mg/g)**	**$q_{e(cal)}$ (mg/g)**	**R^2**	**SSE**
Mosambi peel	0.3146	1.915	0.6221	0.9984	0.4558
Pseudo second order model					
Name of adsorbent	**K_2 (min.$^{-1}$)**	**$q_{e(expt)}$ (mg/g)**	**$q_{e(cal)}$ (mg/g)**	**R^2**	**SSE**
Mosambi peel	0.5499	1.915	1.732	0.9993	0.0091
Elovich equation model					
Name of adsorbent	**β**	**$q_{e(expt)}$(mg/g)**	**$q_{e(cal)}$(mg/g)**	**R^2**	**α**	**SSE**
Mosambi peel	0.0873	1.915	0.4708	0.9588	1.547	0.5687
Intra particle diffusion model					
Name of adsorbent	**K_{ip} (mg/g.min.$^{-0.5}$)**	**$q_{e(expt)}$(mg/g)**	**$q_{e(cal)}$(mg/g)**	**R^2**	**SSE**
Mosambi peel	0.0206	1.915	1.251	0.8639	0.1202
Bangham's model					
Name of adsorbent	**K_0**	**$q_{e(expt)}$(mg/g)**	**$q_{e(cal)}$(mg/g)**	**R^2**	**α**	**SSE**
Mosambi peel	0.039	1.915	1.806	0.9854	0.002	0.0032

Biosorbent Characterization

SEM

The surface morphological characteristics of the mosambi peel were examined by SEM. Fig. 10(a) and 10(b) shows the surface of the mosambi peel before and after the adsorption the fluoride. From these figures we found that the surface of the mosambi peel was very irregular and porous. This porosity of the surface is mainly responsible for the adsorbance capacity of the mosambi peel.

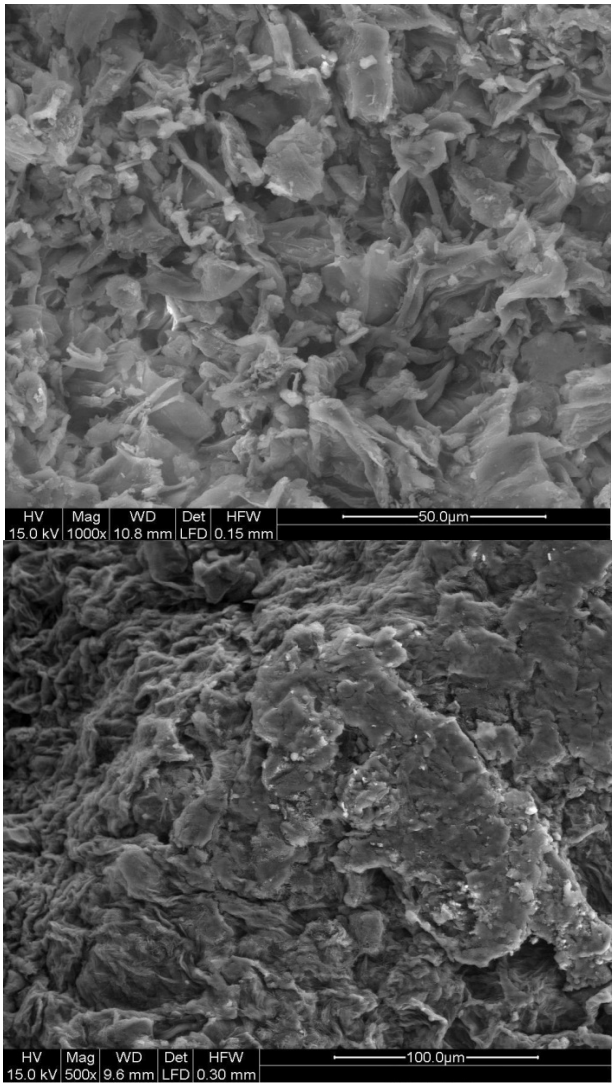

Figure 10: SEM image of Mosambi Peel (a) Before Adsorbtion and (b) After Adsorbtion

EDAX

EDAX analysis was carried out for the characterization of the Mosambi peel's surface before and after adsorption as shown in Fig 11(a) and 11(b). It is evident from the figures that the elements such as oxygen, carbon and a small amount of potassium etc. except fluoride were present in the adsorbent initially but after the adsorption of the fluoride it was found that about 0.71 wt % of fluoride was present on the adsorbent surface. This result confirms the adsorption of fluoride by the mosambi peel.

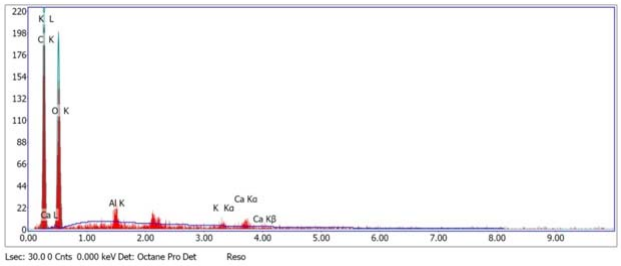

Element	Weight %	Atomic %	Net Int.	Error %
C K	45.23	53.28	55.4	7.89
O K	51.07	45.16	55.46	11.31
AlK	1.43	0.75	5.43	36.15
K K	0.58	0.21	1.36	67.85
CaK	1.69	0.6	3.22	61.77

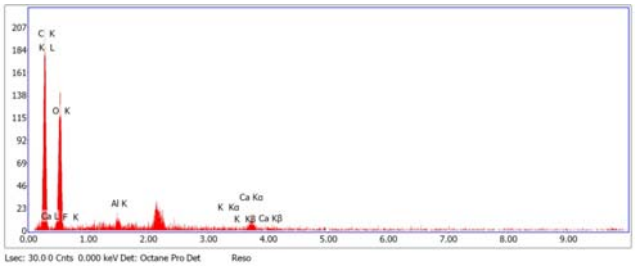

Element	Weight %	Atomic %	Net Int.	Error %
C K	44.04	52.34	50.97	7.91
O K	50.98	45.48	50.54	11.5
F K	0.71	0.53	0.56	91.93
AlK	0.69	0.36	2.41	67.36
K K	0.2	0.07	0.45	78.32
CaK	3.38	1.2	5.97	27.42

Figure 11: EDAX spectra for Mosambi peel (a) Before Adsorption and (b) after adsorption

Conclusion

The present study states that mosambi peel has a considerable potential for the removal of fluoride from the waste water at low cost. The SEM analysis showed that surface porosity was solely responsible for the uptake capacity of the mosambi peel and fluoride removal was evident through EDAX. The rate of adsorption is best explained by pseudo second order model having high correlation coefficient (0.9993). The kinetic data was best fitted with Bangham's model with good correlation coefficient (0.9854) which shows that the adsorption mechanism is controlled by pore diffusion process. It was also found that the removal efficiency of mosambi peel is affected by the pH, contact time, initial fluoride concentration and adsorbent dose. At optimum conditions, the value of these parameters was 7, 40 minute, 20 mg/l and 10g/L respectively for which the removal efficiency was maximum i.e. 94.23%. Thus the use of mosambi peel as a low cost biosorbent for the fluoride removal was proved to be economic feasible in the treatment of industrial waste water.

References

[1]. Singh R. and Maheshwari R.C., Defluoridation of drinking water–a review, Ind. J. Environ. Protec., 21(11), 983–991 (2001)

[2]. Bell M.C. and Ludwig T.G., The supply of fluoride to man: Ingestion from water, Fluorides and Human Health, World Health Organization, Geneva, WHO Monograph Series 59 (1970)

[3]. Malinowska E, Inkielewicz I, Czarnowski W, Szefer P (2008). "Assessment of fluoride concentration and daily intake by human from tea and herbal infusions". Food Chem. Toxicol. 46 (3): 1055–61.

[4]. Murray J.J., A history of water fluoridation, Br. Dent. J., (13), 4250–254 (1973)

[5]. Popat, K. M., P. S. Anand, and B. D. Dasare. "Selective removal of fluoride ions from water by the aluminium form of the aminomethylphosphonic acid-type ion exchanger." Reactive polymers 23, no. 1 (1994): 23-32.

[6]. Amor, Zakia, Bernard Bariou, Nabil Mameri, Mohamed Taky, Stephan Nicolas, and Azzedine Elmidaoui. "Fluoride removal from brackish water by electrodialysis." Desalination 133, no. 3 (2001): 215-223.

[7]. Shen, Feng, Xueming Chen, Ping Gao, and Guohua Chen. "Electrochemical removal of fluoride ions from industrial wastewater." Chemical Engineering Science 58, no. 3 (2003): 987-993.

[8]. Guo, Laodong, Becky J. Hunt, and Peter H. Santschi. "Ultrafiltration behavior of major ions (Na, Ca, Mg, F, Cl, and SO 4) in natural waters."Water Research 35, no. 6 (2001): 1500-1508.

[9]. Matsuura, Takeshi, and S. Sourirajan. "Studies on reverse osmosis for water pollution control." Water Research 6, no. 9 (1972): 1073-1086.

[10]. Simons, R. "Trace element removal from ash dam waters by nanofiltration and diffusion dialysis." Desalination 89, no. 3 (1993): 325-341.

[11]. Chubar, N. I., V. F. Samanidou, V. S. Kouts, G. G. Gallios, V. A. Kanibolotsky, V. V. Strelko, and I. Z. Zhuravlev. "Adsorption of fluoride, chloride, bromide, and bromate ions on a novel ion exchanger." Journal of colloid and interface science 291, no. 1 (2005): 67-74.

[12]. Tembhurkar A.R., Dongre S.R., Comparative studies on fluoride removal using natural adsorbents viz AzadirachtaIndica (neem) and FicusReligiosa (Pipal), IE(I) Journal-EN, (90)18-23 (2009)

[13]. Getachew, T., Hussen, A., & Rao, V. M. (2015). Defluoridation of water by activated carbon prepared from banana (Musa paradisiaca) peel and coffee (Coffea arabica) husk. International Journal of Environmental Science and Technology, 12(6), 1857-1866.

[14]. Mondal, Naba Kr, Ria Bhaumik, Arnab Banerjee, Jayanta Kr Datta, and Tanmoy Baur. "A comparative study on the batch performance of fluoride adsorption by activated silica gel and activated rice husk ash." International Journal of Environmental Sciences 2, no. 3 (2012): 1643-1661.

[15]. Alagumuthu, G. A. N. A. P. A. T. Y., and M. A. R. I. A. P. P. A. N. Rajan. "Kinetic and equilibrium studies on fluoride removal by zirconium (IV): Impregnated groundnut shell carbon." Hemijska industrija 64, no. 4 (2010): 295-304.

[16]. Pollution Prevention and Abatement Handbook Phosphate fertilizer plant, World Bank Group (1998)

[17]. American Public Health Association (APHA), Standard Methods for the Examination of Water and Wastewater, 21st ed., American Public Health Association (APHA), 1015 Fifteenth Street, NW, Washington DC, (2005)

[18]. Sivasankar, V., T. Ramachandramoorthy, and A. Chandramohan. "Fluoride removal from water using activated and MnO 2-coated Tamarind Fruit (Tamarindus indica) shell: Batch and column studies." Journal of hazardous materials 177, no. 1 (2010): 719-729.

[19]. Jamode, A. V., V. S. Sapkal, and V. S. Jamode. "Defluoridation of water using inexpensive adsorbents." Journal of the Indian Institute of Science 84, no. 5 (2013): 163.

[20]. Viswanathan, Natrayasamy, C. Sairam Sundaram, and S. Meenakshi. "Removal of fluoride from aqueous solution using protonated chitosan beads." Journal of hazardous materials 161.1 (2009): 423-430.

[21]. American Public Health Association. "Water Environment Federation." Standard methods for the examination of water and wastewater 19 (1995).

[22]. Meng, F. W. "Study on a mathematical model in predicting breakthrough curves of fixed-bed adsorption onto resin adsorbent." PhD diss., MS Thesis, Nanjing University, China, 2005.

[23]. Ho, Y. S., and G. McKay. "A comparison of chemisorption kinetic models applied to pollutant removal on various sorbents." Process Safety and Environmental Protection 76.4 (1998): 332-340.

[24]. Meenakshi, S., and Natrayasamy Viswanathan. "Identification of selective ion-exchange resin for fluoride sorption." Journal of colloid and interface science 308.2 (2007): 438-450.

[25]. Lagergren, Svenska. "About the theory of so-called adsorption of soluble substances." (1898): 1-39.

[26]. Zhang, Junshe, and Robert Stanforth. "Slow adsorption reaction between arsenic species and goethite (α-FeOOH): diffusion or heterogeneous surface reaction control." Langmuir 21.7 (2005): 2895-2901.

[27]. Aksu, Zümriye, and Sevilay Tezer. "Equilibrium and kinetic modelling of biosorption of Remazol Black B by Rhizopus arrhizus in a batch system: effect of temperature." Process Biochemistry 36.5 (2000): 431-439.

[28]. Aharoni, Chaim, and Moshe Ungarish. "Kinetics of activated chemisorption. Part 2.—Theoretical models." Journal of the Chemical Society, Faraday Transactions 1: Physical Chemistry in Condensed Phases 73 (1977): 456-464.

[29]. Singh, Tej Pratap, and C. B. Majumder. "REMOVAL OF FLUORIDE USING SWEET LEMON PEEL IN BATCH REACTOR: KINETICS AND EQUILIBRIUM STUDIES." (2015).

[30]. WJ Weber Jr., JC Morris; J. Sanit. Eng. Div. Am. Soc. Civ. Eng., 89 (1963), pp. 31–39.

[31]. Qiu, Hui, Lu Lv, Bing-cai Pan, Qing-jian Zhang, Wei-ming Zhang, and Quan-xing Zhang. "Critical review in adsorption kinetic models." Journal of Zhejiang University Science A 10, no. 5 (2009): 716-724.

[32]. Kumar, Eva, Amit Bhatnagar, Minkyu Ji, Woosik Jung, Sang-Hun Lee, Sun-Joon Kim, Giehyeon Lee et al. "Defluoridation from aqueous solutions by granular ferric hydroxide (GFH)." Water research 43, no. 2 (2009): 490-498.

Author's details

[1,2]Department of Chemical Engineering, Bundelkhand Institute of Engineering & Technology, Jhansi-284128 U.P. India

[3]Department of Chemical Engineering, Bundelkhand Institute of Engineering & Technology, Jhansi-284128 U.P. India

Copy for Cite this Article- Deepankar Dev Pandey, Apoorva Tripathi, Tej Pratap Singh, 'Removal Of Flouride From Industrial Waste Water Using Mosambi Peel As Biosorbent: Kinetics Studies,' *International Journal of Science, Engineering and Technology,* Volume 4 Issue 1: 2016, pp. 304- 313.

Vishnu Khetan et al. 2016, Volume 4 Issue 1
ISSN (Online): 2348-4098
ISSN (Print): 2395-4752

International Journal of Science, Engineering and Technology
An Open Access Journal

Design and Fabrication of a Hybrid Solar & Micro Wind Power Generator

[1]Vishnu Khetan, [2]Hari Kumar Singh, [3]Rohit Kumar

Abstract

This paper is concerning to designing of the micro hybrid system using solar energy and wind energy simultaneously. Now a day's electricity is most required facility for the human being. All the conventional energy resources are reducing day by day. So we have to move from conventional to non-conventional energy resources. In this research paper the combination of two energy resources such as i.e. solar and wind energy. The paper defines the design and fabrication of the hybrid solar and micro wind turbine. Solar PV cell and micro wind turbine have a great potential. In this research paper hybrid system we have discuss the design and fabrication of such a system. Hybrid system is simplified design, effectual power production as there is no gear box in the turbine, easiness in the installation, and maintenance coat is low. A hybrid system is design for the generation of power up to 40 W. There are 24 horizontal axis wind turbine in vertical plane is fabricated along with the 10 Solar PV cell of 3.2 W (Max Power). Designing parameter is evaluated and discuss in this research. Various parameter are discusses which affect the efficiency of the both solar PV cell and micro wind turbine.

Keywords- PV array, micro wind turbine, swept area, solidity, coefficient of performance (Cp), power consumption demand, Efficiency, design and fabrication.

Introduction

Now a day's major percentage of the electricity generation is contributed by generation through Coal, Diesel, Hydro, Nuclear sources of energy. The use of such fuel as a primary source of power generation produce very dangerous situation in environment. Hybrid solar & micro wind turbines consist of the small solar panel & micro wind size wind turbine as compare to the large centralized wind turbine. Working principle of the Wind turbines is to convert the kinetic energy of the wind firstly first into rotational kinetic energy in the turbine and then this rotational energy has been converted to the electrical energy via the generator or alternator that can be supplied, via the national grid, for any purpose. The energy which available in the wind and solar for conversion primarily depends on the wind velocity, swept area of the turbine & solar radiation. [1]When planning to establish a wind farm or solar farm its very important to know the probable/expected power and energy output of solar panel and each wind turbine to be able to determine its economic feasibility.

Material and Methodology

The Word 'hybrid' stand for the combination of two dissimilar things, in other word we can say that some things which made by the use of two different thing. Just like in the energy system, two or more different sources of the energy are combined and used to generate/produced the electricity. Hybrid energy system is the combination of two energy sources such as solar and wind, solar and diesel, wind and hydro or wind and diesel. In other word it can also be defined as "Energy system which is fabricated or designed to produce power with the help of two energy sources is called as the hybrid energy system." The main advantages of the hybrid energy system (solar and wind power) has good reliability, effective, efficient, no emission, and lower cost.

In this proposed system solar and micro wind turbine is design and fabricated to generate the power simultaneously. Solar energy and wind energy has more advantageous than any other non-

[1]Corresponding Author's Email: khetan2013@gmail.com

conventional energy sources. Both the energy sources are available in ample amount in all the areas. Thus there is no need to search special location to establish the hybrid system.

Solar Energy

Radiation of the sun is responsible for the generation of the solar energy. On earth, solar energy is present continuously and in abundant quantity. The main benefit is that Solar energy is freely available and it is renewable source of energy. It doesn't emit any harmful gases that mean it is pollution free. Only one problem is associate the with the solar system is that it is not capable to produce any output power in bad weather condition. Efficiency the of the solar energy are very high than any other sources of energy. Life of the solar panel is also very long. Photovoltaic cell is engaged to convert the incident sun radiation in to the electrical energy. PV cells are semiconductor device.

Photovoltaic systems (PV system) incorporate with the series of the solar panels. Solar panels works as converter of the energy from solar to electrical. Solar energy system is composed of one or more than one solar panels, it also include the controller or power converter, battery charger and the interconnections system and mounting for the other components used in the solar energy system.

Wind Energy

Wind energy is renewable energy sources. Wind is an indirect solar energy source. Wind energy is the energy which is taken out from wind. For pulling out the energy from the wind we need wind turbine. Cost of generation of electricity from the wind energy is slightly higher than the solar energy. Maintenance cost is also less for wind energy system. The main advantage of wind energy is that it present nearly 24 hours of the day. There is no emission product during the generating power. Generation of electricity from wind is function of the speed of wind speed. The main limitation of using renewable energy resources are that unavailability of power for all time because solar and wind doesn't available whole a day.

The objective of this project is to design the system such that it will operates at minimum wind velocity. There are 24 micro wind turbines are used to generate power and each micro wind turbine have 3 generator which is connected in series through the bridge rectifier.

Micro wind turbines works as similar to the centralized wind turbines. It also equipped with the self starting with the help of the wind velocity. Micro wind turbine are arrange in horizontal axis in the vertical plane.

Calculation and Tables

For the designing of the hybrid energy system there are so many kind of relative data are required to accurate design the system. Data such as Power consumption demand, Duration of the sun shine where PV cells is going to install, Mean solar intensity (W/m^2) of the area, wind velocity, height and elevation of the area for which the system is design.

Steps Involved in the designing of the hybrid system are as follow:

1. First evaluate the power consumption demand for the load that needs to be supplied by the hybrid system.
2. Next is to divide the total power demand for the solar PV array and wind turbine.
3. After that solar PV array and Wind turbine were design separately according to the power demand from the each system.

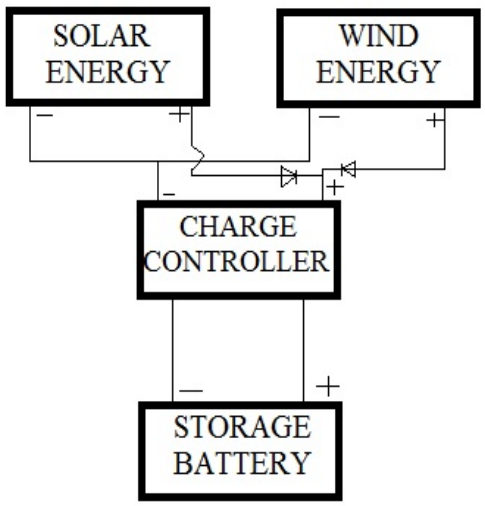

Figure 1: Systematic diagram for Hybrid Solar & Micro Wind Power Generator

Design Calculation

1. Selection of Generator on the basis of Design Calculation

The main target for the micro wind turbine to generate power average 15 W. All the design and fabrication is done on the basis of power generation target.

For Series Configuration, Maximum power we get is 0.7 W from single Turbine At different speed is as follow.

Table 1: Power generated in series configuration

Voltage (V)	2	3	8	10
Current (A)	.015	.017	.045	.07
Power (W)	.03	.051	.36	.70
Velocity of wind (m/s)	2	4	5.5	7

For Parallel Configuration, Maximum power we get is 0.375W from the single turbine is as follow.

Table 2: Power generated in Parallel configuration

Voltage (V)	.3	.5	1.5	2
Current (A)	.01	.05	.09	.11
Power	.003	.025	.135	.22
Velocity of wind (m/s)	2	4	5.5	7

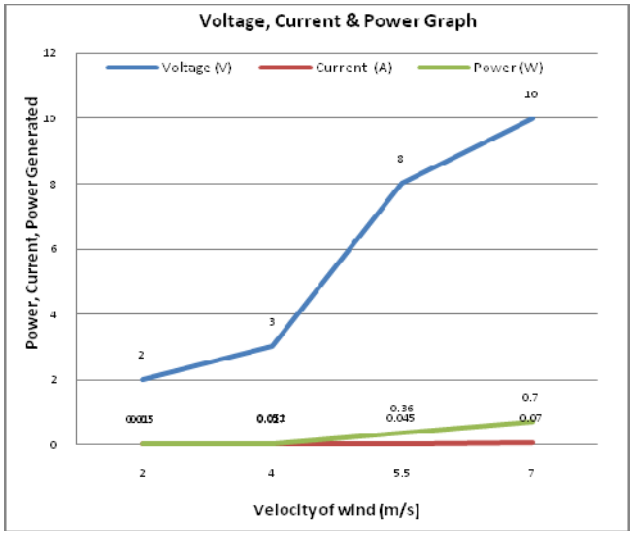

Figure 2: Graph of Voltage, Current & Power obtained in series configuration while increasing the velocity of wind

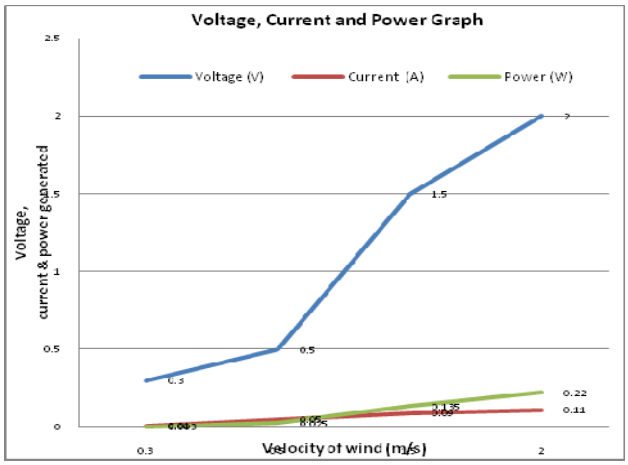

Figure 3: Graph of Voltage, Current & Power obtained in parallel configuration while increasing the velocity of wind

After doing a lot of experiments in connecting these generators into different combination best result are observed into the series combination. So we have design the generator into the series configuration. After connecting the generator, a bridge rectifier is connected to the each generator unit to fix the polarization of the current and to avoid the back flow of current in to generator. Each turbine has 3 generators, turbine is coupled to the main generator and next two generators get the driving power from the main generator with help of rope and pulley drive mechanism. Thus after calculation we get 16.8 W Power from 24 Micro Wind turbines at the wind speed of 7 m/s.

2. Design of Micro Wind Turnbine Blade

The blades of the turbine play a critical role in the efficiency of the turbine and hence it is considered as a strategic component. Mostly multiple blades are used over the turbine in order to achieve the optimum efficiency in the various wind speed. Here we used 6 blade high speed fan which has the capability to gives the better output results.

Specification of the turbine fan are as follow

No. of Turbine blade	:	6 blades
No. of Fan used	:	24 fans
Diameter of the turbine fan	:	23 cm

Diameter of Hub : 8 cm

Swept Area of blade : $0.037\ m^2$

$$\mathbf{WindTurbinePower} = \frac{1}{2} * \rho * A * V^3 * C_p * \eta_g * \eta_b$$

$$Average C_p = \frac{0.36 + 0.07 + 0.21 + 0.20}{4}$$

Average coefficient of performance = 0.21

Where,

P = Power in watts

ρ = Air density (about 1.225 kg/m^3 at sea level, less higher up)

A = Rotor swept area, exposed to the wind (m^2)

Cp = Coefficient of performance (.59 Betz limit is the maximum theoretically possible,.35 for a good design) [4]

V = wind speed in *m/s*

η_g = Generator efficiency (50% for car alternator, 80% or possibly more for a permanent magnet generator or grid-connected induction generator) [4]

η_b = Gearbox/bearings efficiency (depends, could be as high as 95% if good)[4]

Table 3: Coefficient of performance at different speed

Wind Speed (m/s)	Power generated from the 24 Turbine (W)	Theoretical power through 24 turbine (W)	Coefficient of performance
2	0.72	1.95	0.36
4	1.22	15.66	0.07
5.5	8.64	40.72	0.21
7	16.8	83.96	0.20

Two important parameters in the design of the wind turbine rotor are the axial thrust which act as along the direction of the wind flow and other is circumferential force acting along the rotation of the wheel which provides the torque.

Thrust and torque on the turbine rotor

The axial force acting on the turbine rotor is given by:

$$F_x = \frac{\pi}{9}\rho D^2 V_i^2$$

$$F_x = \frac{\pi}{9} * 1.17 * 23^2 * V_i^2$$

Table 4: Thrust force on the blade

Wind Speed (m/s)	Thrust Force (N)
2	0.086
4	0.345
5.5	0.653
7	1.057

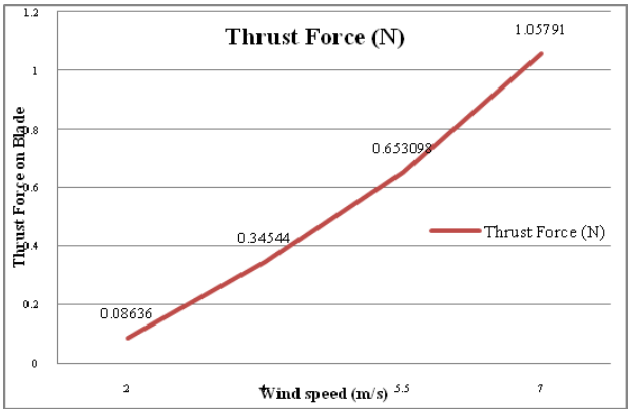

Figure 4: Graph between Winds Speed V/s Thrust force on the blade

Torque on the turbine rotor

The torque on the surface is given by:

$$T_x = (F_x) \times \frac{D}{2}$$

$$T_x = \frac{\pi}{9}\rho D^2 V_i^2 \times \frac{D}{2}$$

Table 5: Torque Generated on the blade

Wind Speed (m/s)	Torque Generated (N-m)
2	0.009
4	0.039
5.5	0.075

7	0.121

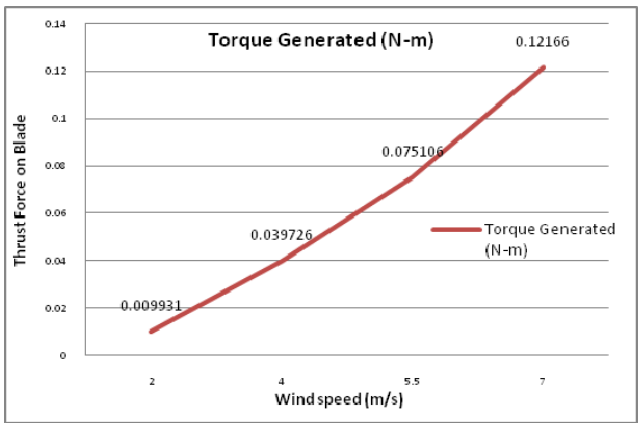

Figure 5: Graph between Wind Speed V/s Torque generated

Solidity (σ)

It is important factor for designing the turbine. It is ratio of blade area to the circumference of rotor.

$$\sigma = \frac{n \times b}{\pi \times D}$$

$$= \frac{6 \times 0.07}{3.14 \times .23}$$

$$\sigma = 0.58$$

n is the number of the blades used, *b* is the width of the blade and *D* is the diameter of the blade.

Swept Area

The swept area refers to the area of the circle created by the blades as they sweep through the air. To find the swept area, use the same equation you would use to find the area of a circle can be found by following equation:

$$Area of single turbine blade = \pi r^2$$

$$Area single turbine blade = 3.14 * .11^2$$
$$= 0.037\ m^2$$
$$Area of\ 24 turbine blade = 24 \times 0.037$$
$$Area of\ 24 turbine blade = 0.88\ m^2$$

Design Calculation for the Solar PV Cell

There are different factor for the designing of the solar PV modules. Some of the important parameter is discuss below which are as follow:

Determine power consumption demands

The first step in designing a solar PV system is to find out the total power and energy consumption of all loads that need to be supplied by the solar PV system as follows:

1. Calculate total Watt-hours per day for each appliance used.

2. Calculate total Watt-hours per day needed from the PV modules

Determine the Size the PV modules

Different size of PV modules will produce different amount of power. To find out the sizing of PV module, the total peak watt produced needs. The peak watt produced depends on size of the PV module and climate condition of the site location. We have design the solar system such that we have to generate the power 25 W through the solar cell.

Determine power consumption demands

Total power needs = (25 W x 8 hours)

= 200 W/day

Total PV panels energy needed = 200 x 1.3

= 260 W/day.

1.3 is multiplication factor (the energy lost in the system)

Determine the Size the PV panel

Number of PV panels needed = 260 / 3.2 × 8

= 10 Module

Minimum requirement = 10 modules to generate the maximum power 260 Wh/day.

So this system should be powered by at least 10 modules of PV cell 3.2 W.

Designing Solar Charge Controller

Sizing

The charge controller is normally rated capacity that it can withstand for the Amperage and Voltage. It kept in mind that the charge controller has sufficient capacity to handle the current from PV array and wind turbine.

According to standard practice, the sizing of charge controller is to take the Short Circuit current (Isc) of the PV array, and multiply it by 1.3

Charge controller rating

= Total short circuit current of PV array and wind turbine x 1.3

= (1.8 A for solar + 1.5 A for wind) ×1.3

= 3.9 A

Thus for the system we have to design such a charge controller which can easily withstand for the above current capacity.

Measuring Photo Voltaic Efficiency

Efficiency of the photovoltaic solar cell is calculated by the capability of a panel to transform the available sunlight into usable energy for human consumption.

The maximum efficiency of a solar photovoltaic panel is determined by the following equation:

$$\eta = \frac{P(Power\ output)}{E(Incident\ solar\ radiation) \times A_c(Collector\ Area)}$$

Area of 10 sets of Collector = 0.25 m^2

Table 6: Calculation of the Efficiency of the Solar Plate as per data of 8th Sept 2015

TIME	Solar Voltage (V)	Solar Current (A)	Solar Power (W)	Solar Radiation W/m^2	Efficiency (η)
10:00	18.70	1.34	25.06	830	12.08
11:00	18.60	1.35	25.11	890	11.29
11:30	19.30	1.46	28.18	940	11.99
12:00	19.40	1.58	30.65	1070	11.46
12:30	19.00	1.50	28.50	1130	10.09
13:00	19.50	1.58	30.81	1140	10.81
13:30	18.40	1.43	26.31	810	12.99
14:00	18.50	1.53	28.31	940	12.04
14:30	18.90	1.52	28.73	1040	11.05
15:00	18.40	0.80	14.72	550	10.71
15:30	18.40	1.04	19.14	640	11.96
16:00	18.58	1.07	19.88	680	11.69

Hence the Efficiency of the solar plate for the design system is 11.50%.

Proposed Formulation

The total power flowing through the system, in addition to the flow of energy generated from solar PV panels and wind turbines can be calculated as.

Mathematically equations for the calculation are:

$$\mathbf{P = N_{wind} \times P_{wind} + N_{solar} \times P_{Solar}}$$

Where,

P is the total power generated.

P_{wind} is the electrical energy produced by the wind.

P_{Solar} is the electrical energy produced by the wind.

N_{wind} is the number of micro wind turbine.

N_{solar} is the number of solar panels used.

Calculations for wind energy

The energy generated by micro wind turbine is given by,

$$\mathbf{P_W = ½.\ \rho\ (AW)\ (V)^3}$$

Where,

P_W is power in watts.

ρ is the density of air in kg/m^3.

A_w is the swept area in m^2.

V is the velocity of wind speed in m/s.

Calculations for solar energy

To estimate the size of Solar PV modules, the needed energy consumption must be estimated. Therefore, the power is calculated as:

$$\mathbf{P_S = Ins\ (t) \times AS \times \eta_{PV}}$$

Where,

Ins (t) = isolation at time t (kw/ m2).

AS = area of single PV panel (m2).

η_{PV} = overall efficiency of the Solar PV panels and dc/dc converters.

Overall efficiency is given by,

$$\eta_{PV} = R_{annual} * P.R.$$

Where,

R_{annual} = Annual average solar radiation on tilted panels

P.R. = Performance ratio, coefficient for losses.

Fabrication

Fabrication of Rotary Foundation

Dimension of Areas is as follow

1. Area required to a single micro turbine is : 25 cm × 28cm (side clearance is included)
2. Thus length required for the micro wind turbine is (25cm × 6cm) 150cm of breadth.
3. Thus height required for the micro wind turbine is (28cm × 4cm) 112cm of height.
4. Area for the wind turbine in the foundation is 1.50 m × 112 m.

Figure 6: Dimension are show with help of figure

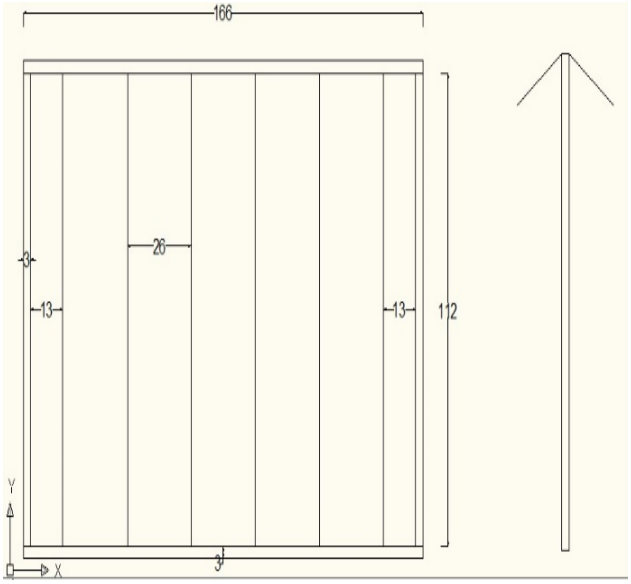

Figure 7: Line diagram with dimension are show with help of figure

Fabrication of Stationary Foundation Base

Material of Stationary base is mild steel. Base is given to stable the panel over it. Stationary base is fixed to the ground through nuts & bolts. Rotary part of the Foundation is attached over it. As shown in the figure that a wheel having teeth are coupled to the stationary base with the help of the bearing.

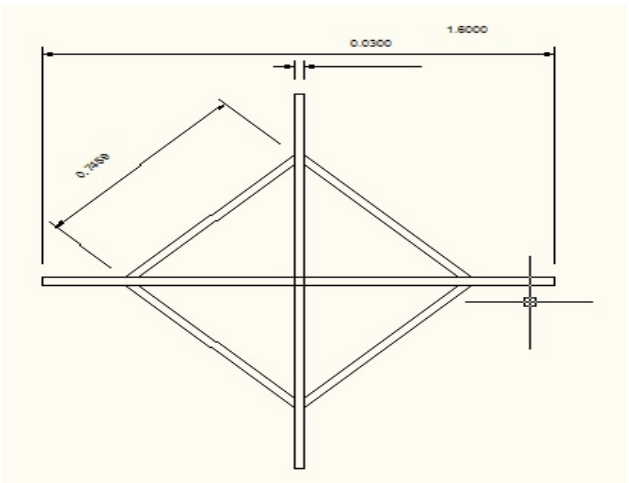

Figure 8: Line diagram and dimension of Base foundation (Dimension in meter)

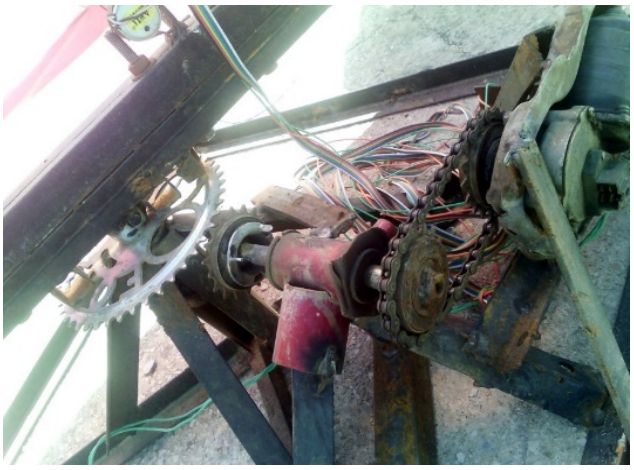

Figure 9: Fabrication of the motor and the wheel along with the gear drive

Experimental Setup and Observation

This experiment was conducted in the energy lab of ISBM building, Suresh Gyan Vihar University, Jaipur Rajasthan. It is assume that the density of air is 1.17 kg/m^3. The reading interval for this experiment was taken 30 minutes i.e. after each interval of 3 minutes reading was taken with the help of different equipment. The experiments were conducted in order to determine the power generated from the hybrid solar and micro wind turbine at different wind speed and different solar radiation. We use anemometer to measure the speed of the wind. Complete experiment is taken at the 4^{th} floor approximately at the height of 25 m from the ground.

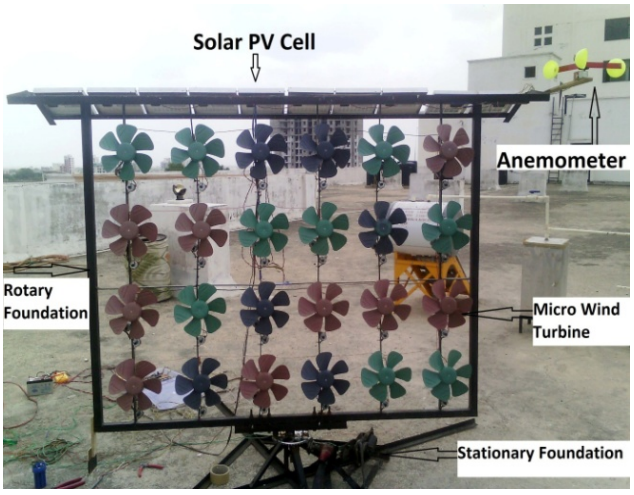

Figure 10: Experimental setup of hybrid solar and micro wind generator

After fabrication and designing of the system, following reading where taken for both the solar and micro wind turbine is as follow:

Table 7 (A): Data of solar voltage, current, power and solar radiation

TIME	Solar Voltage (V)	Solar Current (A)	Solar Power (W)	Solar Radiation
10:00	18.70	1.34	25.06	830
11:00	18.60	1.35	25.11	890
11:30	19.30	1.46	28.18	940
12:00	19.40	1.58	30.65	1070
12:30	19.00	1.50	28.50	1130
13:00	19.50	1.58	30.81	1140
13:30	18.40	1.43	26.31	810
14:00	18.50	1.53	28.31	940
14:30	18.90	1.52	28.73	1040
15:00	18.40	0.80	14.72	300
15:30	18.40	1.04	19.14	640
16:00	18.58	1.07	19.88	680

Table 7 (B): Data of wind voltage, current, power and solar radiation

TIME	Wind Voltage (V)	Wind Current (A)	Wind Power (W)	Wind Speed (m/s)
10:00	17.50	0.93	16.28	3.60
11:00	18.70	0.95	17.77	4.10
11:30	17.90	0.90	16.11	3.50
12:00	17.40	0.98	17.05	5.10
12:30	15.00	0.70	10.50	3.40
13:00	6.20	0.21	1.30	3.80
13:30	9.80	0.31	3.04	3.40
14:00	0.00	0.00	0.00	3.10

14:30	**0.00**	**0.00**	**0.00**	**6.50**
15:00	**0.00**	**0.00**	**0.00**	**3.90**
15:30	**8.05**	**0.10**	**0.81**	**2.10**
16:00	**16.50**	**0.91**	**15.02**	**2.80**

Conclusion

As per the above data, while designing of a solar and micro wind generator, we determine the various deciding factor for the designing of the hybrid power generator. Above data were recorded at equal interval of time and calculated to find out the desire results for the design of the hybrid system. Thus we have come to the point that design for the hybrid solar and micro wind power generator is validated.

Hybrid power generation system is interesting and efficient answer for power generation than conventional energy resources. It has obviously greater efficiency. Hybrid system can be used to remote areas where the transmission of the power through grid is not possible or it unable to reach. Another benefit for using such a system is that generated power can be used at the same place without the investing the extra cost for the transmission of power, and it will also minimize the losses due to transmission.

Recommendation and Future Work

We recommend that to increase the efficiency of the system there is a lot of thing to do in this research. Some of the recommendation is given below:

1. Integration of such a technique to control the pitch angle of the turbine blade will increase the overall efficiency of the system.
2. You may also develop such a tracking system for the wind turbine with doesn't consume the power to track the system.
3. Economic and technical analysis of system should be done.

This combination of renewal Energy source will be highly efficient in all places, mainly in commercial areas where the need of electricity is much more. It doesn't have no effect on environment i.e. free from pollution, at the same time any kind of accident is not possible due to lightning. Renewable energy source is also beneficial to minimize power supply load. With the use this project we can reduce electricity charges. It require very less maintenance charge during fault. The designing of this system is done in such a way that it is very rigid and acts as user friendly equipment. When it is manufactured in a mass production, cost of this hybrid power generator is affordable.

References

[1] M. A. Abdullah, A.H.M. Yatim, Chee Wei, Tan "A Study of Maximum Power Point Tracking Algorithms for Wind Energy System" IEEE First Conference on Clean Energy and Technology CET, pp. 321-326, 2011.

[2] V.K. Rathod, Prof. S.Y. Kamdi, "Design & Fabrication of PVC Bladed Inexpensive Wind Turbine" IOSR-JMCE, e-ISSN: 2278-1684, ISSN:2320-334X,Volume 11, Issue 4 Ver. II (Jul-Aug. 2014) Jul- Aug. 2014, pp. 114-119.

[3] Samuel OfordileAni, "Low Cost Small WindTurbine Generators for Developing Countries" delft university of technology, Institutional Repository, ISBN: 978-94-6203-287-3, March 2013.

[4] Shanikumar, A.K. Mandal, H.K. Singh, "Simulation and Comparison Analysis of Single Rotor Centralized Horizontal Axis Windmill with Integrated Micro Windmill with Horizontal Axis in Vertical Plane " IJLTEMAS, ISSN 2278 – 2540, Volume III, Issue VII, July 2014, pp. 184-186.

[5] Sandeep Kumar, V. K. Garg, "A Hybrid Model Of Solar-Wind Power Generation System" International Journal Of Advanced Research In Electrical, Electronics And Instrumentation Engineering, Vol. 2, Issue 8, August 2013, ISSN (Print) : 2320 – 3765,ISSN (Online): 2278 – 8875, pp. 4107-4116.

[6] Ashish S. Ingole, Prof. Bhushan S. Rakhonde,"Hybrid Power Generation System Using Wind Energy and Solar Energy" IJSRP, Volume 5, ISSN 2250-3153, Issue 3, March 2015, pp. 1-4.Yuanye Xia,, et al " A New Maximum Power Point Tracking Technique for Permanent Magnet Synchronous Generator Based Wind Energy Conversion System" IEEE Transactions On Power Electronics, Vol. 26, No. 12, December 2011.

[7] Yuanye Xia,, et al " A New Maximum Power Point Tracking Technique for Permanent Magnet Synchronous Generator Based Wind Energy Conversion System" IEEE Transactions On Power Electronics, Vol. 26, No. 12, December 2011, pp. 3609-3620.

[8] Kevin Cox, Andreas Echtermeyer,"Structuraldesign and analysis of a 10MW wind turbine blade" Energy Procedia 24, 2012, pp. 194 – 201.

[9] R. K. Singh, M. R. Ahmed, "Blade Design And Performance Testing Of A Small Wind Turbine Rotor For

Low Wind Speed Applications" Renewable Energy 50, 2013 pp. 812-819.

[10] Onder Ozgener,"A small wind turbine system (SWTS) application and its performance analysis", Energy Conversion and Management, elsevier, 2006.

[11] Furkan Dinçer, Mehmet Emin Meral, "Critical Factors That Affecting Efficiency Of Solar Cells", Smart Grid And Renewable Energy, Scientific Research, May 2010.

[12] Suprava Chakraborty, Et Al, "New Location Selection Criterions For Solar Pv Power Plant", International Journal Of Renewable Energy Research, Vol.4, No.4, 2014.

[13] Saurav Kumar1, Et. Al., "Experimental Study Of Optimum Tilt Angle For Solar Pv Panel In Jaipur (Rajasthan)", International Journal Of Science And Research (Ijsr), 2012.

[14] Swami Prakash Srivastava, Et. Al. "Solar Energy And Its Future Role In Indian Economy", International Journal Of Environmental Science: Development And Monitoring, Volume 4 No. 3, 2013.

[15] Kavita Sharma, PrateekHaksar," Designing of Hybrid Power Generation System using Wind energy- Photovoltaic Solar energy- Solar energy with Nanoantenna", IJERA, ISSN: 2248-9622, Vol. 2, Issue 1,Jan-Feb 2012, pp.812-815.

[16] Jyoti Kant, Hari Kr Singh, "Scope and Potential of a Hybrid Solar & Wind Energy System for Jodhpur Region, Case study, "International Journal of Science and Research (IJSR)", ISSN : 2319-7064, Volume 3 Issue 6, June 2014, pp. 1603-1606.

Author's details

[1]M.Tech Dual degree Scholar (Energy Engg.), Department of Mechanical Engineering, Suresh Gyan Vihar University, Jaipur, Rajasthan, Email: khetan2013@gmail.com

[2]Assistant professor, Suresh Gyan Vihar University, Jaipur, Rajasthan, India, Email: harisingh027@gmail.com

[3]M.Tech, Department of Electrical Engineering, Suresh Gyan Vihar University, Jaipur, Rajasthan, Email: rohit.lilha007@gmail.com.

Copy for Cite this Article- Vishnu Khetan, Hari Kumar Singh,, Rohit Kumar, 'Design And Fabrication Of A Hybrid Solar & Micro Wind Power Generator,' *International Journal of Science, Engineering and Technology,* Volume 4 Issue 1: 2016, pp. 314- 323.

Ashish Sharma et al. 2016, Volume 4 Issue 1
ISSN (Online): 2348-4098
ISSN (Print): 2395-4752

International Journal of Science, Engineering and Technology
An Open Access Journal

A Geographical Study of Food Security and Agriculture in India

Ashish Sharma

Abstract

Food security is a challenge for India. Food security has a great relation with agriculture. India is a net agricultural exporter, particularly of milk, fruits and vegetables, and cereals. However, food security is affected by climate change and declining water resources on agriculture output. Economic access to food by about a fourth of the population living below the poverty line is a very big problem in India, despite impressive economic growth in the recent years. Food security is assured by increasing agriculture productivity in India.

Introduction

Food security is a condition related to the supply of food, and individuals' access to it. Concerns over food security have existed throughout history. There is evidence of granaries being in use over 10,000 years ago, with central authorities in civilizations including Ancient China and Ancient Egypt being known to release food from storage in times of famine. At the 1974 World Food Conference the term "food security" was defined with an emphasis on supply. Food security, they said, is the "availability at all times of adequate world food supplies of basic foodstuffs to sustain a steady expansion of food consumption and to offset fluctuations in production and prices".Later definitions added demand and access issues to the definition. The final report of the 1996 World Food Summit states that food security "exists when all people, at all times, have physical and economic access to sufficient, safe and nutritious food to meet their dietary needs and food preferences for an active and healthy life."

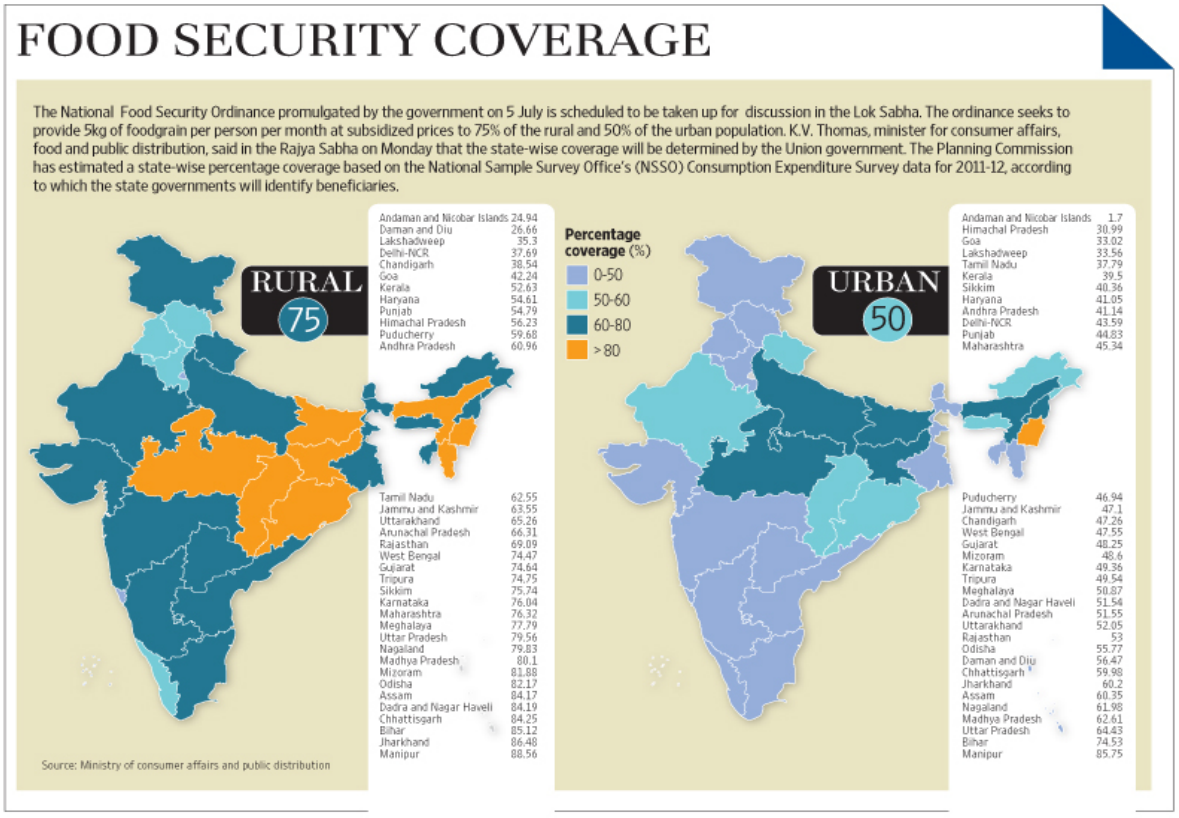

Food security is considered as a major issue since 1970s, with the World Food crisis of 1972-74 and has been a topic of considerable attention since then. The concept of food security would have more meaning if it is understood in line with the legal commitments of the United Nations: the Universal Declaration of Human Rights (1948), which accepts the "right to adequate standard of living," including food; the International Covenant on Economic, Social, and Cultural Rights (1966), which ensures "an equitable distribution of world food supplies in relation to need"; and the Universal Declaration on the Eradication of Hunger and Malnutrition (1974), which declares that "every man, woman, and child has an inalienable right to be free from hunger and malnutrition." Member countries accepted these declarations, responding to food needs of other countries has been left to the discretion of individual surplus-producing countries and the UN has no power to enforce such declarations.

Therefore, a global concept of food security does not guarantee food security at either the household or the national level. The concept of Food Security has been evolving over the last decades with academicians, policy makers and the NGO an activist contributing substantially to the debates on what constitutes food security, the determinants of food security and how it can be ensured at the global, regional, national, state, household and the individual levels. The World Food Conference of 1974, which was organized in the wake of the world food crisis of 1972-74, was largely concerned with world food security wherein it was recognized that it was the common responsibility of all the nations and that international approaches were needed to achieve the improved world food security.

Similarly, the International Conference on Population and Development (1994) highlighted the linkage between the population and the need to evolve global measures to satisfy the growing food needs.

Research Methodology

The study analyses the available secondary information and literature on food security and agriculture in India. Research Methodology is partly descriptive, partly exploratory and partly casual. For this study information has been collected with the help of books, magazines, research articles and reports.

Aim of Study

1. Study of food security and agriculture in India.
2. Study of the new trends in food security.

Pillars of Food Security

The WHO states that there are three pillars that determine food security: food availability, food access, and food use. The FAO adds a fourth pillar: the stability of the first three dimensions of food security over time. In 2009, the World Summit on Food Security stated that the "four pillars of food security are availability, access, utilization, and stability"

1-Avialablity

2-Access

3-Utilization

4-Stablity

Food Security and Agricultural Productivity

The net impact of food security will depend on the many causes mainly global environmental change and the capacity to cope with and recover from global environmental change. On a global level, increasingly unpredictable weather patterns will lead to fall in agricultural production and higher food prices, leading to food insecurity.

This impact of climate change has significant consequences for agricultural productivity and trade of developing countries as well as an increased risk of hunger. The number of people suffering from hunger has increased from under 800 million in 1996 to over 1 billion recently. United Nations population data and projections (UN 2009) show the global population reaching 9.1 billion by 2050, an increase of 32 per cent from 2010. The world's population is expected to grow by 2.2 billion in the next 40 years to 2050, and a significant part of the additional population will be in countries that have difficulties to get food.. Preliminary estimates for the period up to 2080 suggest a decline of some 15–30 per cent of agricultural productivity in the most climate-change-exposed developing countries.

Even the IPCC, says 0.5°C rise in winter temperature would reduce wheat yield by 0.45 tons per hectare in India. Rice and wheat have a total share in total food

grain production in India. Any change in rice and wheat yields may have a significant impact on food security of the country and other crops will also affected by climate change.

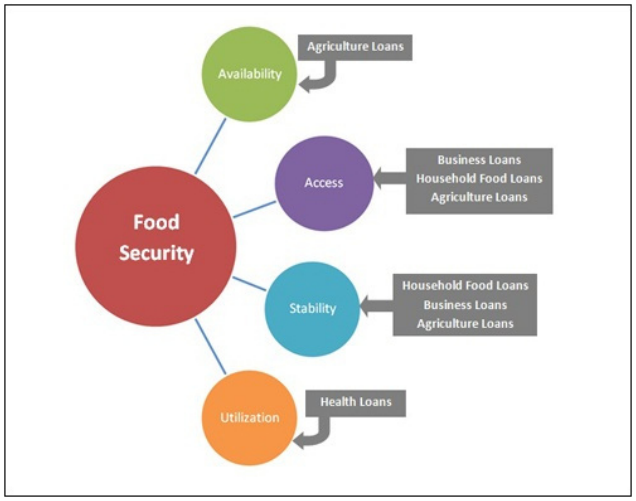

Climate-Smart Agriculture

Smart Climate agriculture is a new trend. FAO (2010a) discusses strategies needed for climate-smart agriculture. It is defined as agriculture that sustainably increases productivity, resilience (adaptation), reduces/removes GHGs (mitigation), and enhances achievement of national food security and development goals.

It provides examples of climate-smart production systems such as soil and nutrient management, water harvesting and use, pest and disease control, resilient eco systems, genetic resources etc. It also discusses about efficient, harvesting, processing and supply chains. Efficient harvesting and early processing can reduce post-harvest losses and preserves food quantity, quality and nutritional value of the product (FAO, 2010a). This approach also ensures better use of co-products and by-producers, either as feed for livestock, to produce renewable energy in integrated systems or to improve soil fertility.

The report says that ‗there is a need for policies, infrastructures and considerable investments to build the financial and technical capacity of farmers (especially small holders) to enable them to adopt climate-smart practices that could generate economic rural growth and ensure food security‖ (p.4, FAO, 2010a).

The study provides the following messages for climate-smart agriculture. Agriculture in developing countries must undergo a significant transformation in order to meet the related challenges of food security and climate change. Effective climate-smart practices already exist and could be implemented in developing country agricultural systems. Adopting an ecosystem approach, working at landscape scale and ensuring intersectoral coordination and cooperation is crucial for effective climate change responses. Considerable investment is required in filling data and knowledge gaps and in research and development of technologies, methodologies, as well as the conservation and production of suitable varieties and breeds. Institutional and financial support will be required to enable smallholders to make the transition to climate-smart agriculture. Strengthened institutional capacity will be needed to improve dissemination of climate- smart information and coordinate over large areas and numbers of farmers. · Greater consistency between agriculture, food security and climate change policy-making must be achieved at national, regional and international levels. Available financing, current and projected, are substantially insufficient to meet climate change and food security challenges faced by the agriculture sector. Synergistically combining financing from public and private sources, as well as those earmarked for climate change and food security are innovative options to meet the investment requirements of the agricultural sector. To be effective in channeling fast-track financing to agriculture, financing mechanisms will need to take sector-specific considerations into account.

Right to Food and National Food Security

The Presidential address to Parliament in 2009 indicates that implementation of the National Food Security Act will provide a statutory basis for a framework which assures food security for all. According to this proposed law, every family below the poverty line in rural as well as urban areas will be entitled by law, to 25 kilograms of rice or wheat per month at Rs. 3 per kilogram. It is felt that the statutory guarantee to food with fixed entitlements to the poor would be an important step in the direction of ensuring food and nutritional security of the country. Although the ongoing ‘targeted public distribution system’ (TPDS) is supposed to provide subsidized food grains to the BPL population, the legislative measure may lead to better accountability

by making the PDS system more responsive in reaching out to the targeted population. Since the announcement of the proposed food security law, several people have raised a number of policy level and operational issues that need to be addressed while extending food guarantee to the citizens through a statutory mandate.

Main Issues under the Proposed Right to Food

Issues under PDS: There has been a serious debate on the question: should the PDS be targeted or universal? The advantage of universal PDS is that targeting errors can be minimized, particularly the exclusion error (exclusion of poor). Also, a right generally implies applicability to the entire population of the nation.

The second issues are who should be covered under BPL and get ration cards? According to Planning Commission estimates, there are 6.52 crore households below the poverty line (based on 1993-94 poverty estimates and population estimates for 2000 from the Registrar General of India (RGI)). However, actual cards issued by states number around 10.68 crore (in some states, nearly the entire population has been issued BPL cards!). The demand of states is that all the 10.68 crore card holders should be included in the BPL list under the Right to Food Act. This would have serious financial implications in terms of food subsidy. The N. C. Saxena committee on BPL population thinks that 50 per cent of the nation's population should be covered under BPL.

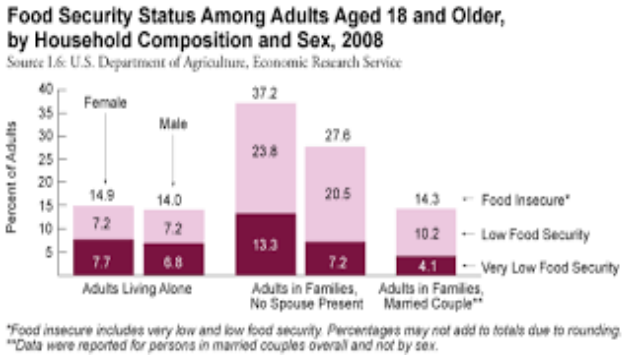

Need for Comprehensive Food Entitlement Act: The proposed national food security law is too narrow. The Right to Food campaign demands a comprehensive 'Food Entitlements Act' that goes beyond the narrow promise of supplying food grains to BPL population.

"Aside from an overarching obligation to protect everyone from hunger, as well as to promote sustainable and equitable food production, essential provisions of the proposed Act include: a universal public distribution system (providing at least 35 kgs of grain per family); special food entitlements for destitute households (including an expanded Antyodaya Programme); consolidation of all entitlements created by recent Supreme

Court Orders (e.g. cooked mid-day meals in primary schools and universalization of ICDS); support for effective breastfeeding (including maternity entitlements and crèches); safeguards against the invasion of corporate interests in food policy; and elimination of all social discrimination in food related matters. Further, the Act must include strong accountability and grievance redressal provisions, including mandatory penalties for any violation of the Act and compensation for those whose entitlements have been denied" (Right to Food Campaign: Right to Food Act, 2009, p.1)

The Right to Food Campaign argues that "any statute enacted ought to, at the very minimum, protect existing legal entitlements created by the Supreme Court orders passed in PUCL Versus UOI currently pending in the Supreme Court, and preferably go beyond". According to the draft prepared by this campaign, the Food Entitlements Act, 2009 should be:

"An Act to ensure dignified economic and social access to adequate food and other requirements of good nutrition for all residents of the country, at all times, in pursuance of their fundamental right to be free from hunger, malnutrition and other deprivations associated with the lack of food." (p.5 of 'Food Entitlements Act, 2009 of Right to Food Campaign).

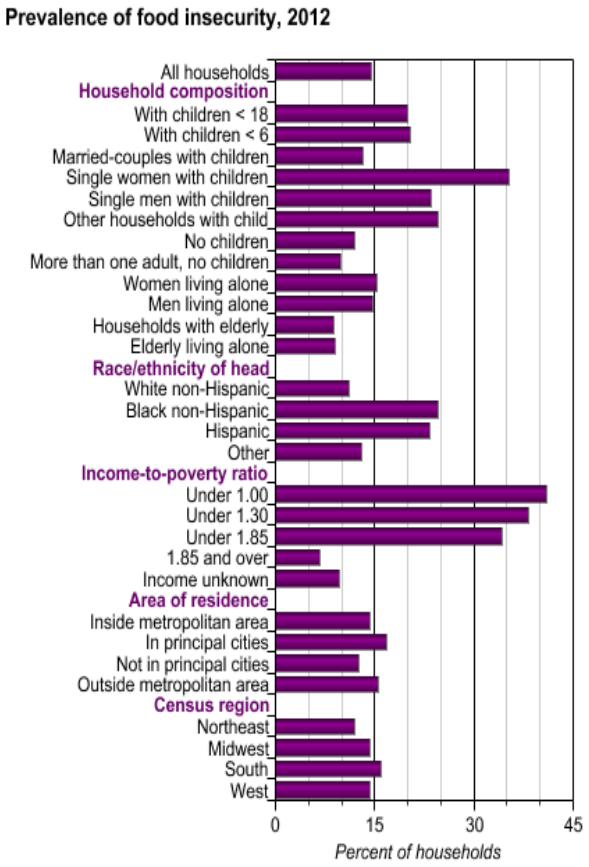

Source: Calculated by ERS using data from the December 2012 Current Population Survey Food Security Supplement.

Our view is that the present National Food Security Act proposed by the government is a narrow one. The alternative draft "Food Entitlements Act, 2009" prepared by the Right to Food Campaign needs to be discussed and the government needs to consider the comprehensive nature of the food insecurity and malnutrition problems prevalent in the country.

Basically, we argue that Right to Food in terms of providing food and nutritional security to all is a much broader concept than the proposed National Food Security Act of providing 25 kilograms of food grains at Rs.3. Many things have to be included in order to have genuine 'Right to Food. India is signatory to many international treaties and the Indian Constitution also indirectly refers to the Right to Food, which is obligatory for the government to fulfill10.

As Dreze (2004)See http//www.righttofoodindia.org/ 9 Ibid 10 More on right to food see Dev (2003, 2008) and Gaiha (2003) mentions, Right to Food can be seen from three perspectives: the Indian Constitution, international declarations, and moral and social right. The core content of the Right to Food refers to availability, accessibility, adequacy, and sustainability.

Conclusion

Food security is most emerging issue now days. During the Green Revolution era, large investments were made on research and development for the irrigated agriculture. The promotion of HYV seed - fertilizer - irrigation technology had a high pay-off and rapid strides of progress were made in food production. But, since last year's agriculture productivity is adversely affected by several causes mainly climate change in India. Agriculture Productivity is a base factor for assuring food security. Government should make a strong action plan for proper implementation of food security act and government should also make a policy for increasing agricultural productivity.

References

Agrawal, A., and N. Perrin. 2008. Climate Adaptation, Local Institutions, and Rural Livelihoods. IFPRI Working Paper W08I-6. Washington, DC: International Food Policy Research Institute.

Antle, J. M., and S. M. Capalbo. 2010. "Adaptation of Agricultural and Food Systems to Climate Change: An Economic Policy Perspective." Applied Economic Perspectives and Policy 32: 386–416.

Axelrod, R., and M. D. Cohen. 2000. Harnessing Complexity: Organizational Implications of a Scientific Frontier. New York: Free Press.

Barnett, J., and S. O'Neill. 2010. "Maladaptation." Global Environmental Change 20: 211–213.

hallinor, A. J. 2009. "Towards the Development of Adaptation Options Using Climate and Crop Yield Forecasting at Seasonal to Multi-decadal Timescales." Environmental Science and Policy 12: 453–465.

Chantarat, S., A. G. Mude, C. B. Barrett, and M. R. Carter. 2012. "Designing Index-Based Livestock Insurance for Managing Asset Risk in Northern Kenya." Journal of Risk and Insurance 80: 205–237.

Chimhowu, A., and P. Woodhouse. 2004. "Customary vs Private Property Rights? Dynamics and Trajectories of Vernacular Land Markets in Sub-Saharan Africa." Journal of Agrarian Change 6 (3): 346–371.

Clarke, H. 2008. "Classical Decision Rules and Adaptation to Climate Change." Australian Journal of Agricultural and Resource Economics 52 (4): 487–504.

Crespo, O., S. Hachigonta, and M. Tadross. 2011. "Sensitivity of Southern African Maize Yields to the Definition of Sowing Dekad in a Changing Climate." Climatic Change 106: 267–283.

De Janvry, A, and E. Sadoulet. 2010. "Agricultural Growth and Poverty Reduction: Additional Evidence." World Bank Research Observer 25 (1): 1–20.

Dercon, S. 1996. "Risk, Crop Choice, and Savings." Economic Development and Cultural Change 44: 485–513.

Douthwaite, B. 2002.Enabling Innovation: A Practical Approach to Understanding and Fostering Technological Change. London: Zed Books.

Dryzek, J. S. 2009. "Democratization as Deliberative Capacity Building."Comparative Political Studies 42: 1379–1402.

Eakin, H., and A. L. Luers. 2006. "Assessing the Vulnerability of Social-Environmental Systems." Annual Review of Environment and Resources 31: 365–394.

Easterling, W. E., P. K. Aggarwal, P. Batima, K. M. Brander, L. Erda, S. M. Howden, A. Kirilenko, J. Morton, J.-F. Soussana, J. Schmidhuber, and F. N.

Ericksen, P.J. 2008."Conceptualizing Food Systems for Global Environmental Change Research." Global Environmental Change 18: 234–245.

Food and Agriculture Organization (November 1996)."Rome Declaration on Food Security and World Food Summit Plan of Action". Retrieved 26 October 2013

Grothmann, T., and A. Patt. 2005. "Adaptive Capacity and Human Cognition: The Process of Individual Adaptation to Climate Change." Global Environmental Change 15: 199–213.

Halstead, P., and J. O'Shea, eds. 1989. Bad Year Economics: Cultural Responses to Risk and Uncertainty. New York: University of Cambridge Press.

Hansen, J., and K. Coffey. 2011. Agro-climate Tools for a New Climate-Smart Agriculture. Copenhagen: CGIAR Research Program on Climate Change, Agriculture, and Food Security.

Howden, S. M., S. J. Crimp, and R. N. Nelson. 2010. "Australian Agriculture in a Climate of Change." In Managing Climate Change, edited by I. Jubb, P. Holper, and W. Cai, 101–111.

Matho, A., 2014. "Climate Change And Its Impact On Agriculture." International Journal Of Scientific and Research Publications, Vol. 4, Issue 4, April 2014.

Raj Patel (20 Nov 2013). "Raj Patel: 'Food sovereignty' is next big idea". Financial Times. Retrieved 17 Jan 2014.

Washington, DC. World Food Programme. 2009. Emergency Food Security Assessment Handbook, 2nd ed. Rome.

Ziervogel, G., S. Bharwani, and T. E. Downing. 2006. "Adapting to Climate Variability: Pumpkins, People, and Policy." Natural Resources Forum 30: 294–305.

Author's details

Research Scholar, Department of Geography, Babu Shobha Ram Arts College (University of Rajasthan), Alwar, Rajasthan, India, Email: ashishsharma2424@rediffmail.com

Copy for Cite this Article- Ashish Sharma, 'A Geographical Study Of Food Security And Agriculture In India,' *International Journal of Science, Engineering and Technology,* Volume 4 Issue 1: 2016, pp. 324- 329.

P. Anitha et al. 2016, Volume 4 Issue 1
ISSN (Online): 2348-4098
ISSN (Print): 2395-4752

International Journal of Science, Engineering and Technology
An Open Access Journal

Synthesis and Characterization of Silver Nanoparticles using Delonix Elata Leaf Extract and Its Anti- Inflammatory Activity against Human Blood Cells

[1]P. Anitha, [2]P. Sakthivel

Abstract

By the review of various literature surveys it has been analyzed that Delonix elata leaf extract has a great medicinal values. The Silver Nanoparticles were prepared by employing the standard procedure. The formation of silver Nanoparticles is confirmed by occurrence of colour change. When Silver Nanoparticles is added with Delonix elata leaf extract, the colour changes from yellow to dark brown which confirms the formation of silver Nanoparticles. The silver Nanoparticles formed have been characterized by UV, FT-IR, XRD and TEM.UV absorbance peak at 230.98nm confirms it as the characteristic peak of silver Nanoparticles. The average sizes of silver Nanoparticles formed by XRD &TEM Analysis are 11.37nm & 11.78nm respectively. Further, these AgNPs formed from Delonix elata leaf extracts has a good anti-inflammatory activity. The anti-inflammatory activity was tested against human blood cells. Hence, the present research aims to open new avenues for the various ailments of medicine with the synthesis of silver Nanoparticles by using leaf extracts like Delonix elata &to bring the anti-inflammatory activity of a medicinal plant to the Scientist's notice, to educate awareness & add values to resources

Keywords: Delonix elata leaf, Silver Nanoparticles, UV, FT-IR, XRD and TEM etc.,

Introduction

Nanoparticles synthesis is usually carried out by various physical and chemical methods like laser ablation, pyrolysis, lithography, chemical vapour deposition, sol–gel techniques and electro-deposition, which are very expensive and hazardous. Although many routes are available for the synthesis of Nanoparticles, there is an increasing need to develop high-yield, low cost, non-toxic and environmentally friendly procedures. Therefore scientists are looking forward for greener methods [1,2]. Green nanotechnology is an area of interest having significant focus in present scenario with important objective of facilitating the manufacture of nanotechnology based eco-friendly products. The development of efficient green chemistry methods for synthesis of metal Nanoparticles has become a major focus of researchers [3]. Among heavy metal Nanoparticles, silver Nanoparticles have received major attention due to unique and tunable surface plasmon resonance (SPR) [4]. Synthesis of silver Nanoparticles with different size range and their self-assembly is considered important due to their potential applications in medicine [5]. In recent years, synthesis of AgNPs has been reported using several plant extracts particularly Prosopis juliflora [6]; Malva parviflora [7]; Hibiscus cannabinus [8]; Ocimum sactum [9]; Sesbania grandiflora [10]; Acalypha indica [11]; Alternathera sessilis [12]; Catharanthus roseus [13]; Ixora coccinea [14] and Mulberry [15]. Delonix elata (L.) Gamble belongs to the family of fabaceae and has been explored for pharmaceutical applications as the leaves and bark of this plant is known to have medicinal properties. The leaf extracts are anti-inflammatory in nature and provide relief from rheumatic problems like pain and stiffness of the joints, especially the knees. It is also known to increase the body heat and pulse rate. The decoction of plant root can be used for relief from abdominal pains. Powdered leaves in proportion with other

herbs are used to cure paralysis and other nervous disorders. Administration of the herbal mixture to younger children is known to prevent polio [16]. Delonix elata (L.) Gamble has been used in the Indian traditional medicine system to treat rheumatism and inflammation.Literature reports on medicinal uses of Delonix elata leaf extract revealed the pharmacological actions like anti-inflammatory activity (Shah et al., 2009)[17] Investigations by many research scholars revealed that Delonix elata possess many activities like anti-inflammatory, in vitro antioxidant activities, anti-arthritic[18,19].All of them found that the Delonix elata extract showed significant and dose dependent activities. Leaves are used for the treatment of bronchitis in infants, fever, malaria, flatulence, and paralysis or as carminative [20]. In our previous study, leaves extract of D. elata has shown remarkable antinociceptive activity [21]. Leaf extract has been screened for anti-inflammatory activity [22]. Particle size distribution curve of the synthesized AgNPs shown reveals that particles obtained are polydisperse mixture, with average diameter 70.01 nm. The zeta potential of the synthesized AgNPs is determined in water as dispersant. The zeta potential is found to be 18.3 mv[23].Recently, microwave heating has been explored as a promising technique for nanoparticle synthesis. In the present study, we first report the reduction of silver ions using Delonix elata leaf extract under microwave irradiation for facile and fast phytosynthesis of silver Nanoparticles (AgNPs). To the best of our knowledge, no reports pertaining to a microwave method by using Delonix elata leaf extract are yet available. The anti-inflammatory property of phyto synthesized silver Nanoparticles was also investigated.

Materials and Methods

Collection of leaf

Fresh leaves of Delonix elata were collected from Trichy, during the month of May and identified by Dr.John Britto, The Director, Rabinat Herbarium and Center for Molecular Systematics, St. Joseph's College (Campus), Trichirappalli-2, Tamil Nadu. India. (Plant authentication no: PN001).

Preparation of leaf extract

The fresh and young leaf samples of Delonix elata was collected & washed thoroughly with sterile double distilled water (DDW). Twenty gram of sterilized leaf samples were taken and cut into small pieces. Finely cut leaves were placed in a 500 ml Erlenmeyer flask containing 100 ml of sterile DDW. After that the mixture was boiled for 5 minutes and filtered. The extract was stored in 4 ^{0}C.

Synthesis of silver Nanoparticles

Silver nitrate was used as precursor in the synthesis of silver Nanoparticles**.** 100 ml of Delonix elata leaf extract was added to 100 ml of 0.1N $AgNO_3$ aqueous solution in conical flask of 250 ml content at room temperature. The flask was thereafter put into shaker (100 rpm) at 50^0 C and reaction was carried out for a period of 12 hrs. Then the mixture is kept in microwave oven for exposure of heat. The mixture was completely dried after a period of 20 minutes and hence Nanoparticles in form of powders were obtained.

Figure 1: Optical photograph of Delonix elata A- 0.1 N $AgNO_3$ solution B- Leaf extract C- Leaf extract + $AgNO_3$ D- Leaf extract + $AgNO_3$(After 30mins) E- Leaf extract + $AgNO_3$(After 1 hr) F- Leaf extract + $AgNO_3$ (After 2 hrs) G- Leaf extract + $AgNO_3$(After 24 hrs)

UV-visible spectroscopy analysis

The colour change in reaction mixture (metal ion solution + leaf extract) was recorded through visual observation. The bio reduction of silver ions in aqueous solution was monitored by periodic sampling of solid and subsequently measuring UV-visible spectra of the solid sample. UV-visible spectra of sample were monitored as a function of time of reaction on the UV-visible spectroscopy and the investigations was carried out using PERKIN ELMER (Lambda 35 model) spectrometer in the range of 190 nm to 1100 nm.

FT-IR measurement

The Fourier transform infrared (FTIR) investigations were carried out using PERKIN ELMER (Spectrum RXI) spectrometer in the range of 400 cm^{-1} to 4000 cm^{-1}.

The functional groups were identified using the peak assignments.

XRD measurement

The sample was drop- coated onto Nickel plate by just dropping a small amount of sample on the plate frequently, allowed to dry and finally thick coat of sample was prepared. The particle size and nature of the silver Nanoparticles was determined using X-ray diffraction (XRD). This was carried out using Rigaku miniflex-3 model with 30kv, 30mA with Cukα radians at 2θ angle.

TEM analysis

Sample is dispersed with acetone and exposed in ultrasonics for 5 minutes.Take a drop of a solution from the samples and drops it on the grid, leave until it dries. After drying, the sample is inserted into TEM instruments using model Tecnai T20 Making in FEI, Netherlands operating at 200KeV Tungsten Filament.

Anti-Inflammatory Activity

The human red blood cell (HRBC) membrane stabilization method

The method as prescribed (Gopalkrishnan et al., 2009; Sakat et al., 2010) was adopted with some modifications. The blood was collected from healthy human volunteer who had not taken any NSAIDS for 2 weeks prior to the experiment and mixed with equal volume of Alsever solution (2 % dextrose, 0.8 % sodium citrate, 0.5 % citric acid and 0.42 % NaCl) and centrifuged at 3,000 rpm. The packed cells were washed with isosaline and a 10 % suspension was made. Various concentrations of extracts were prepared in mg/ml using distilled water and to each concentration, 1 ml of phosphate buffer, 2 ml hypo saline and 0.5 ml of HRBC suspension were added. It was incubated at 37^0C for 30 minutes and centrifuged at 3,000 rpm for 20 minutes and the hemoglobin content of the supernatant solution was estimated spectrophotometrically at 560 nm. Diclofenac (100 Jg/ml) was used as reference standard and a control was prepared by omitting the extracts. The experiments were performed in triplicates and mean values of the three were considered. The percentage (%) of HRBC membrane stabilization or protection is calculated using the following formula,

Percentage of Protection (%) =

(100- OD of drug treated sample/OD of Control) X 100

Albumin denaturation method

The method as prescribed (Sakat et al., 2010) was followed with modifications. The reaction mixture was consisting of test extracts and 1% solution of bovine albumin fraction. pH of the reaction mixture was adjusted using small amount of HCl. The sample extracts were incubated at 37°C for 20 minutes and then heated to 51°C for 20 minutes. After cooling the samples the turbidity was measured spectrophotometrically at 660 nm. Diclofenac sodium was taken as a standard drug. The experiment was performed in triplicates and the mean value of the three was considered. Percent inhibition of protein denaturation was calculated as follows,

Percentage of inhibition (%) =

(OD of Control- OD of Sample/ OD of Control) X 100

Results

UV-visible spectroscopy analysis

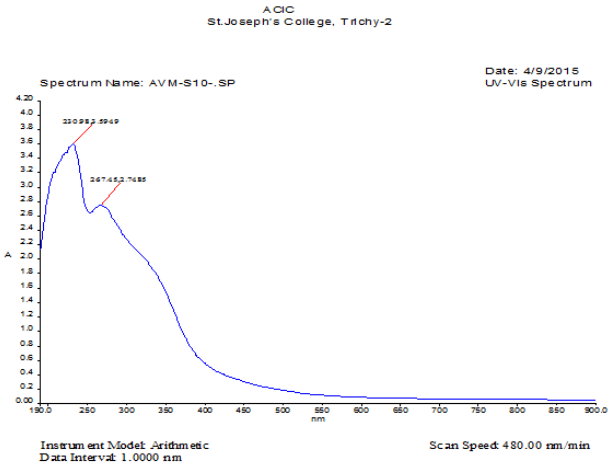

Figure 2: UV-Visible spectrum of synthesized silver Nanoparticles using leaf extracts of Delonix elata.

UV-Vis spectroscopy analysis showed the absorbance band of silver Nanoparticles synthesized using Delonix elata leaf extract at 230.98 nm and confirms the presence of poly-unsaturated and aromatic compound (Isoquinoline) (Advanced strategies in food analysis ,UV/VIS spectrometry by Richard Koplík)

FT-IR measurement

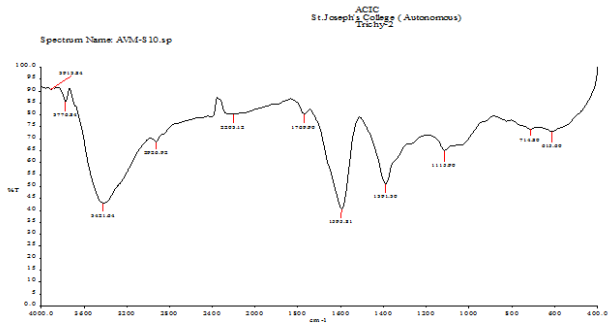

Figure 3: FT-IR spectrum of synthesized silver Nanoparticles using leaf extracts of Delonix elata

The Delonix elata related functional groups were identified using the peak assignments. A strong peak at 3913.84 cm^{-1} and 3776.84 cm^{-1} was assigned to the OH stretching in Phenol group, The sharp and bend peak at 3421.64 cm^{-1} was assigned to OH ,H-bonded alcohol and phenols or medium N-H stretching may be present primary, secondary amines and amides group, The medium peak at 2926.92 cm^{-1} was assigned medium C-H stretching in alkenes, weak peak at 2203.12 cm^{-1} was assigned to –C (triple bond) C- stretching in alkenes group, The strong peak at 1769.90 cm^{-1} was assigned to C=O stretching in carbonyl group, The medium peak at 1595.81 cm^{-1} was assigned to N-H bend in primary amine group, The variable peak at 1391.30 $cm^{-1}$was assigned to C-H bending in alkenes , The medium peak at 1115.90 cm^{-1} was assigned to C-N stretching in aliphatic amine group, The medium peak at 714.80 cm^{-1} was assigned to C-Cl stretching in alkyl halide group and The medium peak at 615.60 $cm^{-1}$was assigned to C-Br stretching in alkyl halides are observed.

XRD measurement

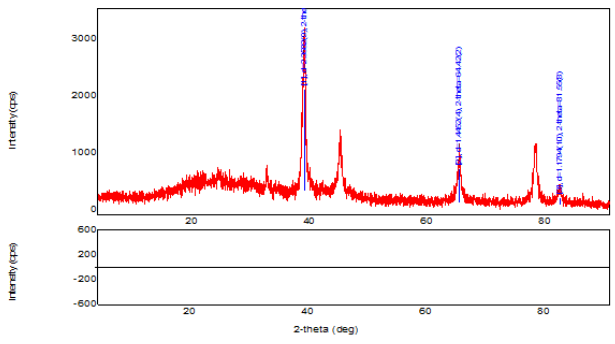

Figure 4: XRD spectrum of synthesized silver Nanoparticles using leaf extracts of Delonix elata

Determination of crystalline size

Average crystallite size of silver was calculated using the Scherrer's formula,

$D = k\lambda / \beta\cos\theta$

D- Average crystallite size: K- Constant: λ- X- ray Wavelength: β- Angular FWHM of the XRD peak at the diffraction angle: θ- Diffraction angle.

By Scherrer's formula, the average size of the particle is approximately found to be 11.37 nm

TEM analysis

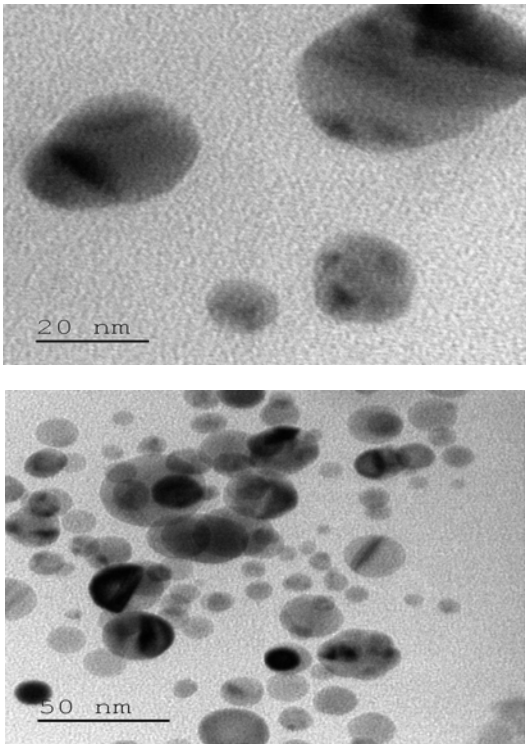

Figure 5: TEM image of synthesized silver Nanoparticles using leaf extracts of Delonix elata

The figure shows the TEM image obtained by the reaction of Delonix elata leaf extract and 0.1N silver nitrate solution separately. The Average size of Delonix elata Ag-NPs by TEM Analysis is found to be 11.78nm.

Anti-Inflammatory Activity

Anti-inflammatory study like human red blood cell (HRBC), membrane stabilization, inhibition of albumin de nutrition indicated that anti-inflammatory activity .The medical use of Delonix elata has a good anti-inflammatory activity. As the concentration of the sample increases, the

percentage of inhibition also increases.

Table 1: Anti-inflammatory activity of human red blood cell (HRBC) by using AgNPs of Delonix elata

S. No	Concentration (µg/ml)	% of Inhibition Membrane Stabilization Mean±S.E.M
1	100	43.19 ± 0.17
2	200	48.73 ± 0.49
3	400	57.51 ± 0.73
4	600	59.28 ± 1.55
5	800	63.32 ± 1.39

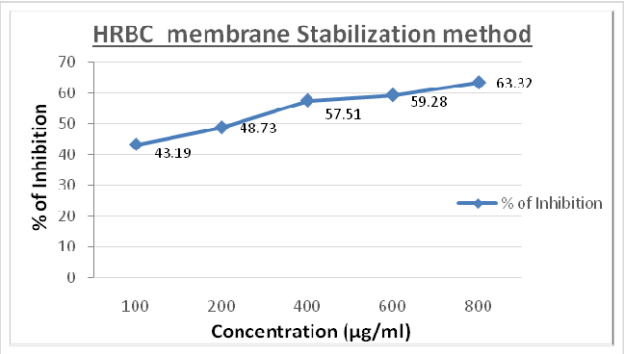

Figure 6: Graphical representation of Anti-inflammatory activity of human red blood cell (HRBC) by using AgNPs of Delonix elata

Table 2: Anti-inflammatory activity of Albumin denaturation methodby using AgNPs of Delonix elata

S. No	Concentration (µg/ml)	% of Inhibition Membrane Stabilization Mean±S.E.M
1	100	40.34 ± 0.48
2	200	45.81 ± 0.39
3	400	56.74 ± 0.73
4	600	58.13 ± 1.21
5	800	60.07 ± 1.18

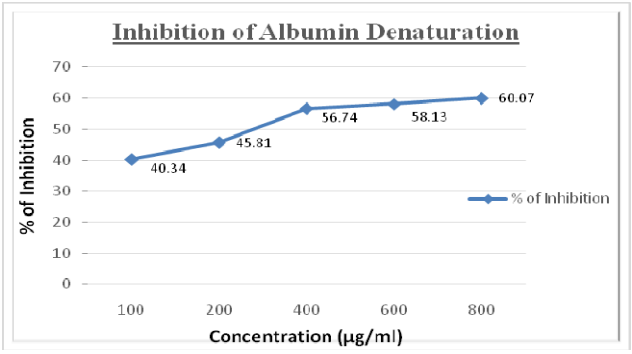

Figure 7: Graphical representation of Anti-inflammatory activity of Albumin denaturation methodby using AgNPs of Delonix elata

Discussion

UV–Vis spectroscopy is an important technique to establish the formation and stability of metal Nanoparticles in aqueous solution [24]. The silver Nanoparticles were formed by adding different concentration of extracts (0.5 ml, 1 ml, 2 ml, 5 ml and 7 ml) with aqueous AgNO3. After 24 hrs, the colour of the solutions changed from pale yellow to yellowish brown and then to deep brown depending on the extract concentration indicating the formation of silver Nanoparticles. The colour changes are due to excitation of surface plasmon vibration in silver Nanoparticles. AgNPs have free electrons, which gives rise to a surface plasmon resonance absorption due to the combined vibration of electrons of the metal Nanoparticles in resonance with the light wave [25]. The synthesized AgNPs display a clear and single SPR band with the kmax at 428–432 nm which confirms the reduction of silver ion to metallic silver. As the concentration of the D. elata leaf extract increases, the absorption peak becomes more sharpen and blue shift is observed at 432 nm. This is due to the formation of spherical and homogeneous distribution of silver Nanoparticles. Some unassigned peaks have also been observed suggesting that the crystallization of bio-organic phase [26-29]. FT-IR analysis was carried out to detect the possible biomolecules responsible for the reduction of the metal ions and capping Photograph of AgNO3 and Delonix elata leaf extracts of these silver Nanoparticles. The FT-IR spectrum of leaf broth before reaction shows several absorption bands at 3387, 2345, 1639 and 1543 cm^{-1}. The absorption band at 3387 cm^{-1} is due to OH stretching vibration. The observed two minor bands at 3819 cm^{-1} and 3722 cm^{-1} indicate the presence of phenols (OAH group) and phenolic compound in the plant extract.

The bands at 2345, 1639 and 1543 cm^{-1} indicates the presence of alkane groups (ACAH stretching), amide I band (Carbonyl group (C-O)) and aromatic (C-C) respectively [30,31]. The minor band 1062 cm^{-1} corresponds to CAN stretching alcohols, the band 754,711 and 680 (800–600 cm^{-1}) regions for CAH out of plane bend, which are of characteristic of aromatic phenols. In the case of Nanoparticles, a shift in the absorbance band with decrease in band intensity was observed from 2345 to 2347 cm^{-1} and 1543 to 1546 cm^{-1} implying the binding of silver ions with alkane and aromatic groups of the extract [32]. The spectra also illustrate a prominent shift in the wave numbers (1639–1645 cm^{-1}) corresponding to amide I band. All these reveal the presence of phenolic compounds along with the AgNPs, flavonoids present in the leaf broth of D. elata have been suggested to be responsible for the reduction and stabilization of silver Nanoparticles [33].

Conclusion

The Silver Nanoparticles synthesized using delonix elata leaf extracts were identified first by observing the colour changes of the extract. The colour changed from yellow to dark brown colour during the formation of silver Nanoparticles. The developed Nanoparticles were characterized by UV-vis, TEM, XRD and FTIR measurements and showed good anti-inflammatory activity. This rapid synthesis technique can be a promising method for the preparation of Nanoparticles and can be valuable in environmental, biotechnological, pharmaceutical and medical applications. Silver Nanoparticles formed was characterized by UV, FT-IR, XRD and SEM. UV absorbance at 230.98nm was observed for Silver Nanoparticles. XRD & TEM analysis of the Silver Nanoparticles showed that the average size of Silver Nanoparticles is 11.37 and 11.78nm.

References

1. A.B. Smetana, K.J. Klabunde, C.M. Sorensen, J. Colloid Interfaces Sci. 284 (2005) 521–526.

2. J. Das, M. Paul Das, P. Velusamy, Spectrochim. Acta A 104 (2013) 265–270.

3. S. Priyadarshini, V. Gopinath, N. Meera Priyadarshini, D. Mubarak Ali, P.Velusamy, Colloids Surfaces B 102 (2013) 232–237.

4. Kannan Badri Narayanan, Natarajan Sakthivel, Mater. Res. Bull. 46 (2011) 1708–1713.

5. D. Philip, Spectrochim. Acta A 73 (2009) 374–381.

6. K. Raja, A. Saravanakumar, R. Vijayakumar, Spectrochim. Acta A 97 (2012) 490–494.

7. Mervat F. Zayed, Wael H. Eisa, A.A. Shabaka, Spectrochim. Acta A 98 (2012)423–428.

8. M.R. Bindha, M. Uma devi, Spectrochim Acta A 101 (2013) 184–190.

9. V. SubbaRao, Venkata S. Kotakadi, T.N.V.K.V. Prasad, A.V. Reddy, D.V.R. Sai Gopal, Spectrochem. Acta A 103 (2013) 156–159.

10. J. Das, M. Paul Das, P. Velusamy, Spectrochim. Acta A 104 (2013) 265–270.

11. K.L. Niraimathi, V. Sudha, R. Lavanya, P. Brindha, Colloids Surfaces B 102(2013) 288–291.

12. V.K. Vidhu, S. Aswathy Aromal, Daizy Philip, Spectrochim. Acta A 83 (2011) 392–397.

13. Muthu Karuppiah, Rangasamy Rajmohan, Mater. Lett. 97 (2013) 141–143.

14. Akl M. Awwad, M. Salem, J. Nanosci. Nanotechnol. 2 (4) (2012) 125–128.

15. G. Abd El, M. Hegazi, J. World Appl. Sci. 14 (5) (2011) 679–686.

16. Wijayasiriwardena, C., Chauhan, M.G., Sharma, P.P., Lahiri, S.K., Shah, M.B., 2009. Anti-inflammatory activity of Delonix elata (L.) gambles. Journal of natural remedies.vol. 9(2), 209 – 215.

17. .Wijayasirivardena C, Chauhan NG, Sharma PP, LahiriSK, ShahMB. Anti-inflammatory activities of Delonix elata (L) gamble. J Nat Rem.2009;9(2):209-215.

18. Muruganathan G, and Mohan S. Anti-inflammatory and Anti-Arthritic activities of Delonix elata bark extracts. Int J Res Ayu Pharm.2011;2(6):1819-1821.

19. P. S. Pavithra, V. S. Janani, K. H. Charumathi, R. Indumathy, S. Potala, and R. S. Verma, "Antibacterial activity of plants used in Indian herbal medicine," International Journal of Green Pharmacy, vol. 4, no. 1, pp. 22–28, 2010.

20. K. Pradeepa, V. Krishna, B. G. Harish, Venkatesh, S. S. R. Kumar, and G. K. Kumar, "Antibacterial activity of leaf extract of Delonix elata and molecular docking studies of Luteolin," Journal of Biochemical Technology, vol. 3, pp. S198–S203, 2013.

21. K.Pradeepa, V. Krishna, K. K. Girish, S. Kumar Sr., J. H. Hoskeri, and A. U. Gnanesh, "Antinociceptive activity of

Delonix elata leaf extract," Asian Pacific Journal of Tropical Biomedicine, vol. 2, no. 1, pp. S229–S231, 2012.

22. M. G. Sethuraman and N. Sulochana, "The anti-inflammatory activity of Delonix elata," Current Science, vol. 55, pp. 343–344, 1986.

23. D. Philip, C. Unni, S.A. Aromal, V.K. Vidhu, Spectrochim. Acta A 78 (2011) 899.

24. Vankatasubbaiah Kotakadi, Y. SubhaRao, Susmila Aparana, Gaddam, T.N.K.V. Prasad, A. Varada Reddy, D.V.R. Sai Gopal, Colloids Surfaces B 105 (2013) 194– 198.

25. R. Sathyavathi, M.B. Krishna, S.V. Rao, R. Saritha, D.N. Rao, Adv. Sci. Lett. 3 (2010) 1–6.

26. Anamika Mubayi, Sanjekta Chatterji, M. Prashant, Rai, Geeta Watal, Adv. Mater. lett. 3 (6) (2012) 519–525.

27. Naheed Ahmad, Seema Sharma, Radheshyam Rai, Adv. Mater. Lett. 3 (5) (2012) 376–380.

28. P. Mukherjee, M. Roy, B. Mandal, P. Dey, G.K. Mukherjee, P.K. Ghatak, J. Tyagi, A.K. Kale, J. Nanotech. 19 (2008) 075103.

29. C. Dipankar, Murugan, Colloids Surfaces B 98 (2012) 112–119.

30. S.Kaviya, J.Santhanalakshmi, B.Viswanathan, J.Muthumary, K.Srinivasan, Spectrochim. Acta A 79 (2011) 594–598.

31. R. Raut, S.L. Jaya, D.K. Niranjan, B.M. Vijay, S. Kashid, Curr. Nanosci. 5 (2009) 117–122.

32. G. Rajakumar, A. Abdul Rahuman, Acta Trop. 118 (2011) 196–203.

33. N. Asmathunisha, K. Karthiresan, Anburaj, M.A. Nabeel, Colloids Surfaces B 79 (2010) 488–493.

Author's details

[1]Assistant Professor, Department of Physics, Roever College of Engineering and Technology, Perambalur, Tamilnadu, India, Email: anithasai2013@gmail.com

[2]Associate Professor, Department of Physics, Urumu Dhanalakshmi College, Trichy, Tamilnadu, India.

Copy for Cite this Article- P. Anitha and P. Sakthivel, 'Synthesis and characterization of silver nanoparticles using Delonix elata leaf extract and its Anti-inflammatory activity against human blood cells,' *International Journal of Science, Engineering and Technology,* Volume 4 Issue 1: 2016, pp. 330- 336.

Md Jafri Ahsan et al. 2016, Volume 4 Issue 1
ISSN (Online): 2348-4098
ISSN (Print): 2395-4752

International Journal of Science, Engineering and Technology
An Open Access Journal

Development and Performance Evaluation of Forced Convection Batch Type Steam Blancher

[1]Mohd Kaleem, [2]Er. Kailash Chandra Yadav, [3]Md Jafri Ahsan

Abstract

The study was conducted for development and performance evaluation of Forced Convection Batch Type Steam Blancher. The polyphenol oxidase (causes enzymatic browning) inactivation of potato slices (0.25 inch length) after Forced Convection Steam Blanching at different steam pressures (1.0 kg/cm^2 and 1.5 kg/cm^2) for time interval of 1-5 minutes was carried out. Polyphenol Oxidase activity of raw potato (control) was found to be 125.4 Units ml^{-1} and after blanching at a pressure of 1.0 kg/cm^2 for 1 min in potato slices (0.25 inch length) was found to be 28.8 Units ml^{-1} and for 2 min was found to be 10.8 Units ml^{-1}. No polyphenol oxidase activity had been observed after blanching for 3, 4 and 5 minutes. No polyphenol oxidase activity had been observed after blanching at a pressure of 1.5 kg/cm^2 for 1, 2, 3, 4 and 5 minutes for the same potato slice length. Polyphenol oxidase inactivation time decreased as steam pressure increased. Forced Convection Steam Blanching promotes enzyme inactivation at faster rate due to high heat transfer coefficient of condensing steam. The present findings will help to design the blanching conditions with minimum physico-chemical and nutrient changes of final product.

Keywords: Forced Convection Steam Blanching, polyphenol oxidase Inactivation, steam pressure, potato slices.

Introduction

Indian has made a good progress on horticultural map of the world with a total annual production of horticultural crops touching over 149 million tones. Indian is the second largest producer of fruit (45.5 million tones) and vegetables (90.8 million tones) in the world, contributing 14.45% of the total world production of fruits and vegetables respectively (Anonymous, 2007).

India's share in the world trade of horticultural processed products is less than 1%. This compares very unfavorably with countries like Malaysia (83%), Philippines (78%), Brazil (70%) and United State (70%). India's major exports are in fruit pulp, pickles, chutney, canned fruits and vegetables, concentrated pulp and juices, dehydrated vegetables and frozen fruits and vegetables (Anonymous, 2007).

Table 1: Vision strategy and action plan for trade of horticultural food products in India

Year	World exports (million tones / annum)	India's export (million tones/ annum)	India's share (%)	Growth rate (%)
2003	522	8	1.5	-
2010	770	15	2.0	14
2015	1020	30	3.0	15

(Anonymous, 2007)

Vegetable are seasonal and perishable in nature. Blanching is one of the methods to prevent enzymatic activity and give extended shelf life with good quality and sensory attributes and make them available at reasonable cost.

Table 2: Nutritional value of raw potato

Nutritional value per 100 g	
Energy	321 kj
Carbohydrate	19g
Starch	15g
Dietary fiber	2.2g
Fat	0.1g
Protein	2.0g
Water	75g
Thiamin (Vit. B1)	0.08 mg
Riboflavin (Vit. B2)	0.03 mg
Naicin (Vit. B3)	1.1 mg
Vitamin B6	0.25 mg
Vitamin C	20 mg
Calcium	12 mg
Iron	1.8 mg
Magnesium	23 mg
Phosphorus	57 mg
Potassium	421 mg
Sodium	6 mg

(Hijmans and Spooner, 2001)

Review of Literature

Blanching

Blanching is an important unit operation for processing of vegetables. The purpose of blanching is to inactivate enzymes along with destruction of microorganisms and reduces the extra cellular gases so that product quality is retained maximum as fresh (Van and Copley, 1963).

Guerrant *et al.,* (1947) found that blanching was beneficial in many ways having detrimental effect particularly on the water–soluble nutrients. Prolonged hot water blanching resulted in considerable loss of carbohydrates, protein and mineral while steam blanching could eliminate these losses to a great extent.

Lee (1958) reported that blanching had also proved to improve textural quality of products.

Van and Copley (1963) reported that blanching of fruits and vegetables is principally followed to inactivate the enzymes responsible for enzymatic and oxidative browning. The common blanching includes hot water, steam and chemical blanching. The loss of nutrient takes place during blanching. The nutrients are also affected by temperature and time of blanching.

Morris (1974) reported that blanching operation involves a short and quick heat treatment to the material, for which usually hot water is used for uniform heating and higher heat transfer rate.

Patil *et al.,* (1978) reported that effect of blanching on fenugreek at different temperature for different time in combination with chemicals like NaCl, KMS. The blanched and sun dried product was compared with sun dried sample which was more acceptable than sun dried product.

Onyami and Badifu (1987) reported that steam blanching is more superior to water blanching on the basis of nutrient retention and overall acceptability. Addition of sodium bicarbonate to the steam blanch improved the quality and overall acceptability of the vegetable compared to water blanched vegetables.

Rice *et al.,* (1990) studied the losses of nutrient in blanching operation. They found steady increase in diffusion coefficient with increase in temperature and blanching time. The value of diffusion coefficient was independent of the dimensions and volume of sample.

Nath *et al.,* (1991) studied the effect of water blanching, water blanching KMS dipped, sulphite dipped, salt treated and brine blanching on bitter gourd rings. Best reconstitutability and total chlorophylls were resulted in water blanching sulphite dipped and brine blanching.

Maharaj and Clement (1994) reported that in blanching the herb shado Beni (Eryngium foetidium) in hot water at 96^0C using a quick dip step followed by drying in the indirect drier reduced the loss of green colour, normally observed without pre-

treatment. Blanching did not affect the drying rate behavior of the herb.

Gill *et al.,* (2003) investigated effect of blanching on the texture, colour and sensory properties of soybeans. Blanching was carried out at 80, 90 and 100^0C for 10-30 min. followed by immersion in cold water for one min. Under these conditions blanching reduced greenness to a similar extent. Treatment at 100^0C for 10 min. led to smallest loss in nutrient content and resulted in the softest texture according to both instrumental and sensory analysis.

Enzymatic Browning

Enzymatic browning of foods during processing and storage, especially during manufacture of fruit and vegetable products decrease the sensory properties of products due to associated changes in the colour, flavour and softening besides nutritional properties. Therefore its control is essential to preserve the quality of the food (Ozemir, 1997).

Krotov *et al.,* (1971) concluded that green pea PPO require 2.5 min. at 90^0C and only 1 min. at 95^0C.

Galeazzi and Sgarbieri (1978) concluded that banana PPO is inactivated in 1.5 min. at 80^0C.

Mondy *et al.,* (1979) concluded that high nitrogen levels have been related to a greater tendency to brown in potatoes.

Vamos (1981) studied that enzymatic browning is not only restricted to discoloration, undesirable taste can also be produced and loss of nutrients, quality may results .

Molhar and Friedman (1990) concluded that the pH of potato is between 5.0 to 5.2 and this makes it susceptible to PPO activity. Enzymatic browning leads to the destruction of vitamin-C due to oxidative degradation.

Asaka amd Hayashi (1991) concluded that the application of low pressure results in pressure – induced membrane damage with consequent enzyme activation. In fact, pear PPO was activated after pressure treatment at 400 MPa for 10 min at 25^0C.

Zawistowski *et al.,* (1991) concluded that blanching and cooking are effective methods for prevention of enzymatic browning. PPO is an enzyme of low thermal stability although difference in heat stability are reported for different cultivars and PPO isoforms.

Materials and Methods

Procurement of raw materials

The study was conducted with good quality of potato procured from the local market of Allahabad. The vegetable was free from any kind of damage. All the trials were carried out in the laboratory of Department of Food Process Engineering, Sam Higginbottom Institute of Agriculture, Technology and Sciences, Allahabad-U.P.

Equipment used

Some of the equipments, Glassware and chemicals that were employed during the course of the study are given below.

Electronic weighing balance

Electronic weighing balance is an instrument used to weigh very small quantities of samples with precision. It was used to weigh 0.1 g catechol for preparing 0.1% catechol reagent.

Mixer grinder

It is a motor operated device consisting of stainless steel jar having stainless steel teethes in it. It was used to grind and mix the potato sample.

Centrifuge

The centrifuge is a motor operated device which works using the sedimentation principle, where centripetal acceleration causes more dense substance to separate out along the radial direction (the bottom of the tube), by the same token, lighter objects will tends to move to the top of the tube. It was used to separate denser substances from supernatant portion (enzyme extract) from potato mixture.

Spectrophotometer

A UV/visible – light spectrophotometer of wavelength ranges from 190-900 nm was used. It is a device used to measure light intensity as a function of light source wavelength. It was used to measure the change in absorbance per 30 sec. at a wavelength of 480 nm for determining PPO activity in potato extract.

Volumetric flask

100 ml capacity volumetric flask was taken for preparing 0.1% catechol and 100 ml standard pH-7 buffer.

Filtering cloth

Butcher's linen or dress linen with approximately 45 threads per square inch was used for sieving ground potato sample.

Collection and preparation of chemical and reagents

Reagents and their preparation

The various reagent used in the analysis were 0.1% catechol and standard pH 7 buffer.

1) Preparation of 0.1% catechol: weigh 0.1 g catechol and dissolve it in 100ml distill water in a 100 ml volumetric flask.

2) Preparation of standard pH-7 buffer: dissolve one standard pH-7 buffer tablet in 100 ml distill water in a 100 ml volumetric flask.

Experimental plan

The experimental variables with their ranges, selected for the performance evaluation of Forced Convection Batch Type Steam Blancher were shown in table 3.

Table 3: Experimental variables for Forced Convection Steam Blanching with their levels and range

S. No.	Independent variables	Experimental range	Levels
1.	Blanching time	1-5 Minutes	1, 2, 3, 4, 5 min.
2.	Steam pressure	1.0-1.5 kg /cm^2	1.0, 1.5 kg/cm^2
3.	Potato slice length	0.25 inch	0.25 inch

Development of Forced Convection Batch Type Steam Blancher

For conducting the experiments on steam blanching, a forced convection batch type steam blancher was developed (Corcuera *et al.,* 2004). It was fabricated in the local workshop of Naini, Allahabad. The steam blancher was fabricated keeping in view that the steam is being supplied from both the sides at uniform pressure and safe in use. It consists of following parts.

1. Cubical box
2. Tray with sieve
3. Steam supply and control
4. Drain valve
5. Control valve
6. Solenoid valve
7. Nozzles
8. Condensed steam outlet
9. Pressure gauge
10. Safety valve
11. Arrangement for temperature measurement

Development of blanching box

A cubical box of 838 x 508 x 508 mm size was fabricated by using 1 mm thick stainless steel sheet (304 quality), recommended for food processing equipments (Durward, 2007). Provision to fix the nozzles at top and bottom face was made. At front face of the box, at the center, a horizontal rectangular slot of 838 x 75 mm was cut for in and out movement of tray. All the joints of the box were soldered with a soldering filler material consisting of 60% tin and 40% lead, having melting point between 183 to 190 °C (Rahn, 1993). At the opening of the front face of box, RTS (Room Temp. Vulcanizing) Silicon Sealant paste (Salistic 723) was used as a gasket to prevent leakage of steam. It meets FDA requirements [FDA requirement number: 21CFR177-2600 (food contact), MIL-A-46106 parts I & II.]. When it was applied, become flexible rubber like structure. They can withstand temp. extremes from -65 to 232 °C. They are resistant to steam, oil, chemicals and ultra violet light.

Development of tray with sieve

A tray with sieve shown in fig.1 was fabricated. The size was 810 x 482 x 70 mm was fabricated by 1 mm thick stainless steel sheet (304 quality), recommended for food processing equipments (Durward, 2007). At the bottom of the sieve two vertical stainless steel strips (2mm thick) equidistant from each other was used to support the sieve.

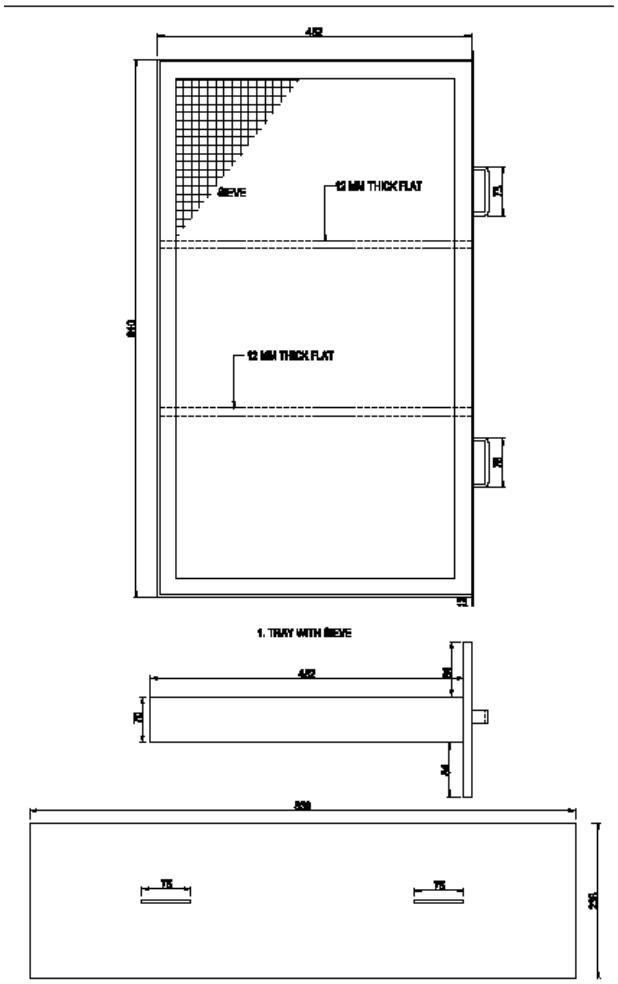

Figure 1: Tray with Forced Convection Batch Type Steam Blancher

Steam supply and control

A ½ inch diameter Stainless steel SS304 reinforced PTFE Hose, working temp. -50 to 210 °C, having working pressure of 256 kg/cm^2 was connected to the outlet of boiler from one end and other to the control valve of blancher which further connected to solenoid valve which is electrically operated and helps in instantaneous switch on and switch off of steam flow. PTFE or Teflon pipe was tightly fitted. After control value, steam was passed via solenoid valve in two directions upward and downward with the help of copper tubes. Other necessary attachments were made as shown in fig. 2.

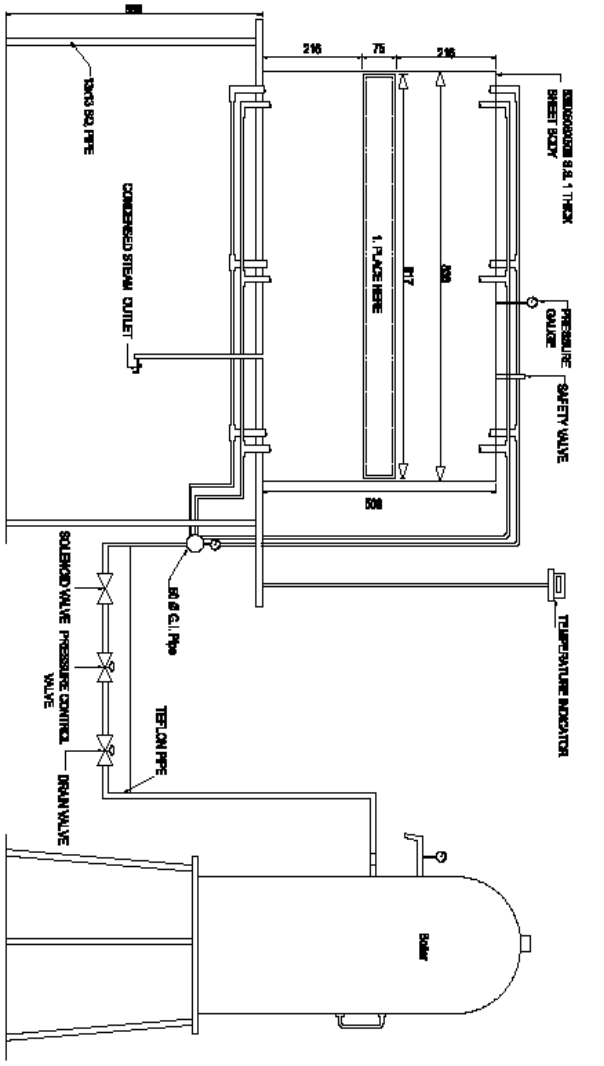

Figure 2: Schematic diagram of forced convection batch type steam blancher

Forced Convection Steam Blanching of potato slices

For performing Forced Convection Steam Blanching, fresh potatoes were procured from the local market of village Mahewa, Allahabad.

The outline of sample preparation has been shown in fig. 3.

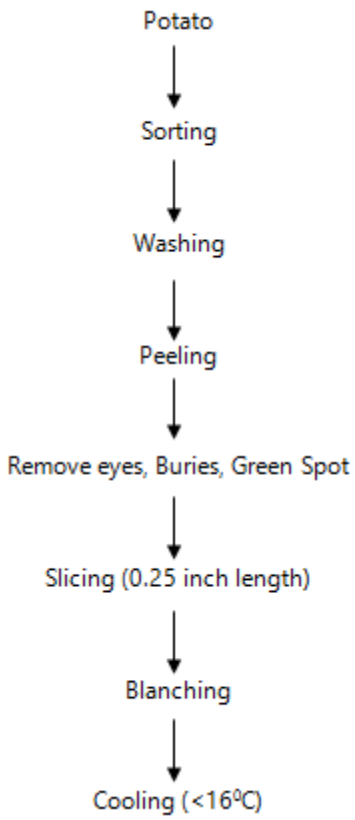

Figure 3: Flow chart for blanching of potato slices

Potato was sliced in uniform length as per the experimental design. A weight amount of slices were placed in the tray of developed blancher. The blanching time and steam pressures were selected as per the experimental design.

Determination of polyphenol oxidase activity

Browning of the cut surface of some fruits and vegetables is due to the presence of a group of enzymes called polyphenol oxidase. These enzymes are released by the broken cells and they catalyze the reaction between colourless molecules called polyphenols and molecular oxygen. This reaction creates compounds and these new compounds can spontaneously cross react with one another to form black brown complexes called melanin. One example of a substrate of these enzyme is catechol, hence the alternative name "catechol oxidase" for the enzymes. Catechol is oxidized initially to the orange compound benzoquinone which is then converted to melanin is spontaneous but slow.

Catechol + oxygen $\xrightarrow{\text{Polyphenol oxidase}}$ **benzoquinone + water** $\xrightarrow{\text{slowly}}$ **melanin**

Polyphenol oxidase assay

1. An extract of potato was made by grinding in a mixer grinder with an equipment mass of distill water.

2. The extract was strain through muslin cloth, then the filtrate was centrifuge at 5000 RPM for 15 min for the removal of remaining solids.

3. The clear supernatant portion was taken without any solid particles into another flask.

4. The visible light source was switch onn and the spectrophotometer was set at a wavelength of 480 nm for potato at 25^0C was measured.

5. The cuvett was placed with 4 ml std. pH 7 buffer solution and 0.1 ml of 0.1% catechol. Then the lid was closed. The "Clab" button was pressed and waiting was done until the led reads "0.000".

6. Another cuvett was taken and added with 2 ml standard pH 7 buffer and 2ml of 0.1% catechol were added, the time was noted and then 0.1 ml enzyme extract was added, quickly the contents of the tube was mixed. Then it was placed into a spectrophotometer. The readings of absorbance at regular intervals were taken.

7. A graph was plotted for the change in absorbance against time. An increase in absorbance was due to the formation of benzoquinone, the product of the reaction. The initial slope of the graph gives a measure of the polyphenol oxidase activity of the potato extract.

The enzymatic activity was calculated as:

$$Units\ ml^{-1} = \frac{\Delta A_{480\,nm} / \min}{(0.001) \times ml\ enzyme\ in\ reaction}$$

1 unit of enzyme causes a change in absorbance at A_{480nm} of 0.001 per minute, under the assay condition of 25 ^{0}C, under specified condition. Procedure (Bauer *et al.,* 1980) was employed.

Results and Discussion

This chapter deals with the results obtained from the different experiments of the present investigation.

Developed Forced Convection Batch Type Steam Blancher

The developed Forced Convection Batch Type Steam Blancher was tested for its pressure range desired to perform the experiment. It was found that the control of steam pressure and blanching time were easier, while in operation. Due to nozzles the steam used to have high velocity. It raised the temp. of the sample at faster rate, as it had high valve of heat transfer coefficient (rate of heat flow in unit time through unit area when there was a unit temp. difference between the surface of the sample and surrounding). The value of heat transfer coefficient depends upon fluid velocity. Capacity of blancher was found to be 1.65 kilogram per batch.

Polyphenol oxidase assay

Polyphenol oxidase (causes enzymatic browning) was analyzed according to the method of (Bauer *et al.,* 1980). Polyphenol oxidase activity was measured for raw potato (control) and for forced convection steam blanched potato slices.

For determining polyphenol oxidase activity, a graph was plotted for the change in absorbance against time. An increase in absorbance is due to the formation of benzoquinone, the product of the reaction. The initial slope of the graph gives a measure of polyphenol oxidase activity of potato extract. Polyphenol oxidase activity was measured from the increase in absorbance at 480nm using spectrophotometer. The reaction was monitored for 330 Sec. All the experiments were replicated thrice and average values were used in analysis.

Enzymatic, activity was calculated in terms of Units ml^{-1} under the assay condition at 25^0C.

Polyphenol oxidase activity of raw potato (control)

Polyphenol oxidase activity (causes enzymatic browning) of raw potato (control) = 125.4 Units ml^{-1} (table 4. and fig. 4.).

Table 4: Absorbance table for polyphenol oxidase activity of raw potato (control) at intervals of 30 Sec.

Absorbance at 480 nm	**Time (Sec.)**
0.027	30
0.032	60
0.040	90
0.045	120
0.053	150
0.058	180
0.068	210
0.073	240
0.079	270
0.085	300
0.091	330

Standard deviation (σ) = 2.17 x 10^{-2}

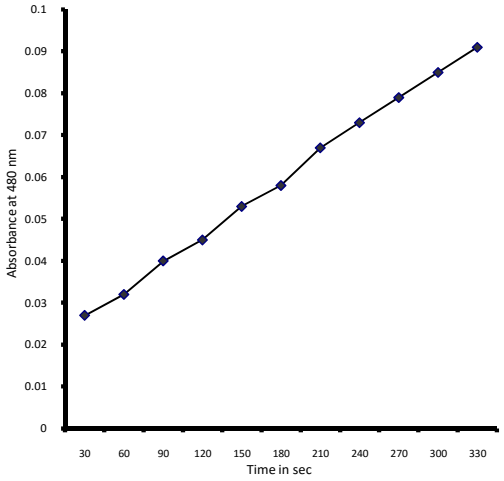

Figure 4: Absorbance Vs time graph for polyphenol oxidase activity of raw potato (control)

Polyphenol oxidase activity of potato slice (0.25 inch length) after Force Convection Steam Blanching at a pressure of 1.0 kg/cm^2 for 1 min

Polyphenol oxidase activity (causes enzymatic browning) of potato slice (0.25 inch length) after Forced Convection Steam Blanching at a pressure of 1.0 kg/cm^2 for 1 min. = 28.8 Units ml^{-1} (table 5 and fig. 5).

Table 5: Absorbance table for polyphenol oxidase activity of potato slice (0.25 inch length) after Forced Convection Steam Blanching at a pressure of 1.0 kg/cm^2 for 1 min. at intervals of 30 Sec

Absorbance at 480 nm	Time (Sec.)
0.022	30
0.023	60
0.024	90
0.025	120
0.027	150
0.029	180
0.030	210
0.032	240
0.034	270
0.036	300
0.038	330

Standard deviation (σ) = 5.43 x 10^{-3}

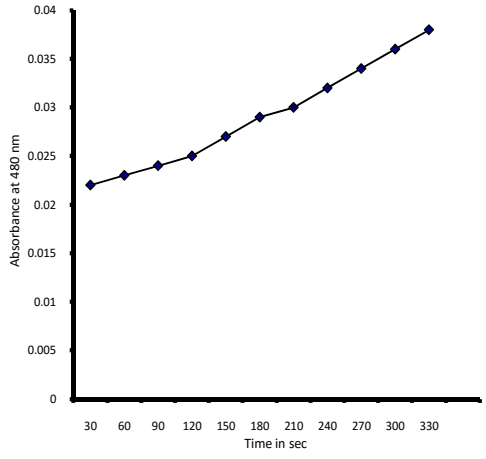

Figure 5: Absorbance Vs time graph for polyphenol oxidase activity of potato slices (0.25 inch length) after Forced Convection Steam Blanching at a pressure of 1.0 kg/cm^2 for 1 min

Polyphenol oxidase activity of potato slices (0.25 inch length) after Forced Convection Steam Blanching at a pressure of 1.0 kg/cm^2 for 2 min

Polyphenol oxidase activity (causes enzymatic browning) of potato slice (0.25 pinch length) after Forced Convection Steam Blanching at pressure of 1.0 kg/cm^2 for 2 min. = 10.8 Units ml^{-1} (table 6 and fig. 6).

Table 6: Absorbance table for polyphenol oxidase activity of potato slices (0.25 inch length) after Forced Convection Steam Blanching at a pressure of 1.0 kg/cm^2 for 2 min. at intervals of 30 Sec.

Absorbance at 480 nm	Time (sec)
0.000	30
0.001	60
0.002	90
0.002	120
0.003	150
0.003	180
0.004	210
0.004	240
0.005	370
0.005	300
0.006	330

Standard deviation (σ) = 2.02 x 10^{-3}

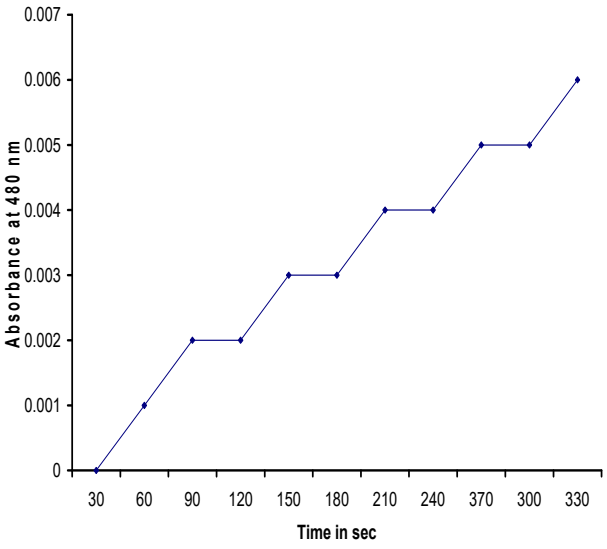

Figure 6: Absorbance Vs time graph for polyphenol oxidase activity of potato slices (0.25 inch length) after Forced Convection Steam Blanching at a pressure of 1.0 kg/cm^2 for 2 min

Polyphenol oxidase activity of potato slices (0.25 inch length) after Forced Convection Steam Blanching at a pressure of 1.0 kg/cm^2 for 3 min

No polyphenol oxidase activity (cause enzymatic browning) was observed in potato slices (0.25 inch length) after Forced Convection Steam Blanching at a pressure of 1.0 kg/cm^2 for 3 min.

Polyphenol oxidase activity of potato slices (0.25 inch length) after Forced Convection Steam Blanching at a pressure of 1.0 kg/cm^2 for 4 min

No polyphenol oxidase activity (cause enzymatic browning) was observed in potato slices (0.25 inch length) after Forced Convection Steam Blanching at a pressure of 1.0 kg/cm^2 for 4 min.

Polyphenol oxidase activity of potato slices (0.25 inch length) after Forced Convection Steam Blanching at a pressure of 1.0 kg/cm^2 for 5 min

No polyphenol oxidase activity (cause enzymatic browning) was observed in potato slices (0.25 inch length) after Forced Convection Steam Blanching at a pressure of 1.0 kg/cm^2 for 5 min.

Polyphenol oxidase activity of potato slices (0.25 inch length) after Forced Convection Steam Blanching at a pressure of 1.5 kg/cm^2 for 1 min

No polyphenol oxidase activity (cause enzymatic browning) was observed in potato slices (0.25 inch length) after Forced Convection Steam Blanching at a pressure of 1.5 kg/cm^2 for 1 min.

Polyphenol oxidase activity of potato slices (0.25 inch length) after Forced Convection Steam Blanching at a pressure of 1.5 kg/cm^2 for 2 min

No polyphenol oxidase activity (cause enzymatic browning) was observed in potato slices (0.25 inch length) after Forced Convection Steam Blanching at a pressure of 1.5 kg/cm^2 for 2 min.

Polyphenol oxidase activity of potato slices (0.25 inch length) after Forced Convection Steam Blanching at a pressure of 1.5 kg/cm^2 for 3 min

No polyphenol oxidase activity (cause enzymatic browning) was observed in potato slices (0.25 inch length) after Forced Convection Steam Blanching at a pressure of 1.5 kg/cm^2 for 3 min.

Polyphenol oxidase activity of potato slices (0.25 inch length) after Forced Convection Steam Blanching at a pressure of 1.5 kg/cm^2 for 4 min

No polyphenol oxidase activity (cause enzymatic browning) was observed in potato slices (0.25 inch length) after Forced Convection Steam Blanching at a pressure of 1.5 kg/cm^2 for 4 min.

Polyphenol oxidase activity of potato slices (0.25 inch length) after Forced Convection Steam Blanching at a pressure of 1.5 kg/cm^2 for 5 min

No polyphenol oxidase activity (cause enzymatic browning) was observed in potato slices (0.25 inch length) after Forced Convection Seam Blanching at a pressure of 1.5 kg/cm^2 for 5 min.

Polyphonel oxidase activity of raw potato (control) and Forced Convection Steam Blanched potato slices (0.25 inch length) at a pressure of 1.0 kg/cm^2 and a pressure of 1.5 kg/cm^2 for blanching time of 1-5 min

The potato slices (0.25 inch length) were blanched by using Forced Convection Steam Blancher at a pressure of 1.0 kg/cm^2 and 1.5 kg/cm^2 for time intervals for time intervals of 1-5 min.

Further inactivation time for pressure 1.0 kg/cm^2 was longer than that for 1.5 kg/cm^2, table 7.

Table 7: Polyphonel oxidase activity of raw potato (control) and Forced Convection Steam Blanched potato slices (0.25 inch length) at a pressure of 1.0 kg/cm^2 and a pressure of 1.5 kg/cm^2 for blanching time of 1-5 min

Enzymatic activity	**Samples**
125.4 Units ml $^{-1}$	Raw potato (control)
28.8 Units ml^{-1}	Blanching for 1 min. at a pressure of 1.0 kg/cm^2
10.8 Units ml^{-1}	Blanching for 2 min. at a pressure of 1.0 kg/cm^2

Nil	Blanching for 3 min. at a pressure of 1.0 kg/cm^2
Nil	Blanching for 4 min. at a pressure of 1.0 kg/cm^2
Nil	Blanching for 5 min. at a pressure of 1.0 kg/ cm^2
Nil	Blanching for 1 min. at a pressure of 1.5 kg/cm^2
Nil	Blanching for 2 min. at a pressure of 1.5 kg/cm^2
Nil	Blanching for 3 min. at a pressure of 1.5 kg/cm^2
Nil	Blanching for 4 min. at a pressure of 1.5 kg/cm^2
Nil	Blanching for 5 min. at a pressure of 1.5 kg/cm^2

Conclusion

1. The developed Forced Convection Batch Type Steam Blancher was easy to operate as there was strict control over time and steam pressure range applied.

2. The polyphenol oxidase activity (causes enzymatic browning) of blanched potato slices decreased as steam pressure range increased.

3. Forced Convection Steam Blanching results in better control on energy utilization as it takes lesser time because of high heat transfer coefficient.

4. Forced Convection Steam Blanching helps in enhancing the keeping quality of potato slices by preventing enzymatic browning.

Suggestions for Future Work

1. Effect of Forced Convection Steam Blanching on quality characteristics of dehydrated product be studied during storage at ambient and referization temp..

2. Forced Convection Steam Blanching be done in combination with chemicals, potassium meta bisulphate and sodium chloride and their effect over quality of product be studied.

Effect of Forced Convection Steam Blanching on enzymatic activity of polyphenol oxidase (causes enzymatic browning) be studied in different fruits like mango, apple, banana etc. and vegetables like mushroom, lettuce etc. as they are highly susceptible to enzymatic browning because their pH lies between the range of 5-7.

References

Ahvenainen, R. (1996). New approaches improving the shelf –life of minimally processed fruit and vegetables trends. Food Sci. Technol, 7:pp. 179-187.

Arroqui, C. A., Lopex, A. E. and Irsed, P.V. (2003). Mathematical model of heat transfer and enzyme inactivation in an integrated blancher cooler. J. of Food engineering, 58(1):pp. 512-225.

Asaka, M. and Hayashi, R. (1991). Activation of polyphenoloxidase in pear fruit by high pressure treatment. Agric. Biol Chem., 55(9):pp. 2439-2440.

Bauer, R. D., Campbell, J. A., Loseschen, R. L. and Wolf, J. L. (1980). Laboratory Manual Chemistry for the allied Health Sciences. Prentice-Hall, Inc; Engle wood Ciffs, 36:pp. 657-665.

Corcuera, J. I., Ralph, P., Cavalieri and Joseph, R. P. (2004). Blanching of Food. Encylopedia of Agricultural, Food and Biological Engineering, 51(5):pp. 1201-1203.

Durward, S. A. (2007). Small Scale Food Equipment. Unl Extension Publications, 43:pp. 20-24.

Galeazzi, M. A. and Sgarbieri, V. C. (1978). Banana polyphenol oxidase.Verietal difference and partial Characterization. Int. Congress Food. Sci. Technol. Abst., 37(2):pp. 273.

Gill, H., Jae, Y.S. and Chul, J. (2003). Colour, texture, nutrients content and sensory and values of vegetable soybean as affected by blanching Food Chemistry. Journal of food Science and Technology, 83 (1):pp. 69-74.

Guerrant, N. B., Vavich, M. G., Fardig, O. B. and Ellenberger, H. A. (1947). Effect of duration and temperature of blanching on vitamin retention by certain vegetables. Journal of Food Science and Technology, 38(4):pp. 369-370.

Gupta, S., Lakshmi, J. and Prakash, J. (2008). Effect of Different Blanching treatments on retention in green leafy vegetable. Natural Product Radiance, 7(2):pp. 111-116.

Hijmans, R. .J. and Spooner, D. M. (2001). Geographic distribution of potato species. American Journal of Botany, 88(11): 101-2112.

Iqbal, A. and Ralph P. C. (2001). Blanching of fruit and vegetable. Beverages and Food World, 11.

Kendall, P. (2008). Home freezing of fruit and Vegetables. Home and garden Bulletin No. 10, U. S. Department of Agriculture.

Kim, D. M., Smith, N. L. and Lee, C. Y. (1993). Apple cultivar variations in response to heat treatment and minimal processing. J. Food Sci., 58(4):pp. 1114-1124.

Krotov, E. G., Pluzhnikov, I. I. and Golubyatnikova, L. A. (1971). Inactivation of enzyme system in vegetable prior to freezing. Izv. Vyssh. Zaved Pishch.Tekhno., 5 (1):pp. 42.

Lee, F. A. (1958). The blanching process. Journal of advances in Food research, 8 (2):pp. 56-61.

Lin, S. and Brewer, M. S. (2006). Effect of blanching on quality characteristics of frozen peas. Journal of Food quality, Vol II, 2 Eddition, CABI, Pennsylyania, USA.

Maharaj, V. and Clement, K. S. (1994). Drying the green herb Shado- Beni in a natural cabinet and solar driers. Asian Food Journal, 9(1):pp. 56-60.

Molhar, P. I. and Friedman (1990). Inhibition of browning by sulfur amino acids in apples and potatoes. J. Agric. Food Chem., 38:PP. 1652-1656.

Mondy, N I., Koch, R. L. and Chandra, S. (1979). Influence of nitrogen fertilization on potato discoloration in relation to chemical composition. J. Agric. Food Chem., 27(2): PP. 418-420.

Morris, A. A., Bernett and Burrow, O. J. (2004). Effect of Processing on nutrient content of foods. J. Agric Food Chem., 37:PP. 56-60.

Morris, T. N. (1974) Dehydration of food. Chapman and Hall Ltd., London.

Mukherjee, S. and Chattopadhayay, P. K. (2005). Whirling bed blanching of potato cures and its effect on product quality. Journal of Food engineering, 78:PP. 52-60.

Mustapha, K. (2006). Effect of Polyphenol Oxidae and peroxidase in Algerian stored dates, African Journal of Biotechnology, 62(3):PP. 790-794.

Nath, N., Kuamr, S. and kalra R. (1991). Dehydration of bitter gourd ring. Journal of Food Science and Technology, 28(1):PP. 52-53.

Copy for Cite this Article- Mohd Kaleem, Er. Kailash Chandra Yadav, Md Jafri Ahsan, 'Development And Performance Evaluation Of Forced Convection Batch Type Steam Blancher,' *International Journal of Science, Engineering and Technology,* Volume 4 Issue 1: 2016, pp. 337- 347.

Nadiaye, C., Shi, Y. X. and Zhang, W. (2008). Steam Blanching Effect on Polyphenoloxidase, Peroxidae and Colour of Mango slice. Journal of Food Engineering, 113:PP. 92-95.

Negi, P. S. and Roy, S. K. (2000). Effect of blanching and drying methods on b carotene, ascorbic acid and chlorophyll retention of leafy vegetables. J. Food sci., 28(1):PP. 236-239.

Onyamio and Badifu (1987). Effect of Blanching methods on the nutritional and sensory quality of leafy vegetables. Qualities plantrum plant foods for human nutrition, 37(4): 219-298.

Ozemir, M. (1997). Food Browning and Its control. CRIT. Rev. Food Sci. Nutr., 32:PP. 53-273.

Patil, V. R., Kulkarni, K. and Ingle, U. M. (1978). Effect of blanching factors on quality and durability of sun dried and dehydrated Fenugreek (Methi). Indian Food Packer, 23(1):PP. 32-33.

Pittia, P., Nicoli, M. C., Comi, G. and Massini, R. (1999). Shelf-life extension of fresh-like ready – to– use pear cubes. J. Sci. Food Agric., 79(7):PP. 955-960.

Rahn, A. (1993). "1.1 Introduction"). The Basics of Soldering. John Wiley & Sons.ISBN 0471584711.

Rice, P., Selman, J. D. and Abdul, R. K. (1990). Nutritent retention in hot water blanching of potatoes. International Journal of Food Science and technology, 25:PP. 61-65.

Saltveit, M. E. (1997). Physical and physiological changes in minimally processed fruit and vegetables. In Tomas, B. F. A and Robin, R. J. Edi. "Phytochemistry of fruit and vegetables". Phytochem. Soc. Europe, Clarendon, Oxford, pp. 205-220.

Sapers, G. M. (1993). Browning of foods: control by sulfites, antioxidants and other means. Foods Technol., oct. (10):pp. 75-84.

Seyderhelm, I., Boguslwaski, S., Michaelis, G. and Knorr, D. (1996). Pressure induced inactivation of selected food enzymes. J. Food Sci., 61:pp. 308-310.

Author's details

[1, 3] M. Tech Student, Vaugh School Agricultural Engineering & Technology, SHIATS, Allahabad, India.

[2]Assistant Professor, Vaugh School Agricultural Engineering & Technology, SHIATS, Allahabad, India.

Call for Papers

International Journal of Science, Engineering and Technology globally welcomes research scholars & scientists to publish their full-length papers, reviews, and short communications exploring and to promote diverse and integrated areas of the *Science, Engineering, Technology, Biology, Chemistry, Physics, Geography, Mathematics, Biotechnology and all the related fields of Science and Technology*.

Important Dates

Submission Last Date	25th of Feb, Apr, June, Aug, Oct and Dec
Acknowledgement of Submission	System Auto reply with Paper ID
Review / Acceptance Notification	Within 5 Days of Submission (Fast Peer Review Process) Within 10 Days of submission (Blind peer review process)
Publication Date (Print Version Journal)	30th Feb, Apr, June, Aug, Oct and Dec

For Online Submission

Kindly logon to Website: www.ijset.in/submit/

E-mail: editor@ijset.in I editorinchief.ijset@gmail.com